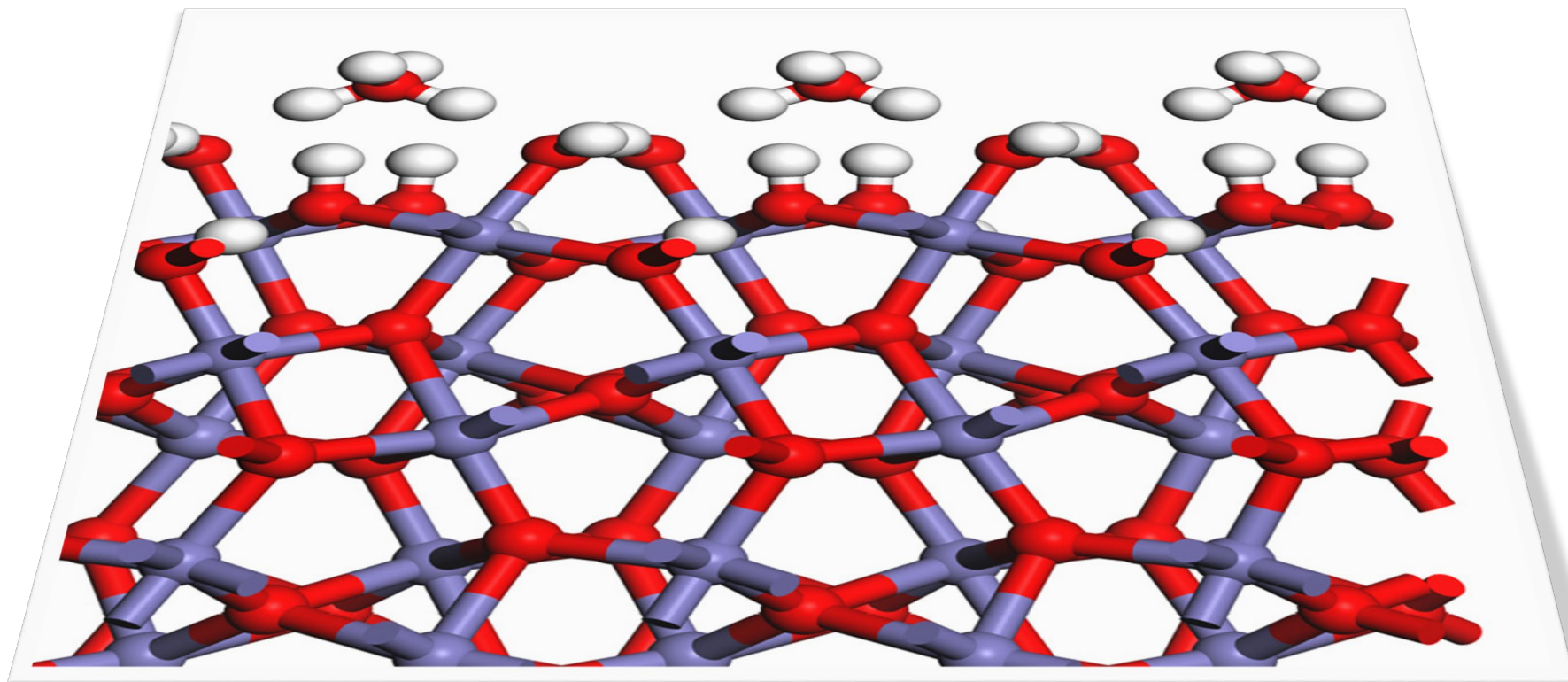


Introduction Surface and Interface Scattering

Peter J. Eng
eng@cars.uchicago.edu
GSECARS
University of Chicago



GeoSoilEnviroCARS 24th National School on Neutron and X-Ray Scattering

July 21st, 2022 Peter J. Eng

Outline

- **Introduction**
- **Diffraction Theory**
- **Crystal Truncation Rod (CTR) Diffraction**
 - Instrumentation
 - Measurement
- **Diffractometer Geometry**
- **Data collection and reduction**
- **Sample Environments**
- **Example Systems**



Surface & Interface Scattering – What can be measured?

- **Surface and interface structure**
 - Atomic level positions of atoms at a surface or interface
 - Growth and dissolution mechanisms (kinetics)
 - Structure and binding modes of adsorbates
 - Structure reactivity relationships
- **Interface electron density profiles @ the atomic scale**



Why use x-rays to Study Surfaces and Interfaces

- **Advantages**

- Large penetration depth allows for in-situ measurements
 - Liquid water, controlled atmospheres, growth chambers, hazardous materials (i.e. radioactive)
 - Provides access to buried interfaces
- Kinematic scattering, simplifies the analysis

- **Disadvantages**

- The generally weak signals requires a synchrotron source
- Systems need to be well ordered and low roughness
- Intense x-ray exposure can alter the system

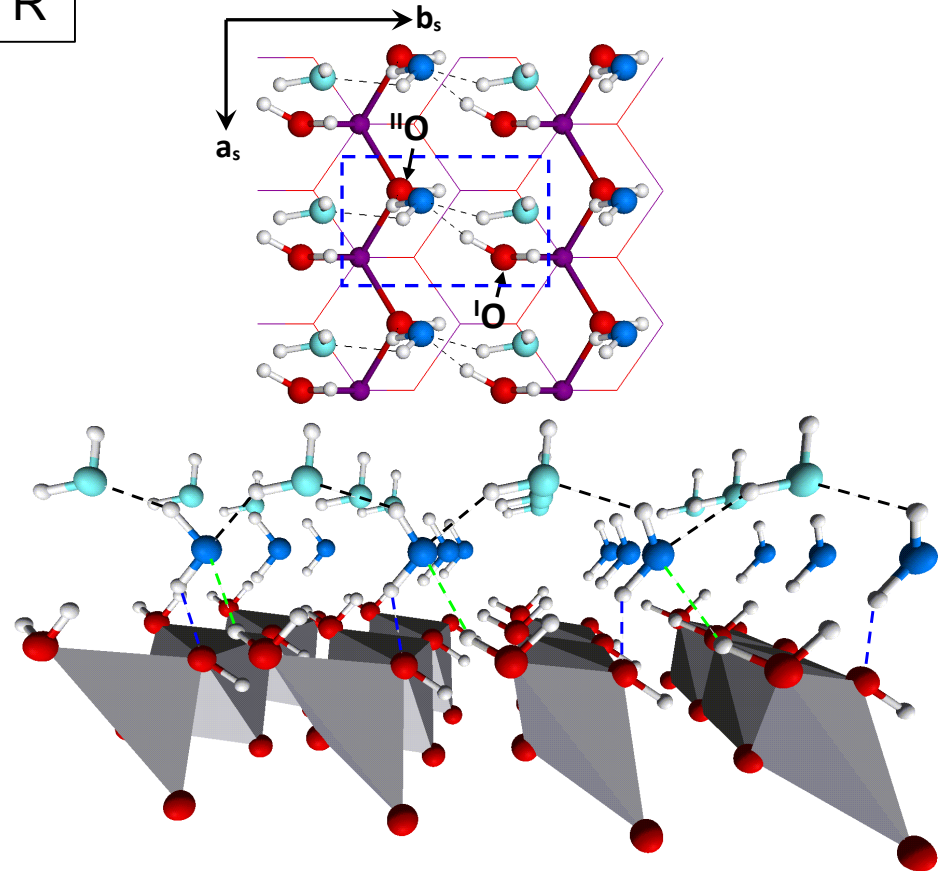
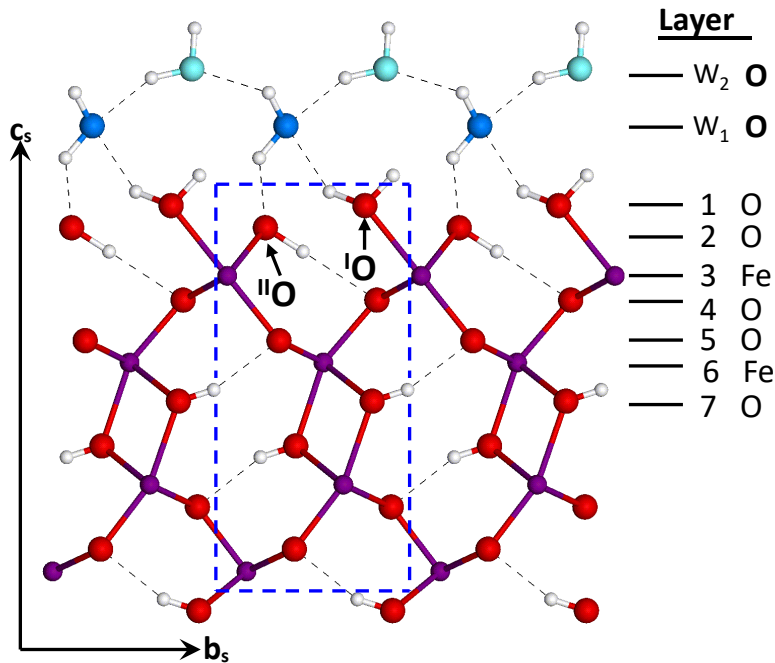
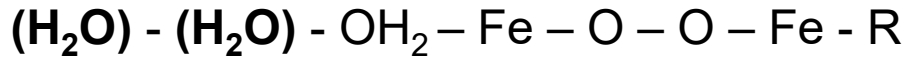


The Results: Goethite – FeOOH (100)

Hydrated goethite (α -FeOOH) (100) interface structure

Double hydroxyl, double water terminated interface with significant atom relaxations

S. Ghose et al. Geochim. Cosmochim. Acta 74, 1943-1953 (2010)



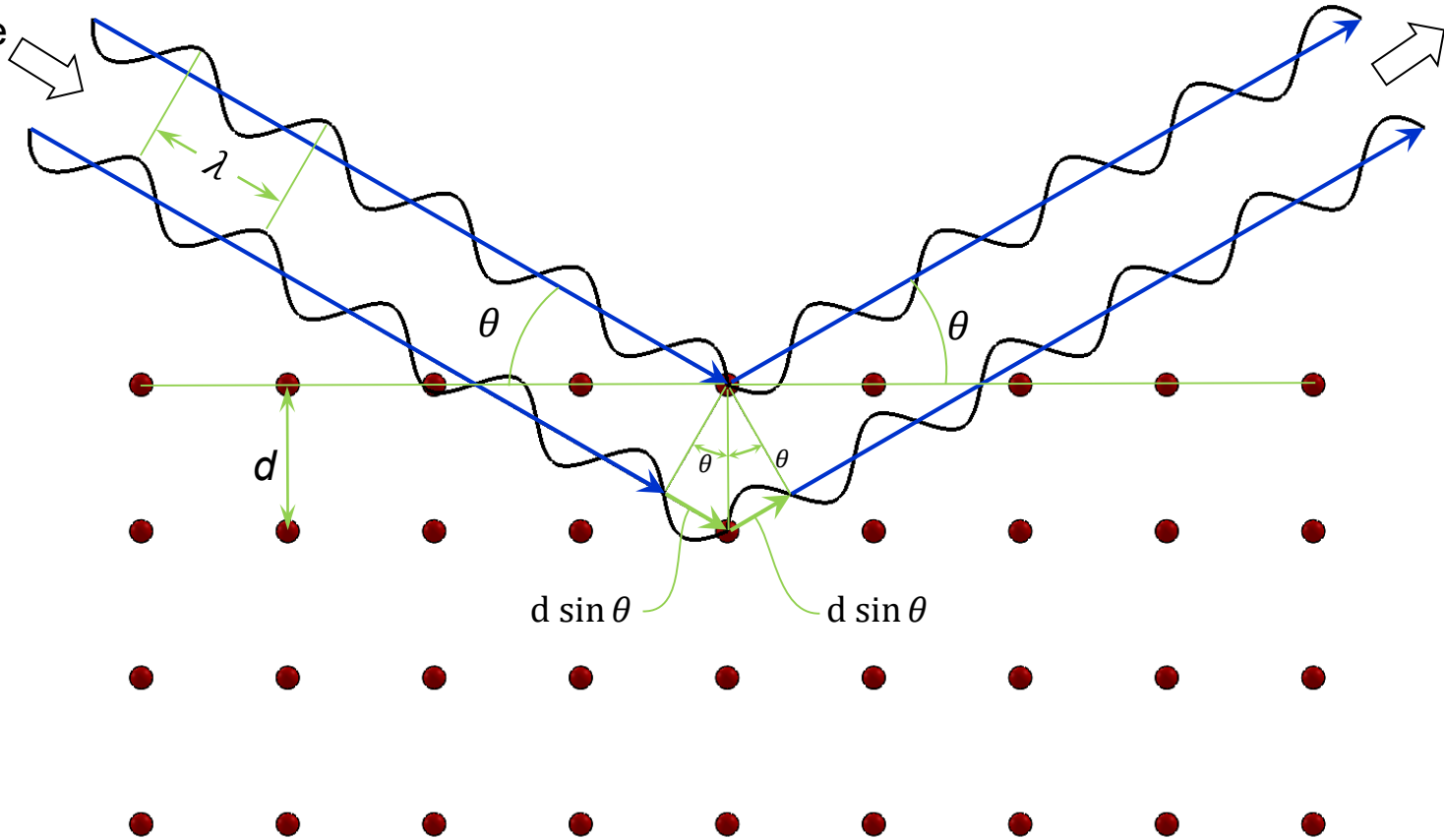
Diffraction – Theory

Constructive interference when:

$$n\lambda = 2d \sin \theta$$

Bragg's Law

Incident
plan wave

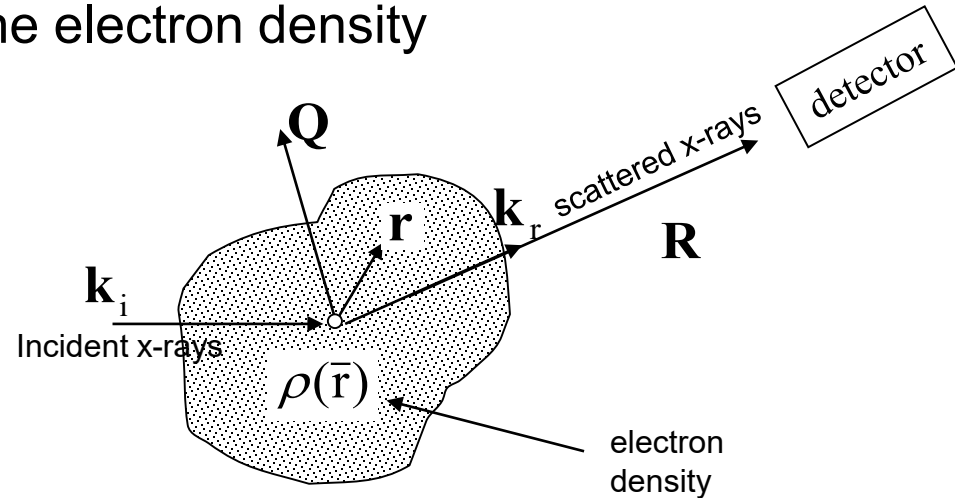


Diffraction – Theory

The scattered intensity into the detector is proportional to the square modulus of the Fourier transform of the electron density

$$I_{\text{det}} = \mathbf{E} \mathbf{E}^* \propto \frac{E_o^2 r_e^2}{R^2} |FT[\rho(\mathbf{r})]|^2$$

Where, $r_e = \frac{e^2}{4\pi\epsilon_0 mc^2} = 2.82 \times 10^{-5} \text{ angstroms}$



$$FT[\rho(\mathbf{r})] \propto \int \rho(\mathbf{r}) e^{i\mathbf{Q}\cdot\mathbf{r}} dV$$

Where, $\mathbf{Q} = \mathbf{k}_r - \mathbf{k}_i$

$$FT[\rho(\mathbf{r})] \propto \sum_n f_{a,n} e^{i\mathbf{Q}\cdot\mathbf{r}_n}$$

$$f_{a,n} = \int \rho_n(\mathbf{r}) e^{i\mathbf{Q}\cdot\mathbf{r}} dV$$

The sum is over all n atoms at \mathbf{r}_n with atomic scattering factors $f_{a,n}$

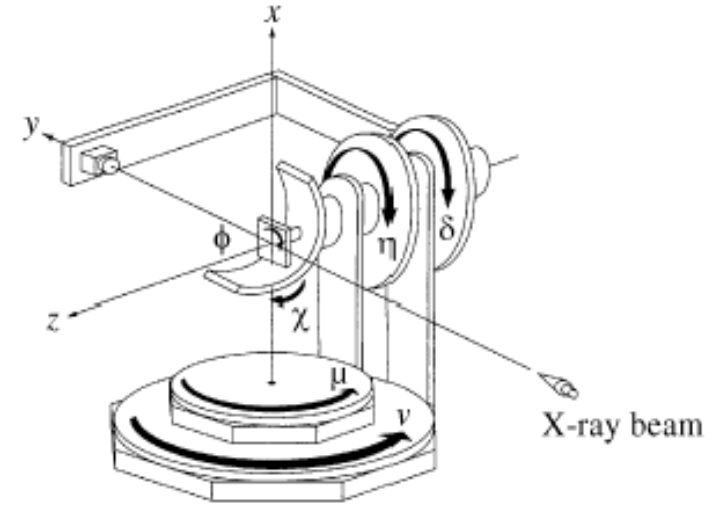
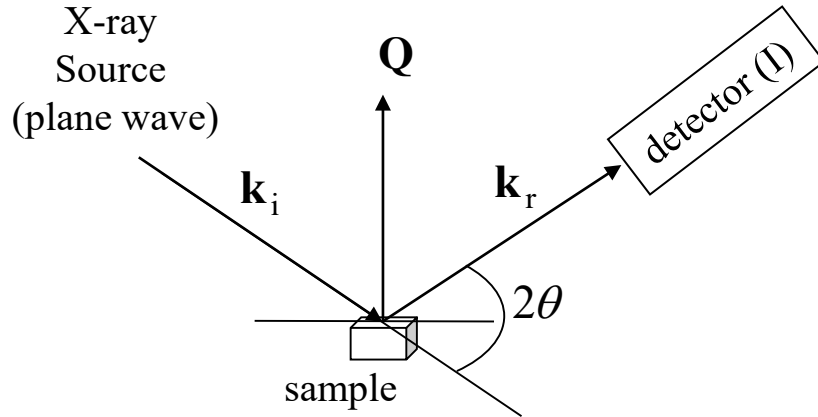
Master Equation for X-ray Scattering from a collection of atoms

$$I = |E(\mathbf{R})|^2 \propto \left| \sum_n f_{a,n} e^{i\mathbf{Q}\cdot\mathbf{r}_n} \right|^2$$



Diffraction – Theory

The instrument measures \mathbf{Q} in the lab



$$\mathbf{Q} = \mathbf{k}_r - \mathbf{k}_i \quad \text{Where,} \quad |\mathbf{k}_r| = |\mathbf{k}_i| = \frac{2\pi}{\lambda}$$

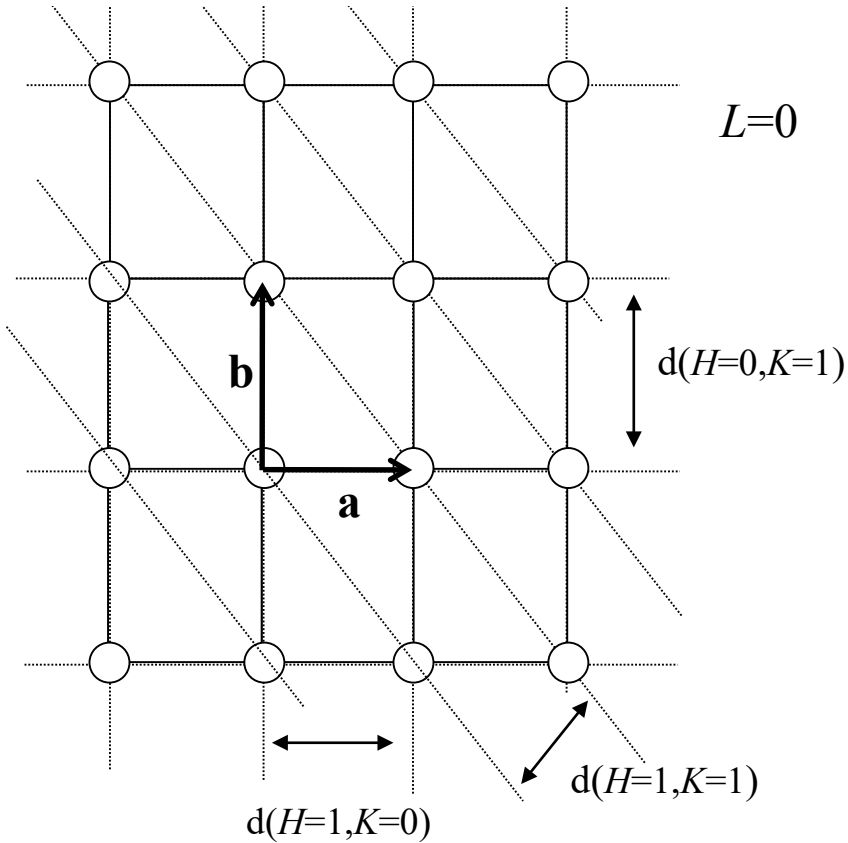
The scattering vector diagram gives:

$$\mathbf{Q} = \hat{\mathbf{Q}} \left\{ 2 \frac{2\pi}{\lambda} \sin 2\theta/2 \right\} \Rightarrow \boxed{|\mathbf{Q}| = \frac{4\pi}{\lambda} \sin 2\theta/2}$$

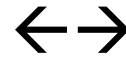


Diffraction – Theory

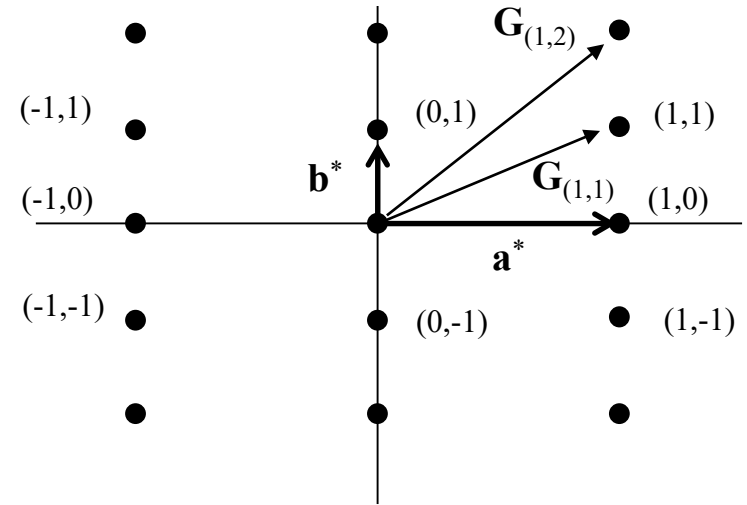
Real Space Planes
(Miller Indices H K L)



(HKL) defines a plane with intercepts: $\frac{\mathbf{a}}{H}$, $\frac{\mathbf{b}}{K}$, $\frac{\mathbf{c}}{L}$



Reciprocal Space Points
(Miller Indices H K L)



$$\mathbf{a}^* = 2\pi \frac{\mathbf{b} \times \mathbf{c}}{\mathbf{a} \cdot \mathbf{b} \times \mathbf{c}} \quad \mathbf{b}^* = 2\pi \frac{\mathbf{c} \times \mathbf{a}}{\mathbf{a} \cdot \mathbf{b} \times \mathbf{c}} \quad \mathbf{c}^* = 2\pi \frac{\mathbf{a} \times \mathbf{b}}{\mathbf{a} \cdot \mathbf{b} \times \mathbf{c}}$$

$$\mathbf{G} = H \mathbf{a}^* + K \mathbf{b}^* + L \mathbf{c}^*$$

$$|\mathbf{G}_{HKL}| = 1/d_{HKL}, \quad \perp (HKL)$$

$$\mathbf{Q} = 2\pi \left(H \mathbf{a}^* + K \mathbf{b}^* + L \mathbf{c}^* \right)$$



Diffraction – Theory

Scattering from a crystal consisting of collection of unit cells

Rewrite \mathbf{r}_n from the master equation as:

$$\mathbf{r}_n = \mathbf{R}_c(n_1n_2n_3) + \mathbf{r}_j(xyz)$$

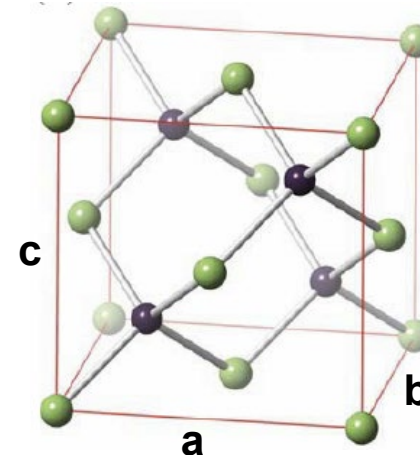
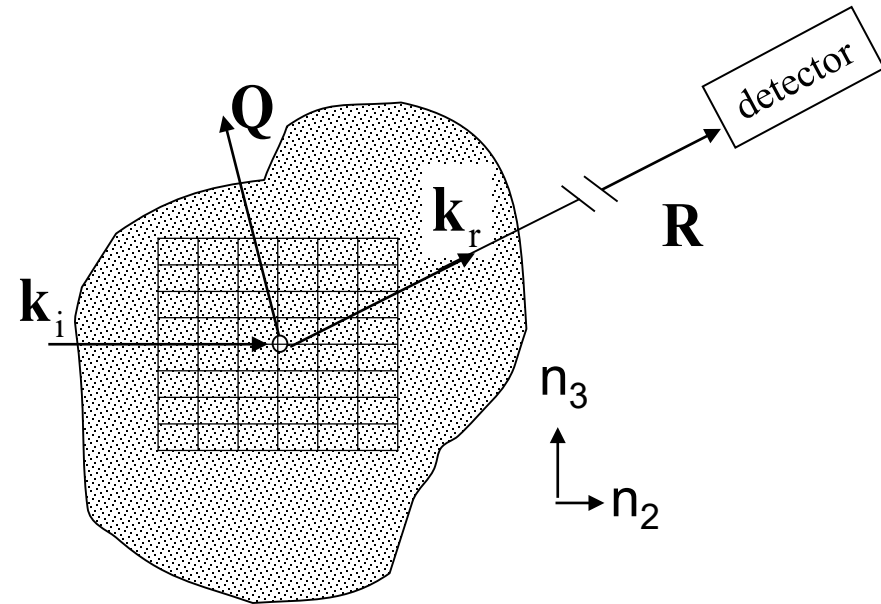
\mathbf{R}_c is the origin of the $(n_1n_2n_3)$ unit cell w/r/to some arbitrary “center”:

$$\mathbf{R}_c(n_1n_2n_3) = n_1 \mathbf{a} + n_2 \mathbf{b} + n_3 \mathbf{c}$$

Where \mathbf{a} , \mathbf{b} , and \mathbf{c} are vectors describing the unit cell

\mathbf{r}_j is the position of the j^{th} atom in the unit cell, expressed in terms of its fractional coordinates (xyz) :

$$\mathbf{r}_j = x_j \mathbf{a} + y_j \mathbf{b} + z_j \mathbf{c}$$



Diffraction – Theory

Using:

$$\mathbf{Q} = 2\pi (H \mathbf{a}^* + K \mathbf{b}^* + L \mathbf{c}^*)$$

Dot products in sum become simple to evaluate

$$\mathbf{Q} \cdot \mathbf{r}_n = \mathbf{Q} \cdot \mathbf{R}_c + \mathbf{Q} \cdot \mathbf{r}_j$$

$$\mathbf{Q} \cdot \mathbf{R}_c = 2\pi(n_1 H + n_2 K + n_3 L) \quad \text{Location of the } n^{\text{th}} \text{ unit cell}$$

$$\mathbf{Q} \cdot \mathbf{r}_j = 2\pi(x H + y K + z L) \quad \text{Location of the atoms within a unit cell}$$



Diffraction – Theory

Substitute for \mathbf{Q} and \mathbf{r}_n in the master equation:

$$E(\mathbf{R}) \propto FT[\rho(\mathbf{r})] = \sum_n f_{a,n} e^{i\mathbf{Q}\cdot\mathbf{r}_n}$$

$$E \propto \sum_{n_1=-\frac{(N_1-1)}{2}}^{\frac{(N_1-1)}{2}} e^{i2\pi n_1 H} \sum_{n_2=-\frac{(N_2-1)}{2}}^{\frac{(N_2-1)}{2}} e^{i2\pi n_2 K} \sum_{n_3=-\frac{(N_3-1)}{2}}^{\frac{(N_3-1)}{2}} e^{i2\pi n_3 L} \sum_{j=1}^m f_{a,j} e^{i\mathbf{Q}\cdot\mathbf{r}_j} e^{-M_j}$$

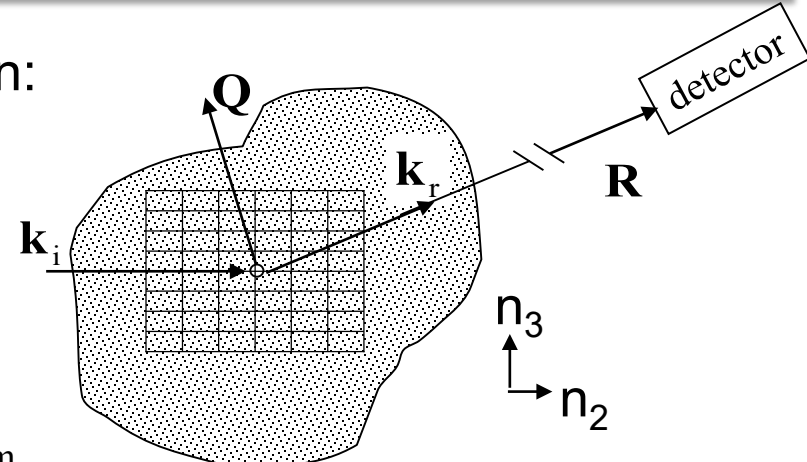
Sum over n_1
 N_1 total cells
 ↓
 $(N_1-1)/2$
 $-(N_1-1)/2$

Sum over n_2
 N_2 total cells
 ↓
 $(N_2-1)/2$
 $-(N_2-1)/2$

Sum over n_3
 N_3 total cells
 ↓
 $(N_3-1)/2$
 $-(N_3-1)/2$

$\sum_{j=1}^m$
 Sum over the m atoms in the unit cell

e^{-M_j}
 Thermal disorder parameter



Simplifying to:

$$E \propto F_c S_1(H) S_2(K) S_3(L)$$

Where F_c is the structure factor of the unit cell:

$$F_c = \sum_{j=1}^m f_{a,j} e^{i\mathbf{Q}\cdot\mathbf{r}_j} e^{-M_j}$$



Diffraction – Theory

The lattice sums can be evaluation using sum the geometric series:

$$S_1(H) = \sum_{-(N_1-1)/2}^{(N_1-1)/2} e^{i2\pi n_1 H} \quad \text{Using:} \quad \sum_{-(N_1-1)/2}^{(N_1-1)/2} k^{n_1} = \frac{k^{\frac{N_1}{2}} - k^{-\frac{N_1}{2}}}{k^{\frac{1}{2}} - k^{-\frac{1}{2}}} \quad \text{Where: } k = e^{i2\pi H}$$

Results in:

$$S_1(H) = \frac{e^{i\pi N_1 H} - e^{-i\pi N_1 H}}{e^{i\pi H} - e^{-i\pi H}} = \frac{\sin(N_1 \pi H)}{\sin(\pi H)}$$

The behavior of the lattice sum when H is close to integer can be determined using L'Hôpital's rule:

$$\lim_{\varepsilon \rightarrow 0} \frac{f(\varepsilon)}{g(\varepsilon)} = \lim_{\varepsilon \rightarrow 0} \frac{f'(\varepsilon)}{g'(\varepsilon)} \quad \longrightarrow \quad \lim_{H \rightarrow \text{int}} \frac{\sin(N_1 \pi H)}{\sin(\pi H)} = \lim_{H \rightarrow \text{int}} \frac{\cos(N_1 \pi H)}{\cos(\pi H)} = N$$

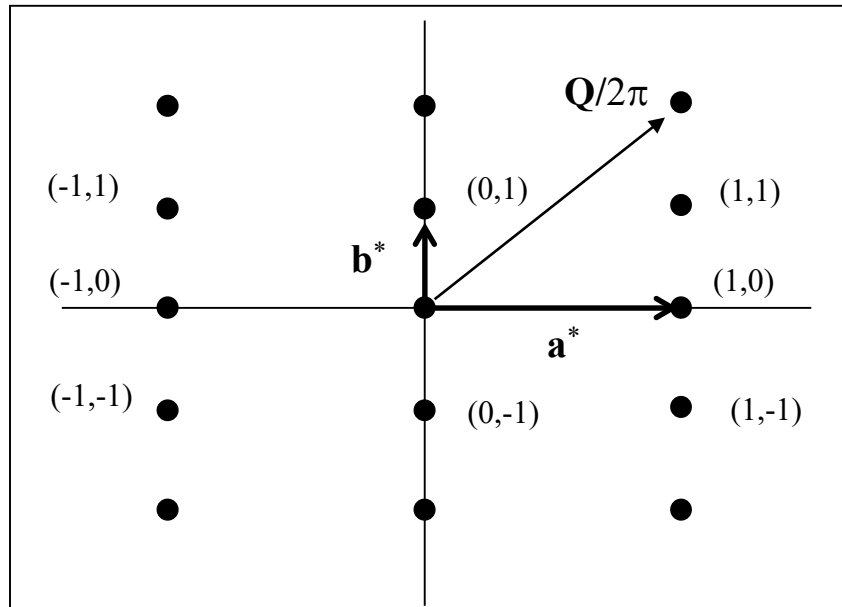
The lattice sum then approaches:

$$S_1(H) \rightarrow N_1 \quad \text{as} \quad H \rightarrow \text{interger}$$



Diffraction – Theory

Scattering intensity at a Bragg point: Where HKL are integers:



$$I \propto |E|^2 \propto |F_c|^2 \frac{\sin^2(N_1\pi H)}{\sin^2(\pi H)} \frac{\sin^2(N_2\pi K)}{\sin^2(\pi K)} \frac{\sin^2(N_3\pi L)}{\sin^2(\pi L)} \rightarrow |F_c|^2 N_1^2 N_2^2 N_3^2$$

Where F_c is the structure factor of the unit cell:
$$F_c = \sum_{j=1}^m f_{a,j} e^{i\mathbf{Q}\cdot\mathbf{r}_j} e^{-M_j}$$



Diffraction – Theory

The structure factor for the unit cell:

$$F_c = \sum_{j=1}^m f_{a,j} e^{i\mathbf{Q}\cdot\mathbf{r}_j} e^{-M_j}$$

using:

$$\mathbf{r}_j = x_j\mathbf{a} + y_j\mathbf{b} + z_j\mathbf{c} \quad (\text{location of the } j^{\text{th}} \text{ atom in the unit cell})$$

$$\mathbf{Q} = 2\pi(H\mathbf{a}^* + K\mathbf{b}^* + L\mathbf{c}^*) \quad (\text{scattering vector in reciprocal space})$$

The dot product is then:

$$\mathbf{Q} \cdot \mathbf{r}_j = 2\pi(x_jH + y_jK + z_jL)$$

Substituting into the structure factor equation gives:

$$F_c = \sum_{j=1}^m f_{a,j} e^{i2\pi(x_jH + y_jK + z_jL)} e^{-M_j}$$



Diffraction – Theory

Example of a Single Crystal of alpha Iron- BCC

Where:

$$a = b = c = 3.61 \text{ \AA}$$

$$\alpha = \beta = \gamma = 90$$

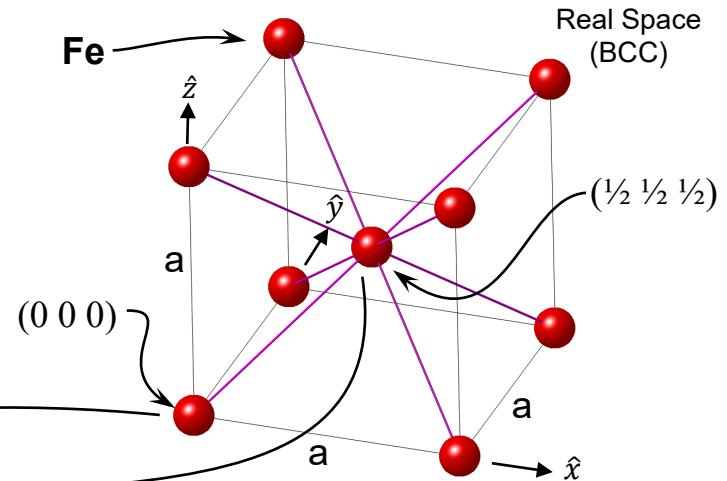
$$F_c = \sum_{j=1}^m f_{a,j} e^{i2\pi(x_j H + y_j K + z_j L)} e^{-M_j}$$

Substituting the coordinates for the two atoms in the crystal:

$$F_c = f_{Fe} \left\{ e^{i2\pi(0H+0K+0L)} + e^{i2\pi\left(\frac{1}{2}H+\frac{1}{2}K+\frac{1}{2}L\right)} \right\} e^{-M_j}$$

$$F_c = f_{Fe} (e^{-M_j}) \{ 1 + e^{i\pi(H+K+L)} \}$$

$$F_c = F \{ 1 + (-1)^{(H+K+L)} \} \Rightarrow \begin{cases} 2F_{Fe} \text{ for, } H + K + L \text{ even} \\ 0, \text{ for, } H + K + L \text{ odd} \end{cases}$$



Diffraction – Theory

Example of a Single Crystal of alpha Iron- BCC

Where:

$$a = b = c = 3.61 \text{ \AA}$$

$$\alpha = \beta = \gamma = 90$$

$$\mathbf{a}^* = 2\pi \frac{\mathbf{b} \times \mathbf{c}}{\mathbf{a} \cdot \mathbf{b} \times \mathbf{c}} \quad \mathbf{b}^* = 2\pi \frac{\mathbf{c} \times \mathbf{a}}{\mathbf{a} \cdot \mathbf{b} \times \mathbf{c}} \quad \mathbf{c}^* = 2\pi \frac{\mathbf{a} \times \mathbf{b}}{\mathbf{a} \cdot \mathbf{b} \times \mathbf{c}}$$

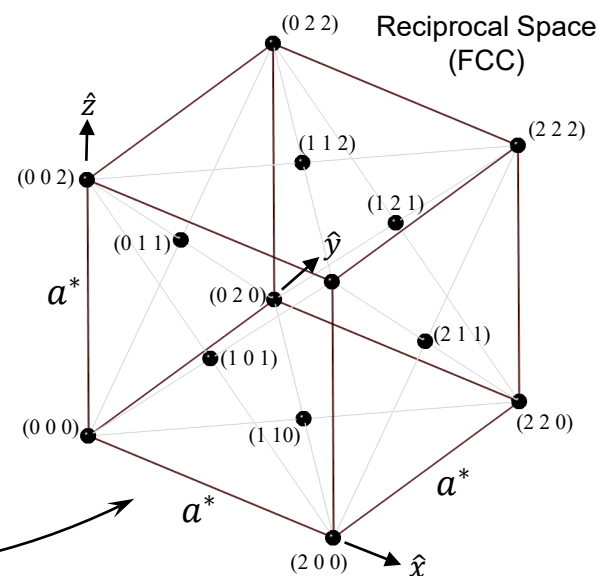
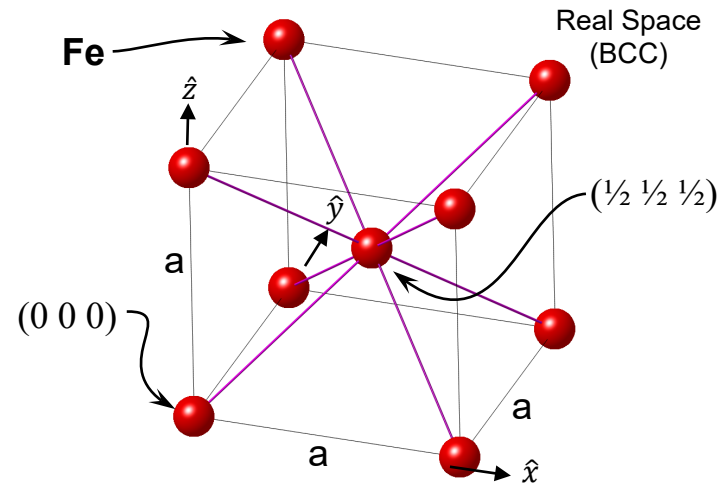
$$\mathbf{a}^* = 2\pi \frac{a^2 (\hat{y} \times \hat{z})}{a^3 \hat{x} \cdot (\hat{y} \times \hat{z})} \quad \mathbf{b}^* = 2\pi \frac{a^2 (\hat{z} \times \hat{x})}{a^3 \hat{y} \cdot (\hat{z} \times \hat{x})} \quad \mathbf{c}^* = 2\pi \frac{a^2 (\hat{x} \times \hat{y})}{a^3 \hat{z} \cdot (\hat{x} \times \hat{y})}$$

$$\mathbf{a}^* = \frac{2\pi}{a} \hat{x} \quad \mathbf{b}^* = \frac{2\pi}{a} \hat{y} \quad \mathbf{c}^* = \frac{2\pi}{a} \hat{z}$$

$$a^* = b^* = c^* = 1.74 \text{ \AA}^{-1}$$

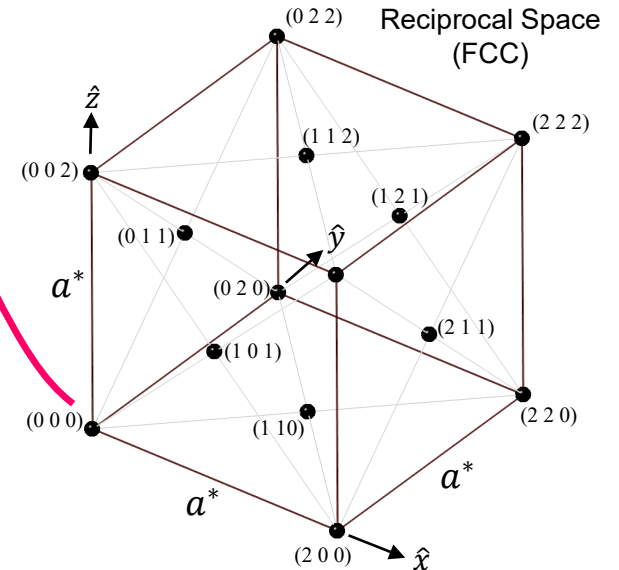
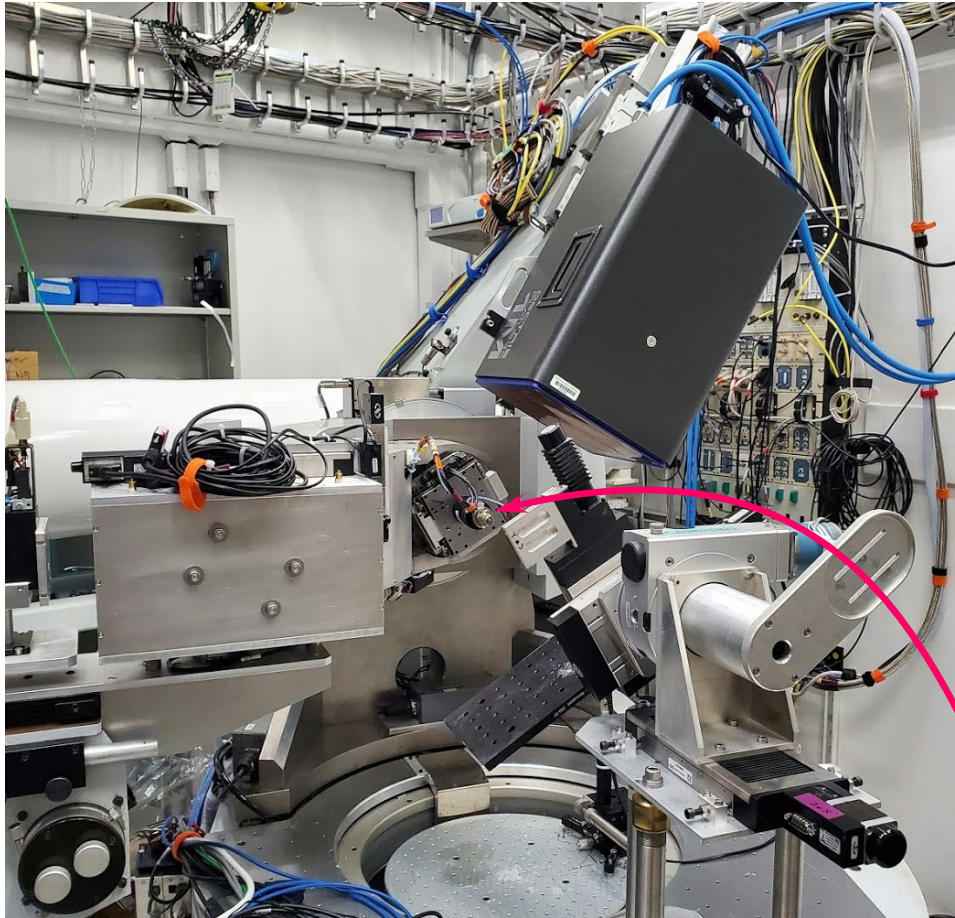
$$F_c = F \{ 1 + (-1)^{(H+K+L)} \} \Rightarrow \begin{cases} 2, \text{ for } H + K + L \text{ even} \\ 0, \text{ for } H + K + L \text{ odd} \end{cases}$$

“Selection rule”

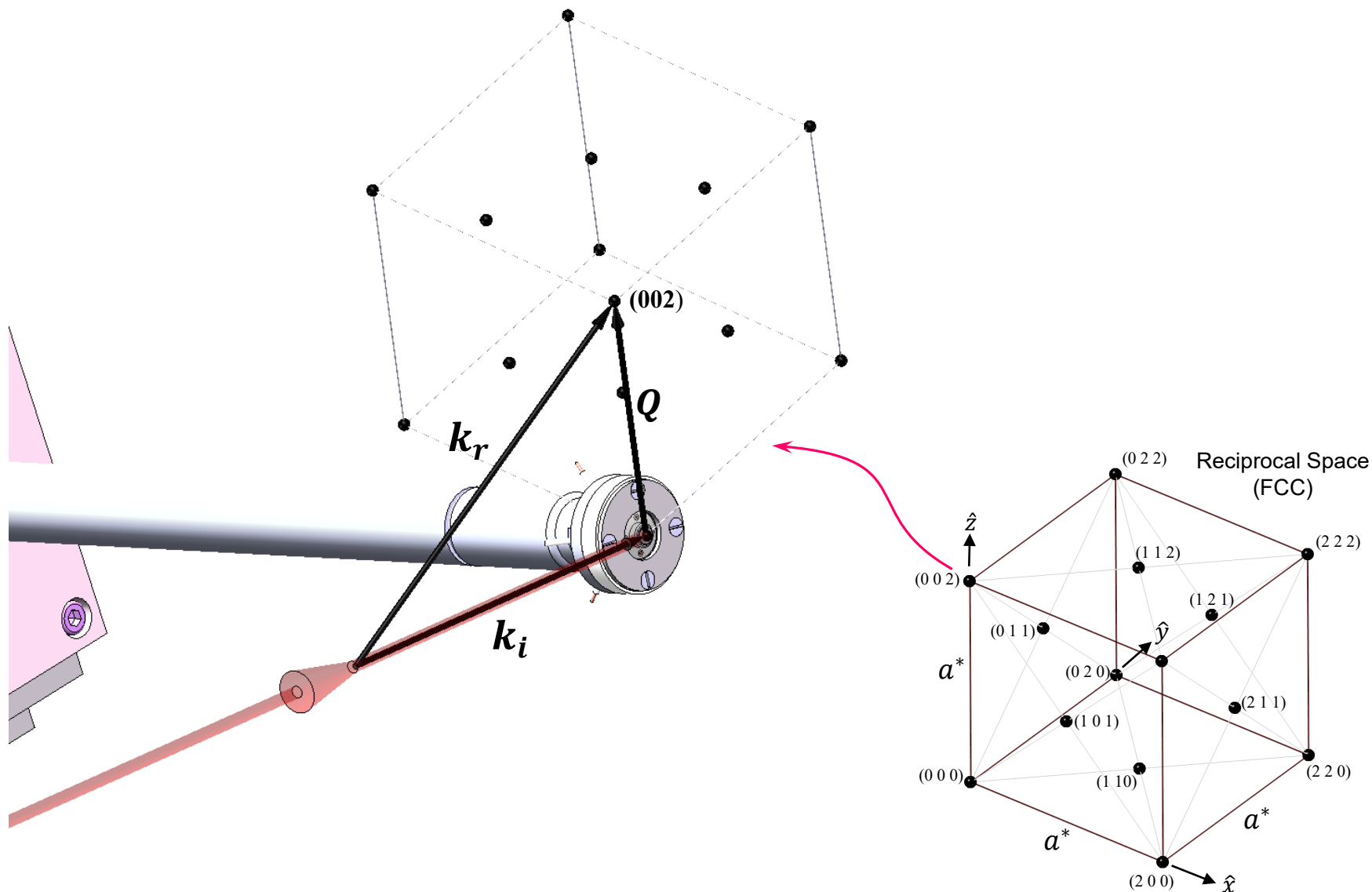


Diffraction – On the Instrument

GSECARS 13BMC Diffractometer

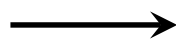


Diffraction – On the Instrument



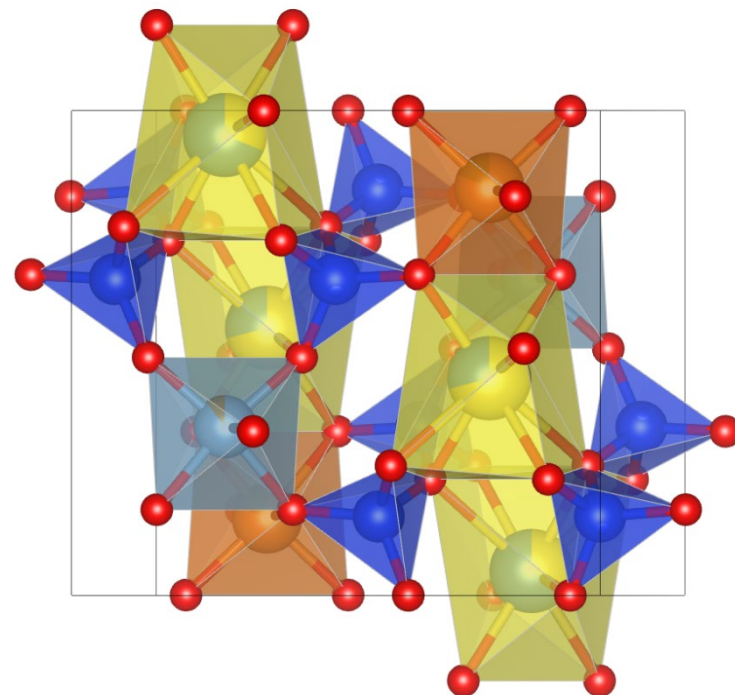
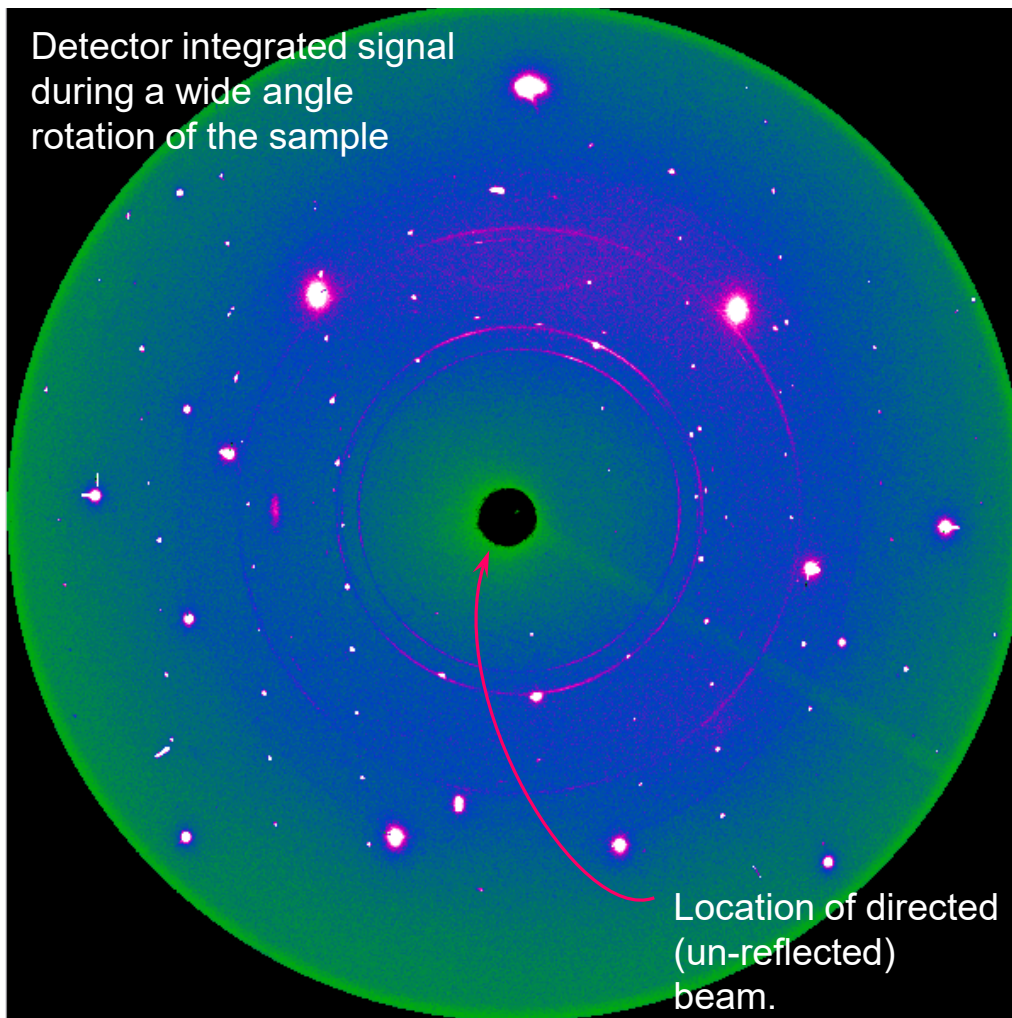
Diffraction – Single Crystal

Single Crystal diffraction data



Single Crystal structure refinement

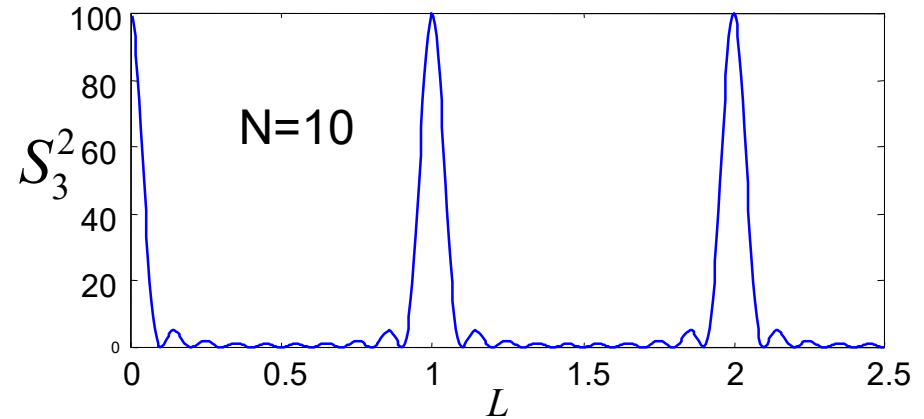
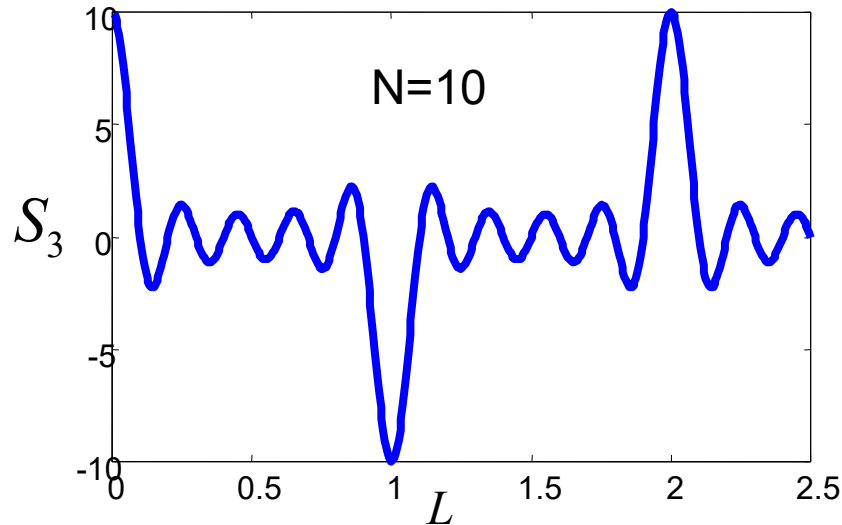
Detector integrated signal during a wide angle rotation of the sample



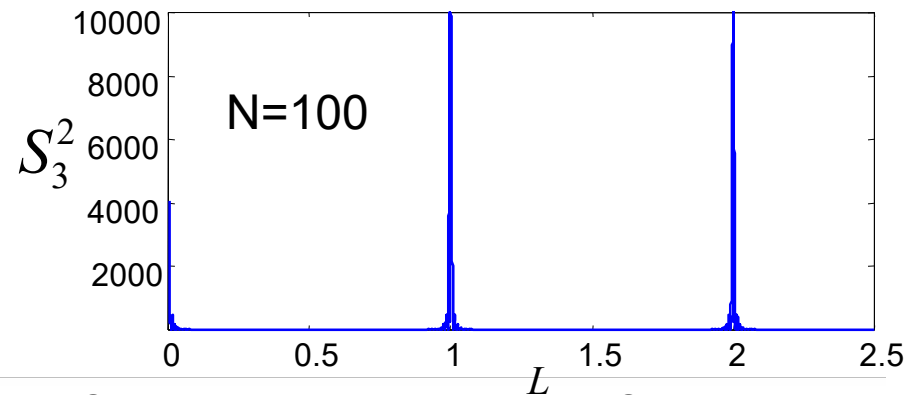
Diffraction – Theory

What about the scattering away from Bragg peak (slit functions)

$$S_3(L) = \sum_{-(N_3-1)/2}^{(N_3-1)/2} e^{i2\pi n_3 L} = \frac{\sin(N_3\pi L)}{\sin(\pi L)} \rightarrow N_3 \text{ as } L \rightarrow \text{integer}$$

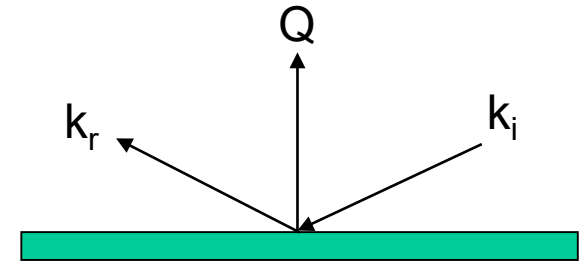
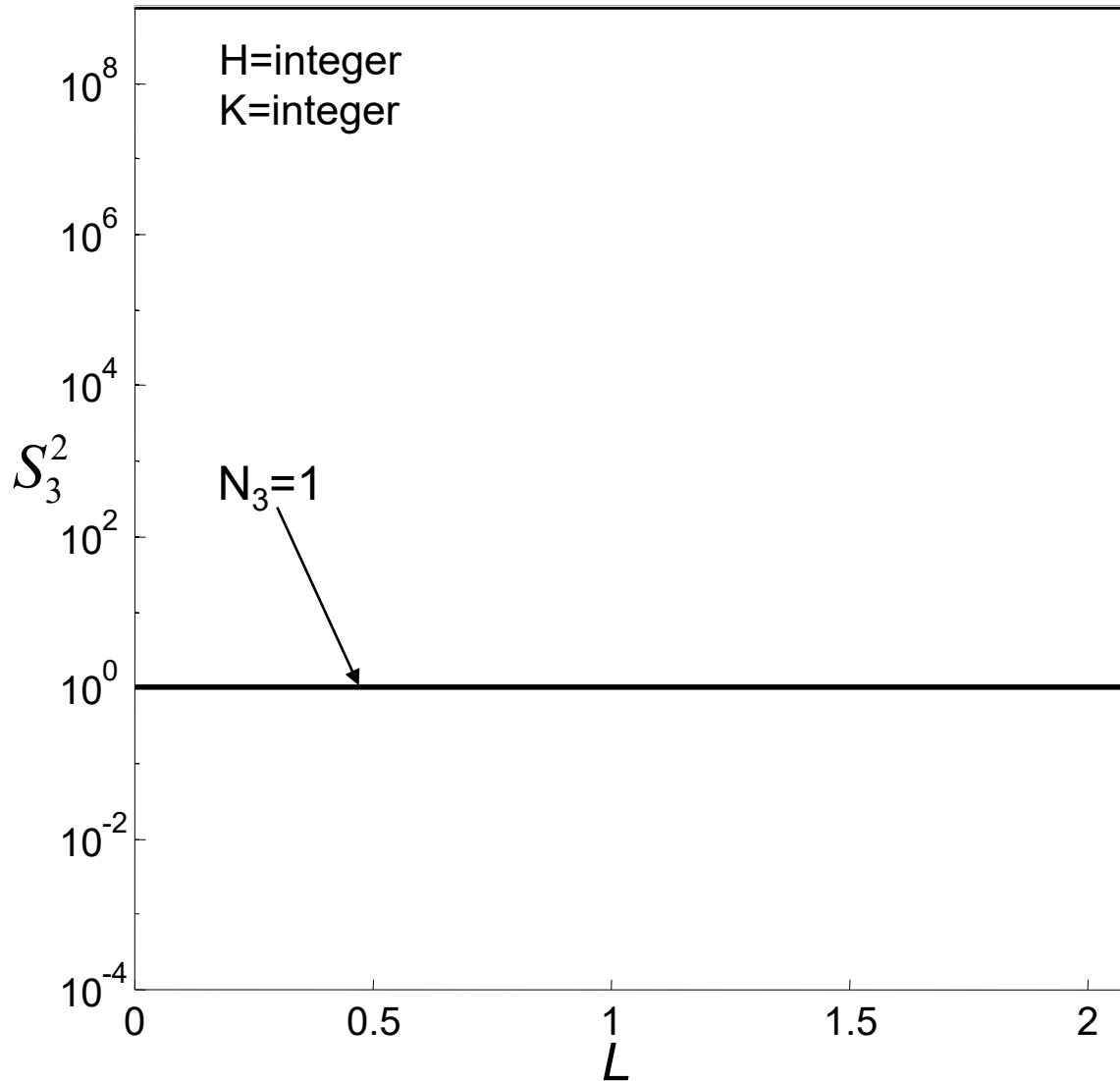


- Intensity is small for non-integer values.
- But its not zero if the xtal is a finite size!



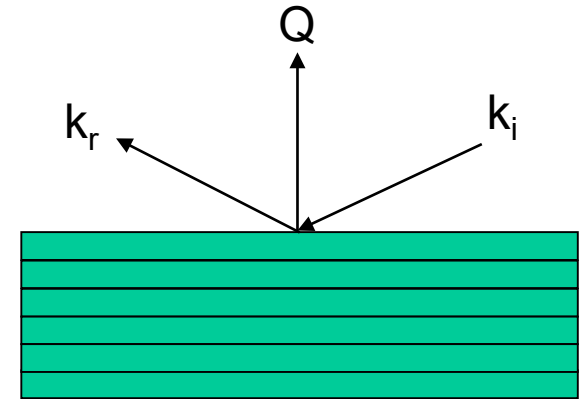
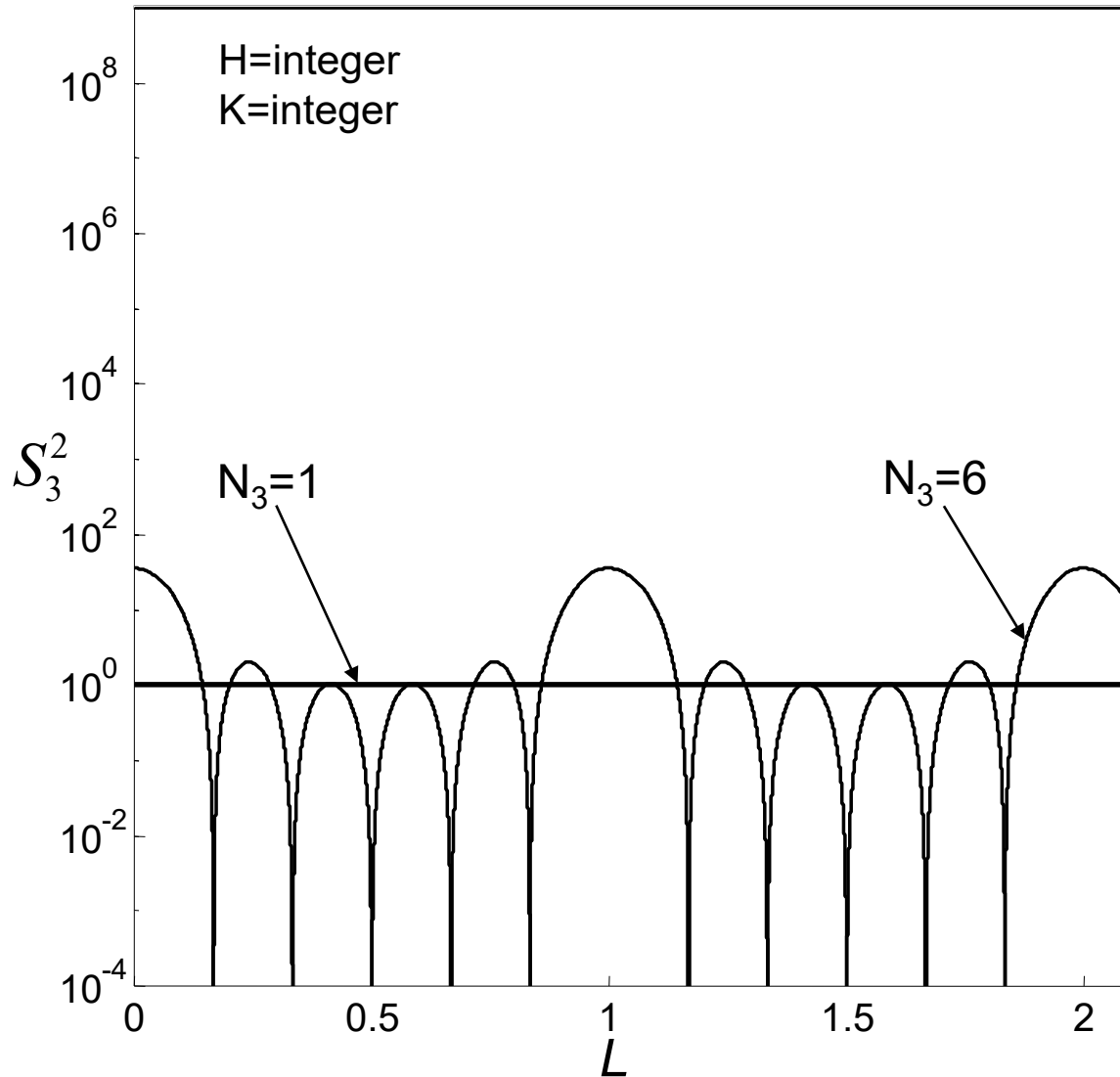
Diffraction – Theory

Intensity variation between Bragg peaks as a function of xtal dimension



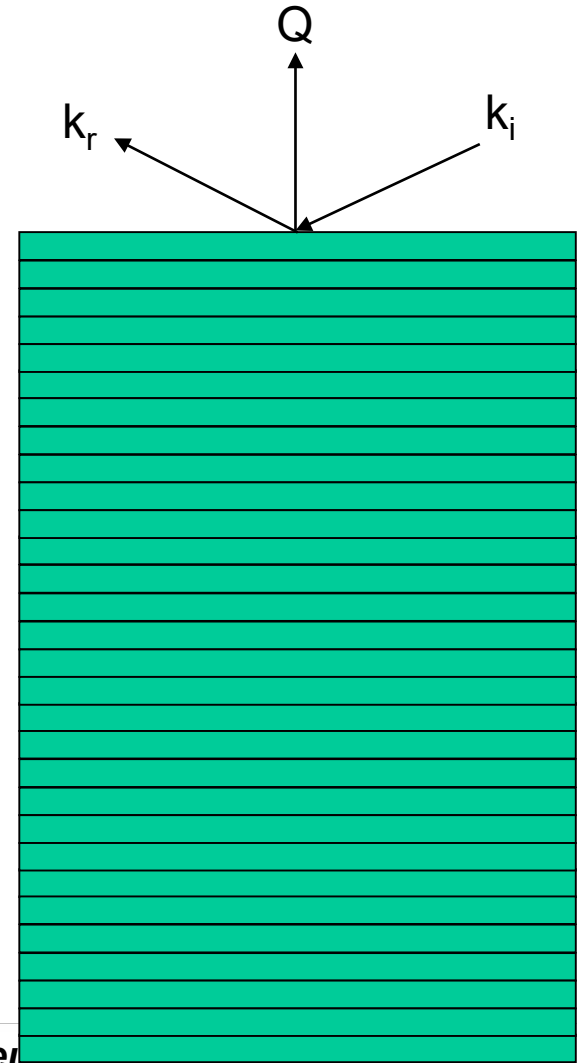
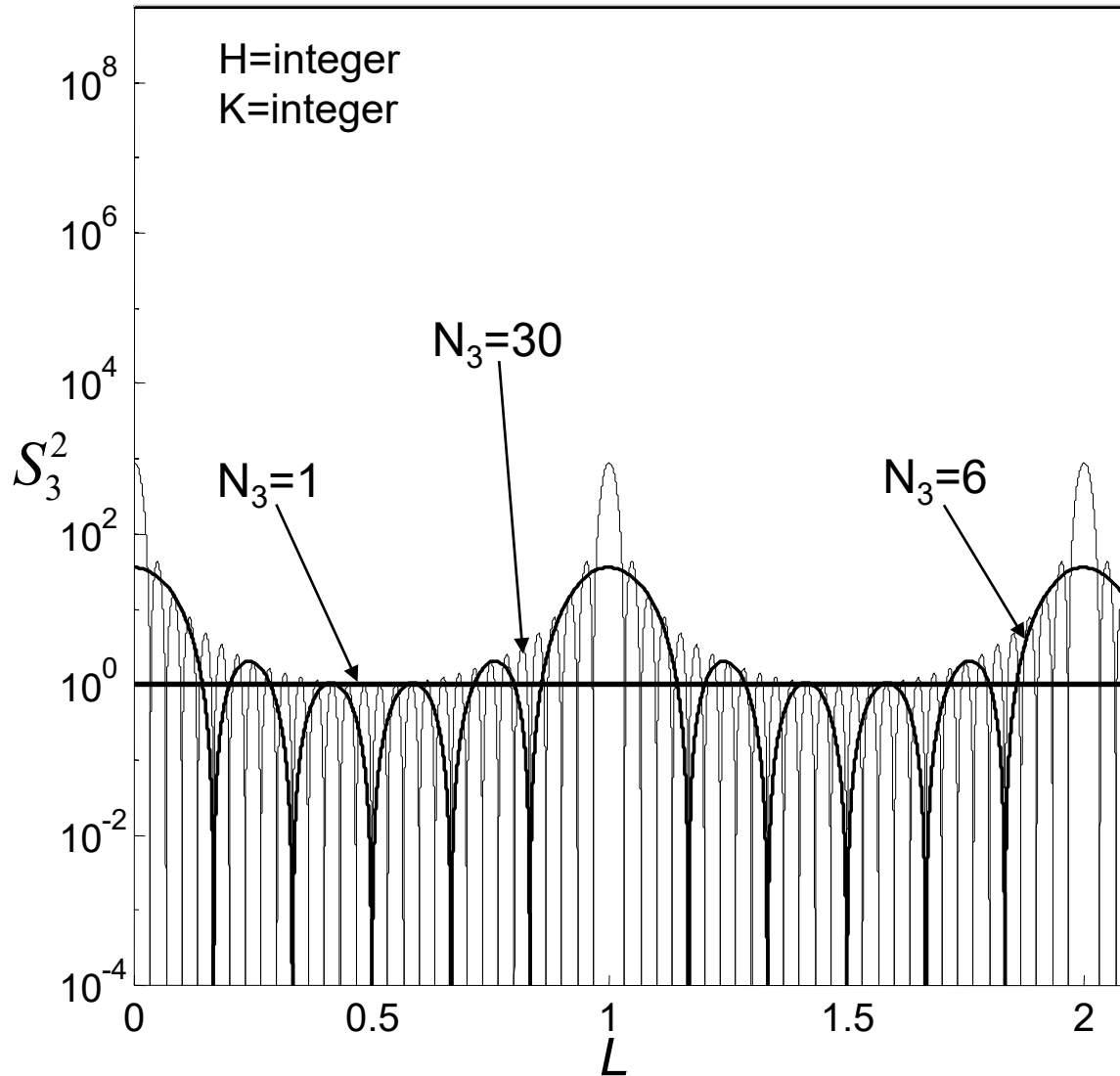
Diffraction – Theory

Intensity variation between Bragg peaks as a function of xtal dimension



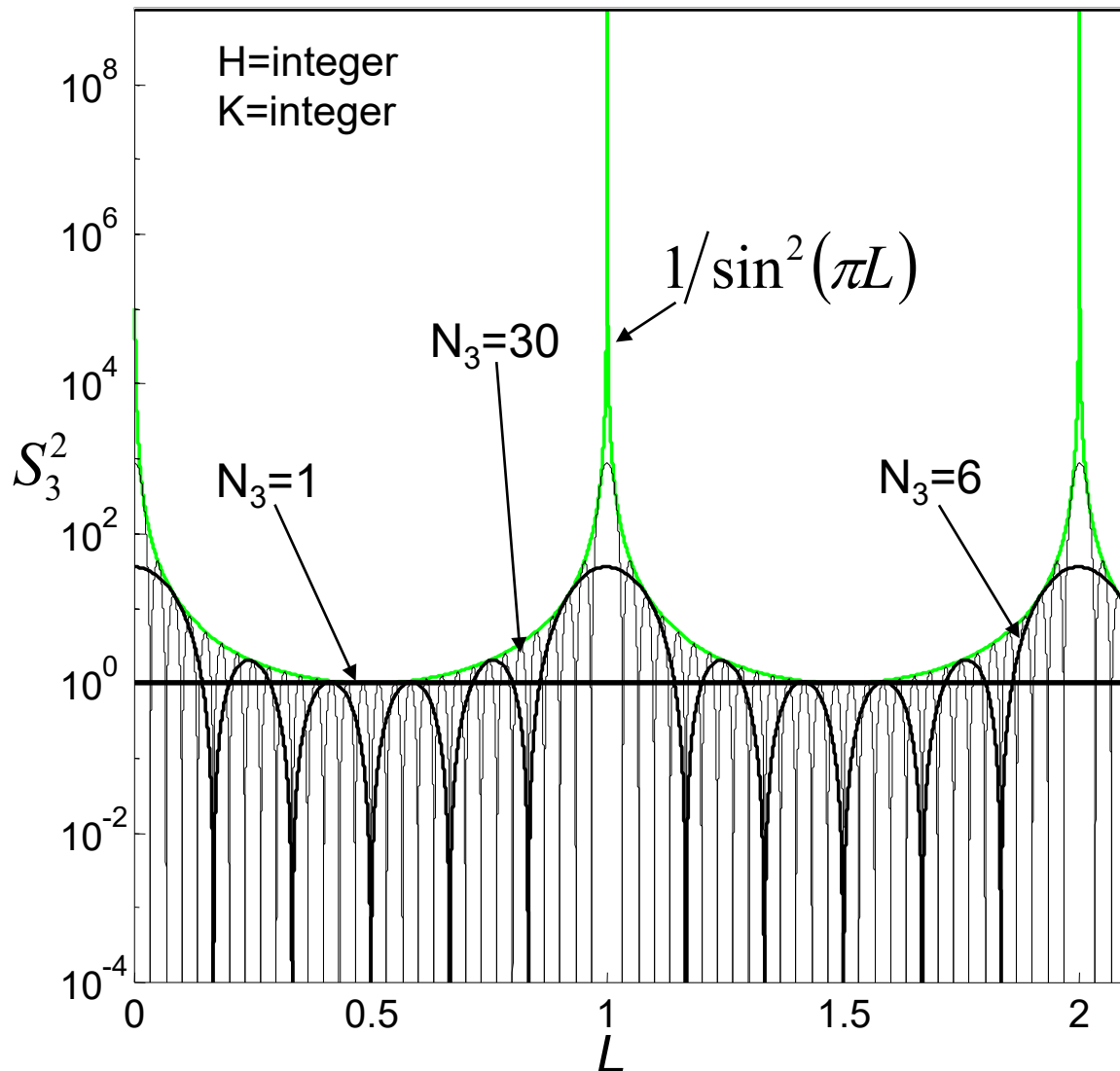
Diffraction – Theory

Intensity variation between Bragg peaks as a function of xtal dimension

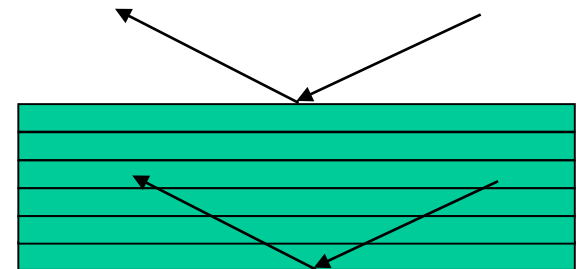


Diffraction – Theory

Intensity variation between Bragg peaks as a function of xtal dimension



- For $N=1$ no oscillations, scattering from a single layer.
- Oscillations for $N>1$ due to interference between x-rays scattering from the top and bottom

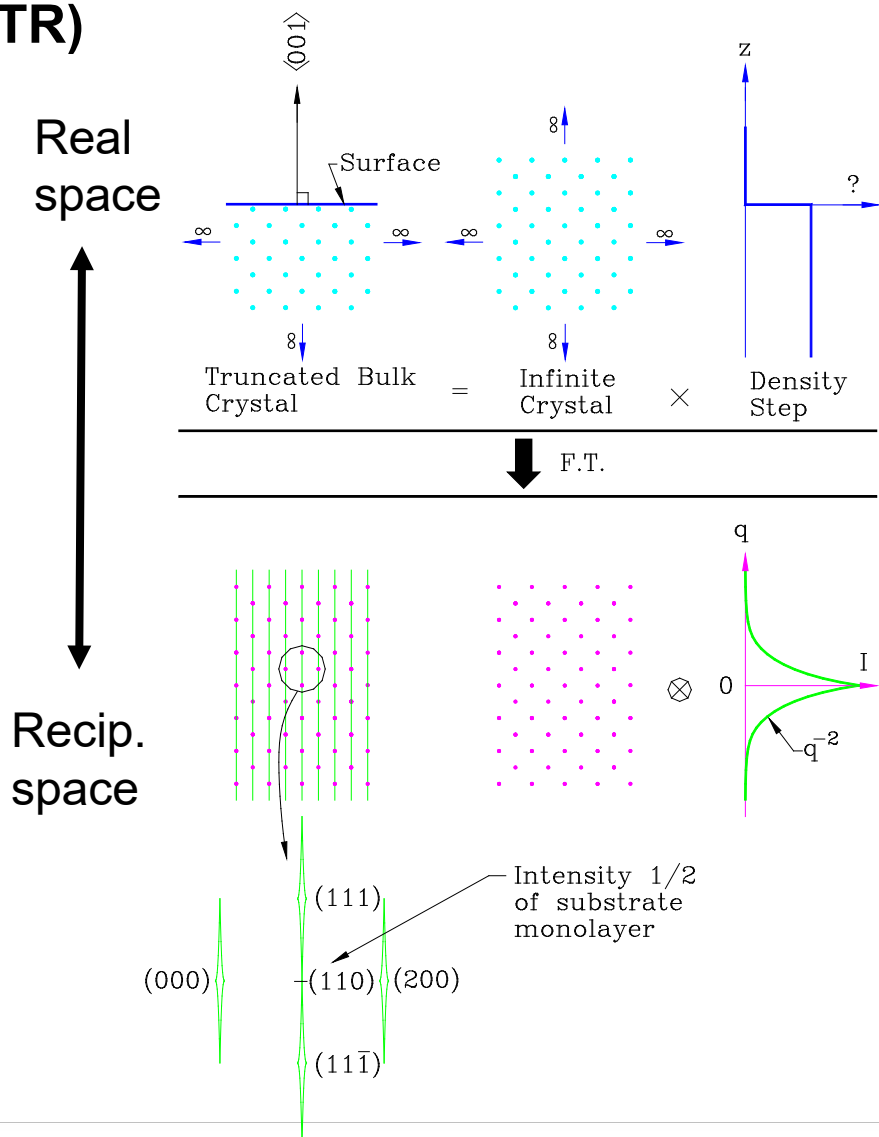


- Intensity variation follows the $1/\sin^2$ profile
- At mid-point (anti-Bragg) the intensity is the same as from a single layer!



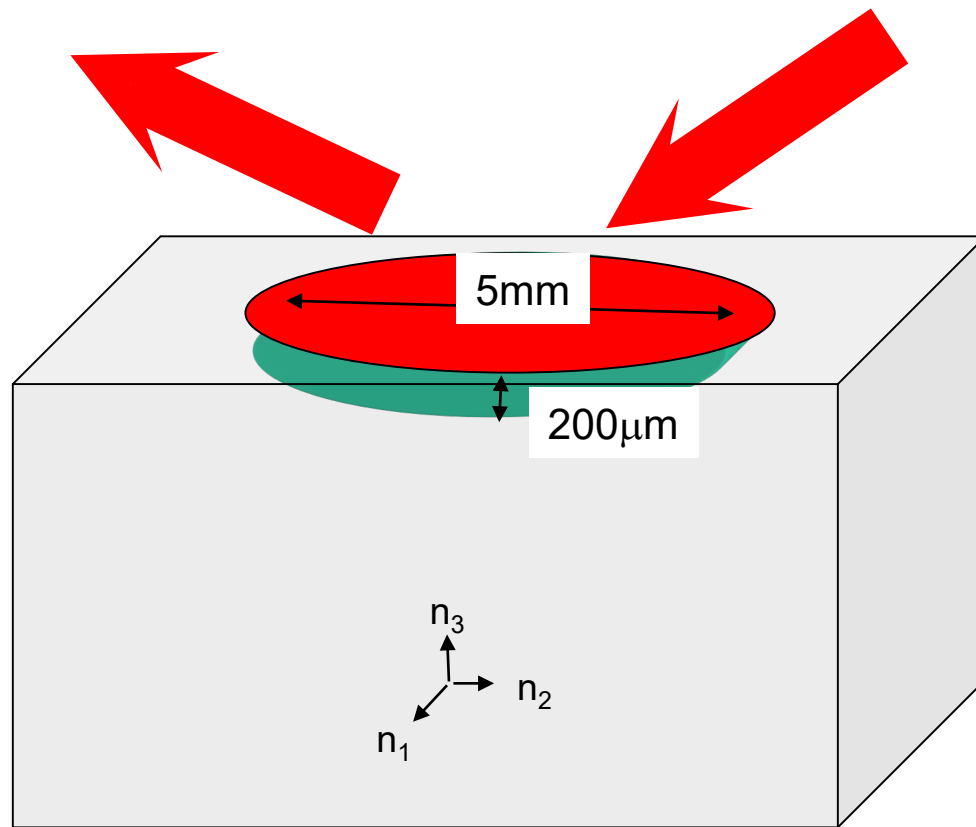
CTR Diffraction – Theory

Crystal truncation rods (CTR)



CTR Diffraction – Theory

- The sharp boundaries of a finite size (i.e. small) crystal results in intensity between Bragg peaks
- However, for a large single crystal in the Bragg geometry a better model for a surface is a semi-infinite stacking of slabs



The crystal in this geometry appears infinite in-plane, and semi-infinite along the n_3 direction

CTR Diffraction – Theory

Return to the sums and take large N_1 and N_2 and sum n_3 from 0 (the surface) to $-\infty$

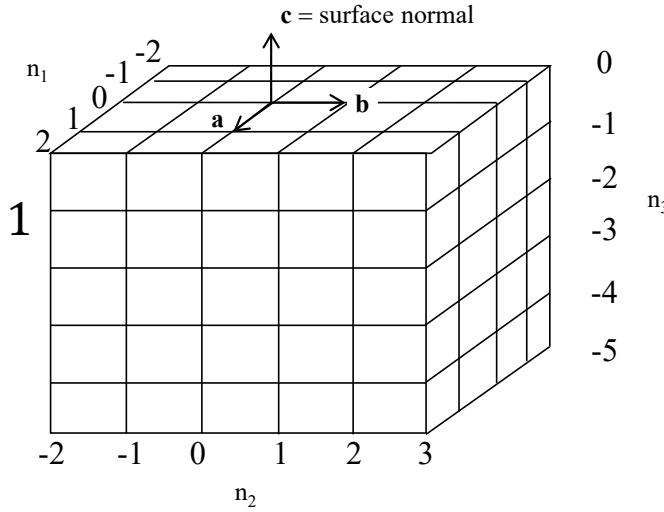
(001) surface termination

$$E \propto F_c \sum_{-(N_1-1)/2}^{(N_1-1)/2} e^{i2\pi n_1 H} \sum_{-(N_2-1)/2}^{(N_2-1)/2} e^{i2\pi n_2 K} \sum_{-\infty}^0 e^{i2\pi n_3 L}$$

$$F_{ctr} = \sum_{-\infty}^0 e^{i2\pi n_3 L} \text{ Evaluate using: } \sum_{-\infty}^0 k^{n_3} = \frac{1}{1-k}, |k| < 1$$

$$F_{ctr} = \sum_{-\infty}^0 e^{i2\pi n_3 L} = \frac{1}{(1 - e^{i2\pi L})}$$

$$|F_{ctr}|^2 = \left| \frac{1}{1 - e^{i2\pi L}} \right|^2 = \frac{1}{2 - (e^{i\pi 2L} + e^{-i\pi 2L})} = \frac{1}{2(1 - \cos(2\pi L))} = \frac{1}{4\sin^2(\pi L)}$$



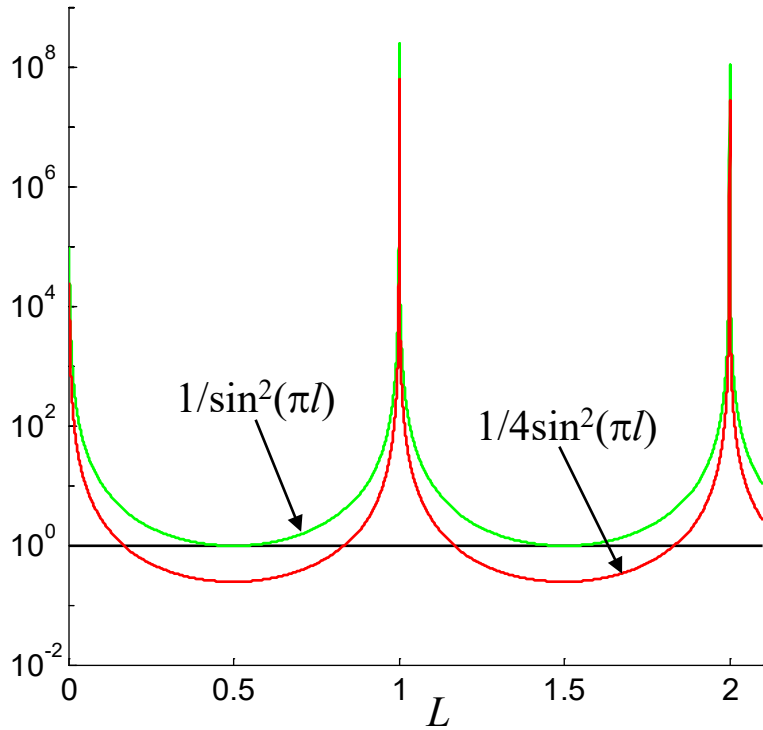
$$I \propto N_1^2 N_2^2 |F_c(HKL)|^2 |F_{ctr}(L)|^2 \quad \text{Where: } |F_{ctr}|^2 = \frac{1}{4\sin^2(\pi L)}$$



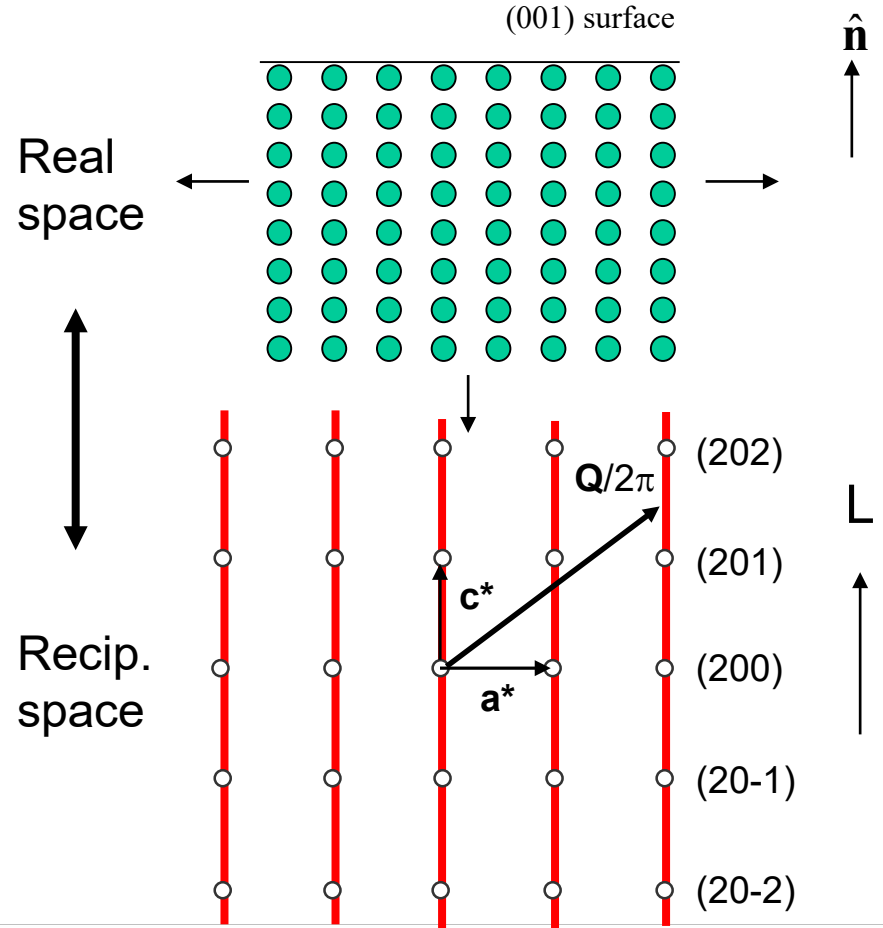
CTR Diffraction – Theory

This is the origin of the crystal truncation rod:

- For integer H and K the intensity is proportional to $N_1 \times N_2 \times F_{\text{ctr}}(L)$
- For non-integer H and K, S_1 and $S_2 \sim 0$, i.e. no sharp boundary in-plane
- Therefore, rods only occur in the direction perpendicular to the surface (n_3 direction)



F_{ctr} lower at anti-Bragg than finite xtal. because the CTR only scatters from one side of the xtal.

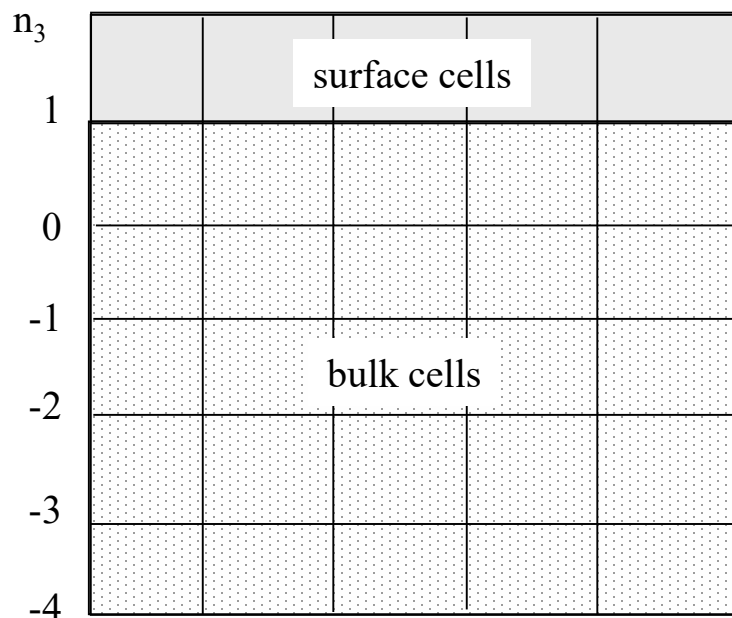


CTR Diffraction – Theory

The scattering between Bragg peaks along a CTR results from a sharp termination of the crystal, and has a well defined functional form. But what does that tell us about the interface structure?

$$I \propto N_1^2 N_2^2 |F_c(HKL)|^2 |F_{\text{CTR}}(L)|^2$$

F_c contains all the structure information (e.g. atomic coordinates). But so far we've assumed all cells are structurally equivalent. What if we add a surface cell with a different structure factor?



$$E_T = E_{\text{bulk}} + E_{\text{surf}}$$

$$E_{\text{bulk}} = N_1 N_2 F_{c, \text{bulk}}(HKL) F_{\text{CTR}}(L)$$

$$E_{\text{surf}} = N_1 N_2 F_{c, \text{surf}}(HKL) e^{i2\pi L}$$



CTR Diffraction – Theory

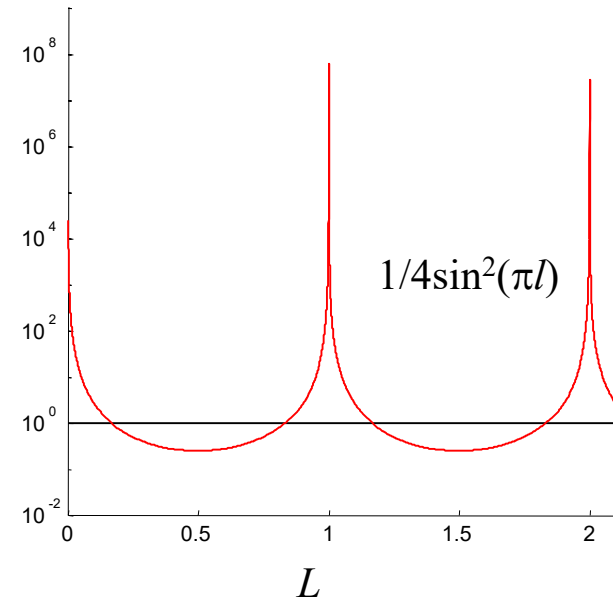
Therefore final expression:

$$I \propto N_1^2 N_2^2 \left| F_{c,bulk}(HKL) F_{ctr}(L) + F_{c,surf}(HKL) \right|^2$$

$$F_c = \sum_{j=1}^n f_j e^{i\mathbf{Q}\cdot\mathbf{r}_j} e^{-M_j} \quad \mathbf{Q}\cdot\mathbf{r}_j(xyz) = 2\pi(xH + yK + zL)$$

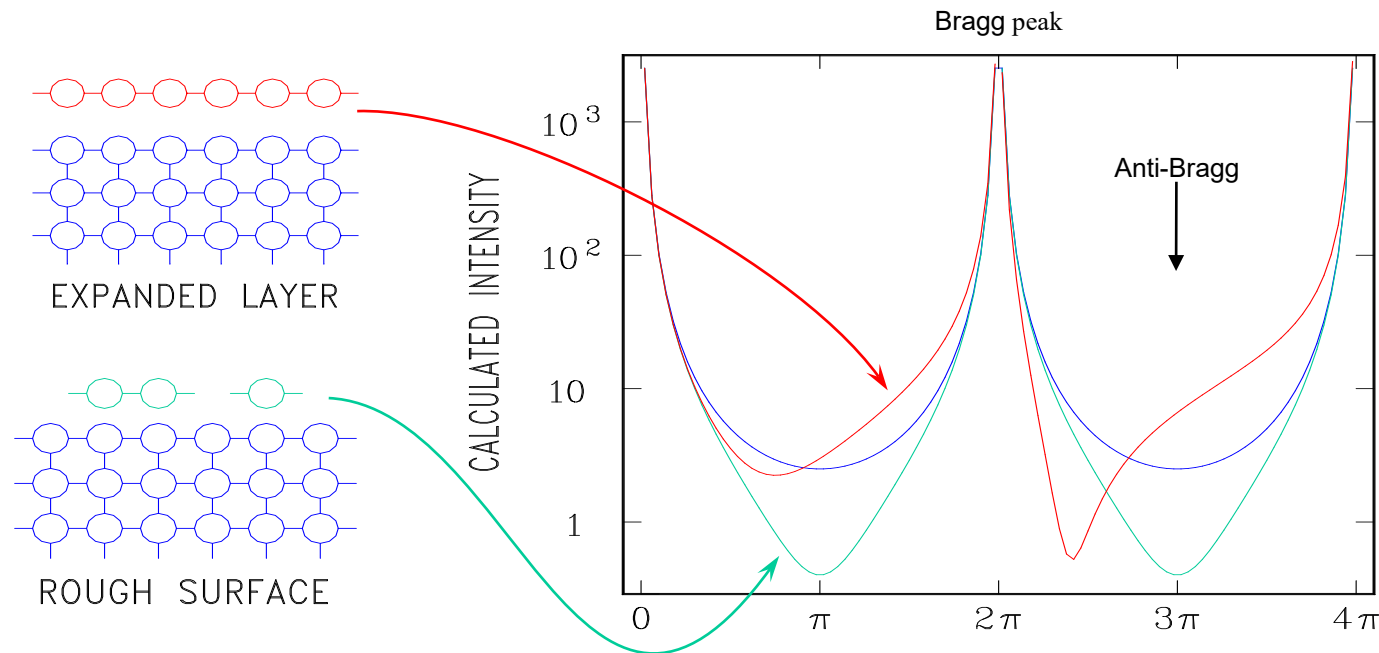
$$F_{ctr} = \sum_{-\infty}^0 e^{i2\pi n_3 L} = \frac{1}{(1 - e^{i2\pi L})}$$

- In the mid-zone between Bragg peaks $F_{CTR} \sim 1$
- Therefore the “bulk” scattering and “surface” are of similar magnitude between Bragg peaks, i.e. sensitive to **one** bulk cell (modified by F_{ctr}) and **one** surface cell I
- The “surface” and “bulk” sum in-phase or interfere if the F_{surf} , is different from the F_{bulk})
- Near Bragg peaks the surface signal is completely swamped: $I_{Bragg} / I_{CTR} > 10^6$



CTR Diffraction – Theory

Influence of surface structure:



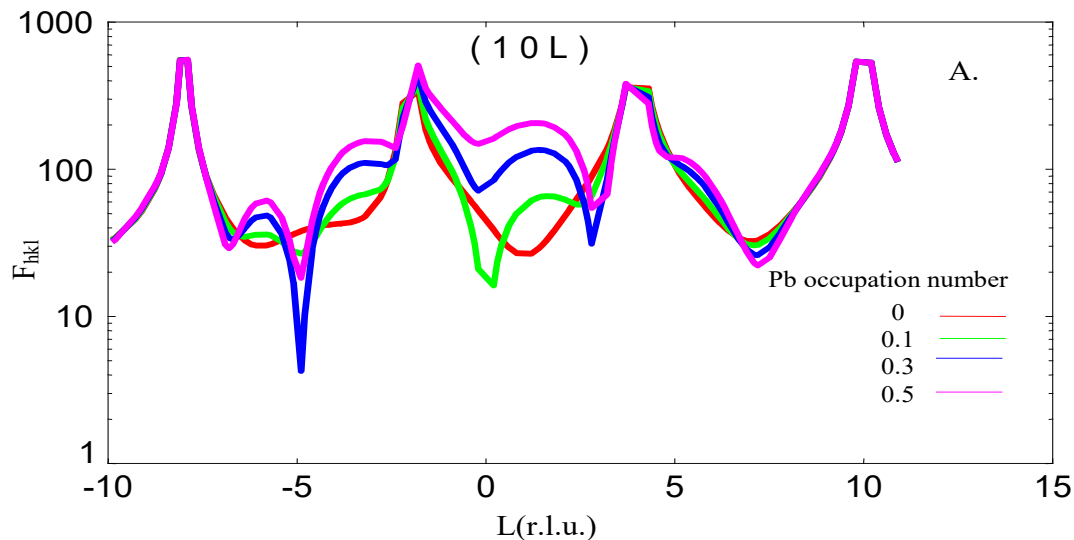
Observe several orders of magnitude intensity variation with changes in surface:

- atomic site occupancy
- relaxation (position)
- presence of adatoms
- roughness

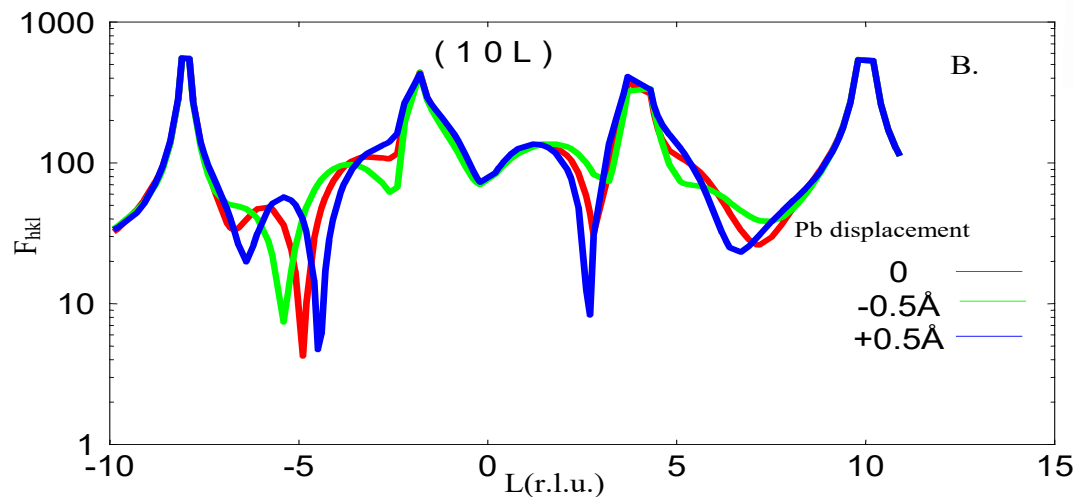


CTR Diffraction – Theory

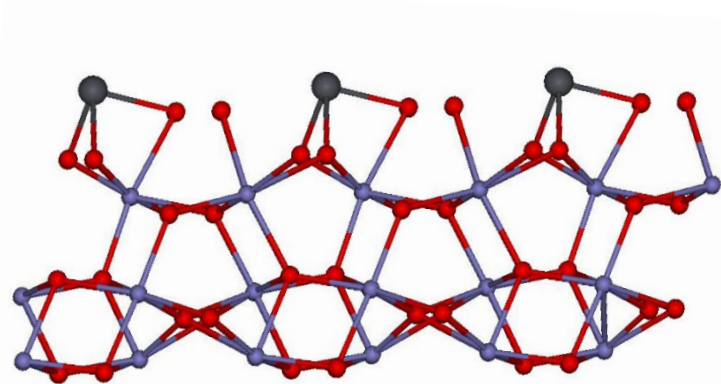
Simulations of Pb/Fe₂O₃



A. Calculations as a function of surface coverage

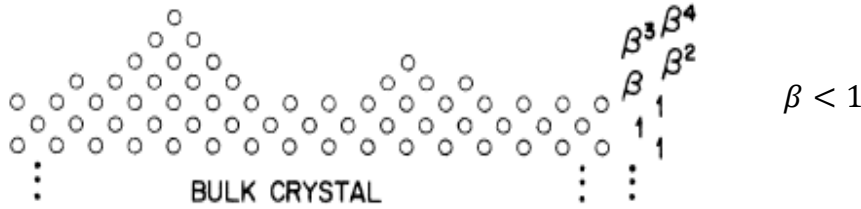


B. Calculations as a function of the z-displacement (along the c-axis), the Pb occupation number is fixed at 0.3.



CTR Diffraction – Theory

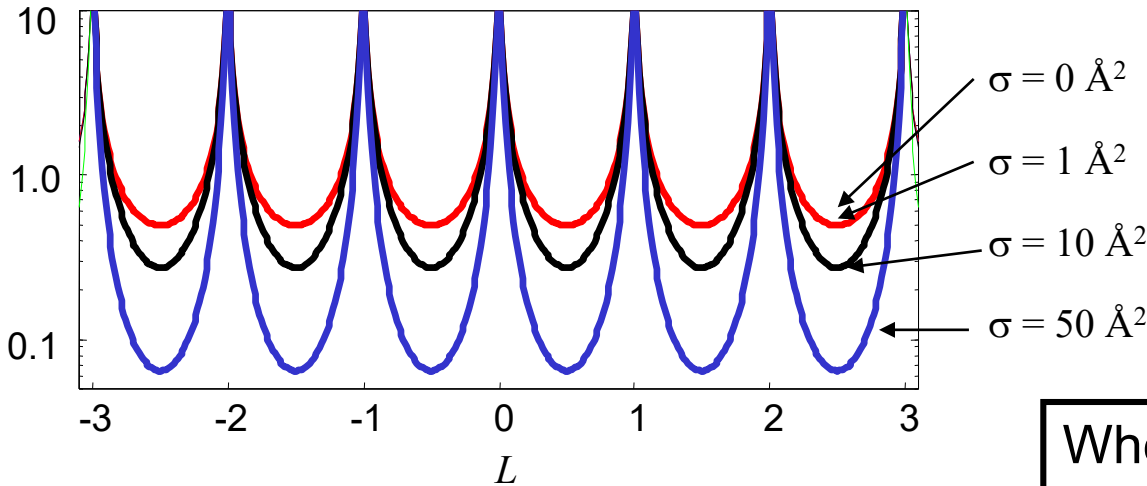
Roughness “kills” rod intensity



Robinson β model

Scattering between different height features cause destructive interference

$$|B(L)|^2 = \frac{(1 - \beta)^2}{1 - \beta^2 - 2\beta \cos(\pi L)}$$



$$\sigma_{rms} = \frac{\beta^{\frac{1}{2}}}{1 - \beta} d_{\perp}$$

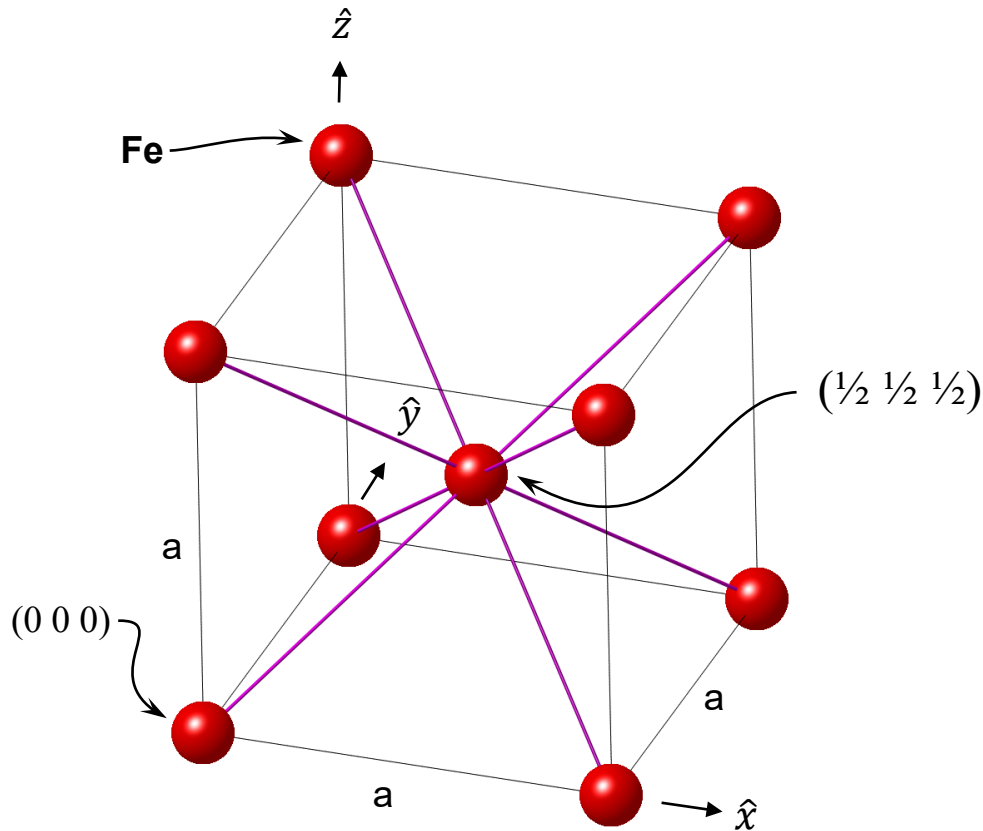
Distinguish roughness from structure because roughness is uniform decrease in intensity

When the roughness is too large the CTR is no longer measurable above background!

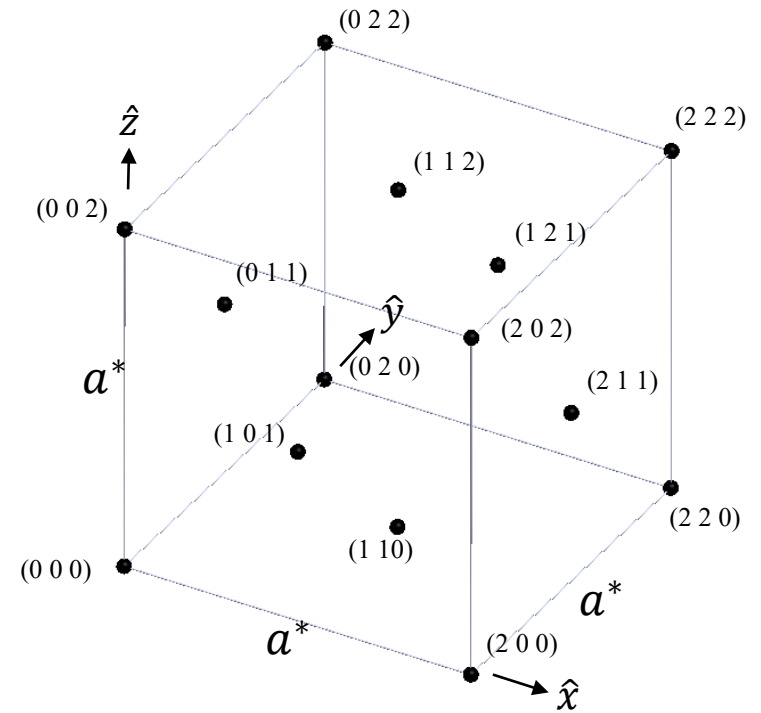


CTR Diffraction – Theory

Real Space (BCC)

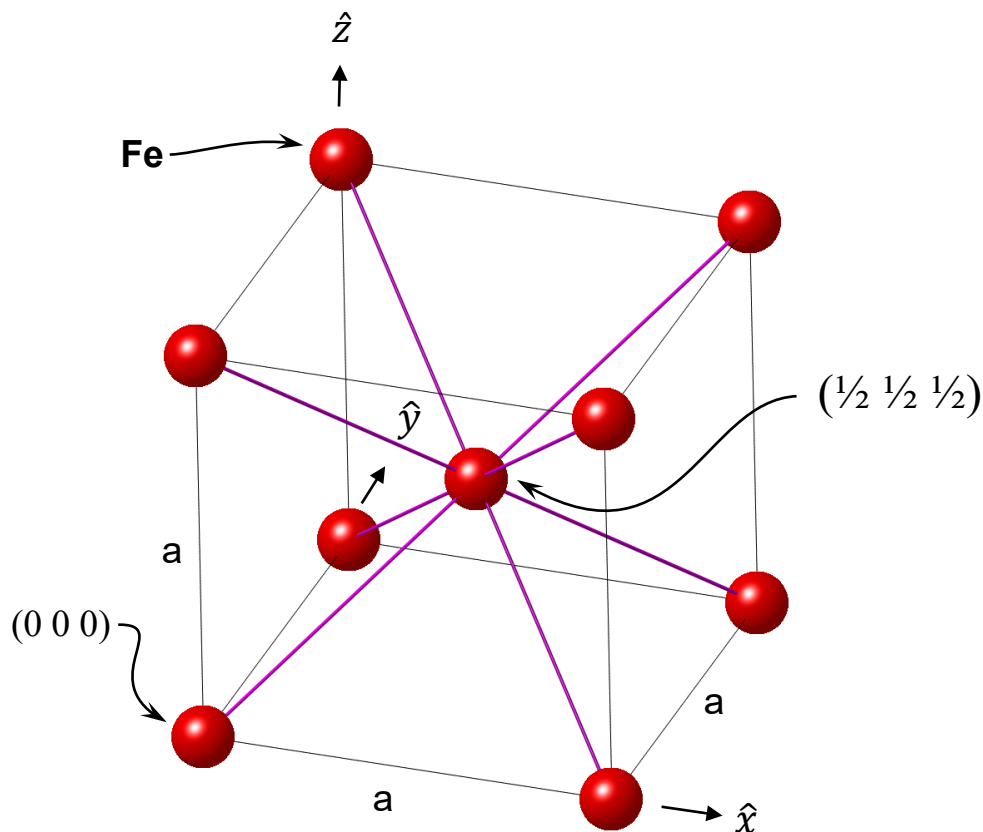


Reciprocal Space (FCC)

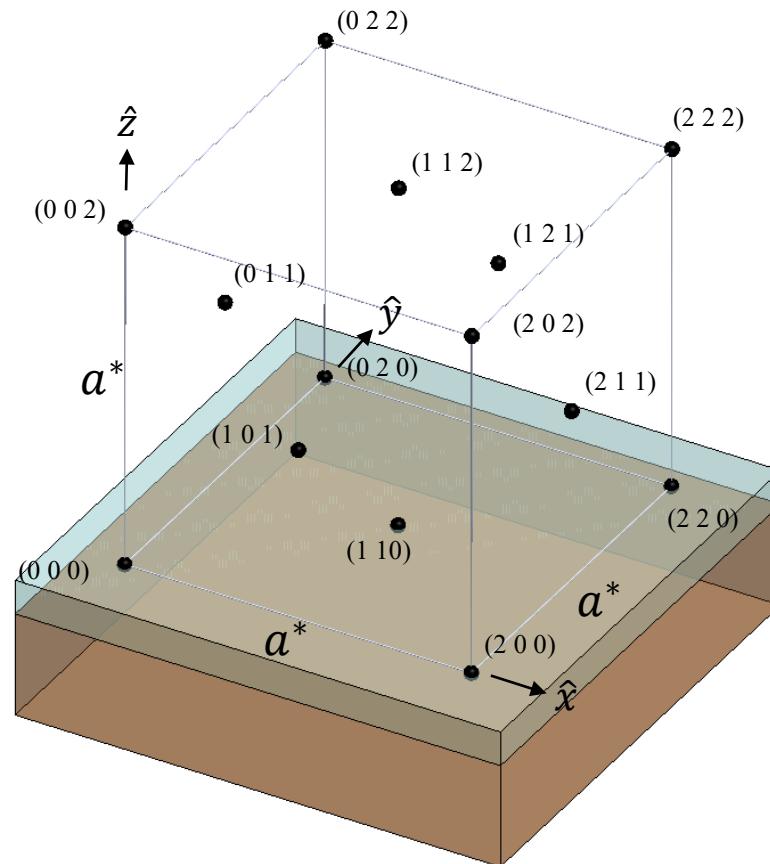


CTR Diffraction – Theory

Real Space (BCC)

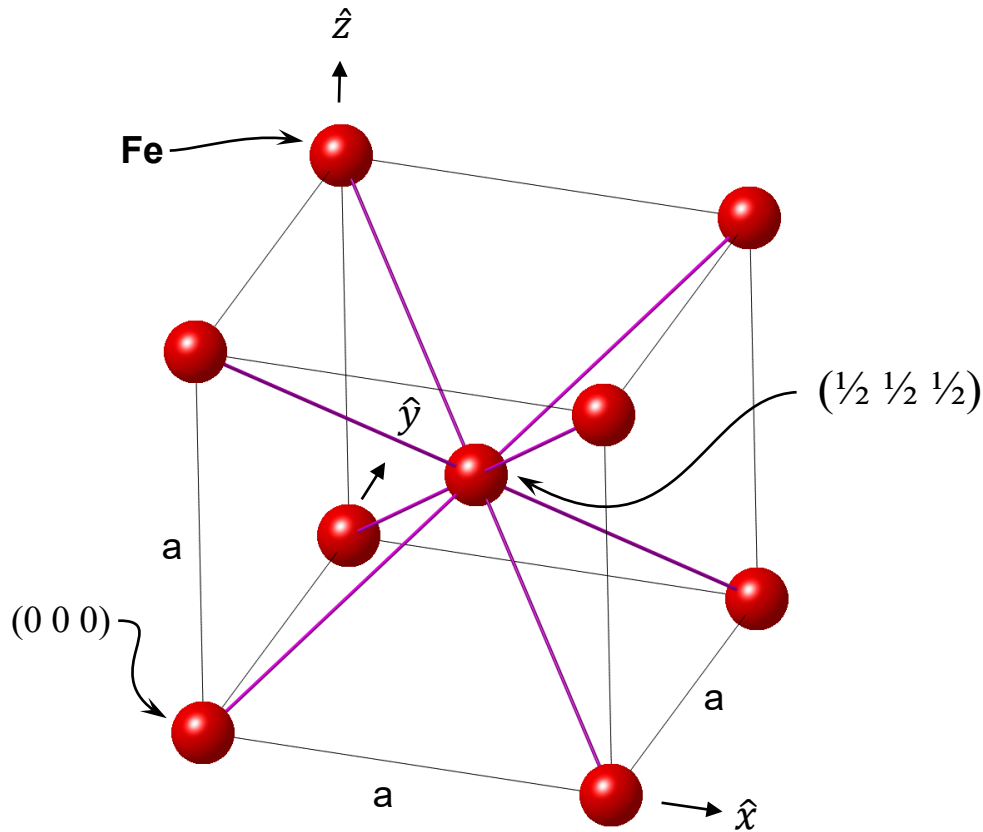


Reciprocal Space (FCC)
With a surface

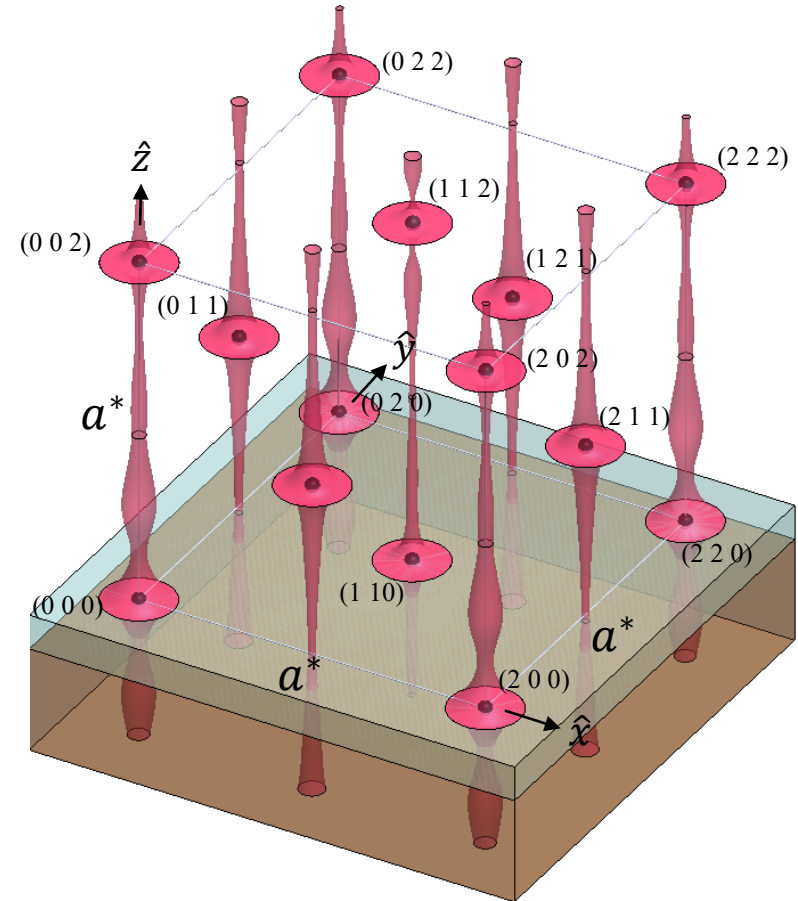


CTR Diffraction – Theory

Real Space (BCC)

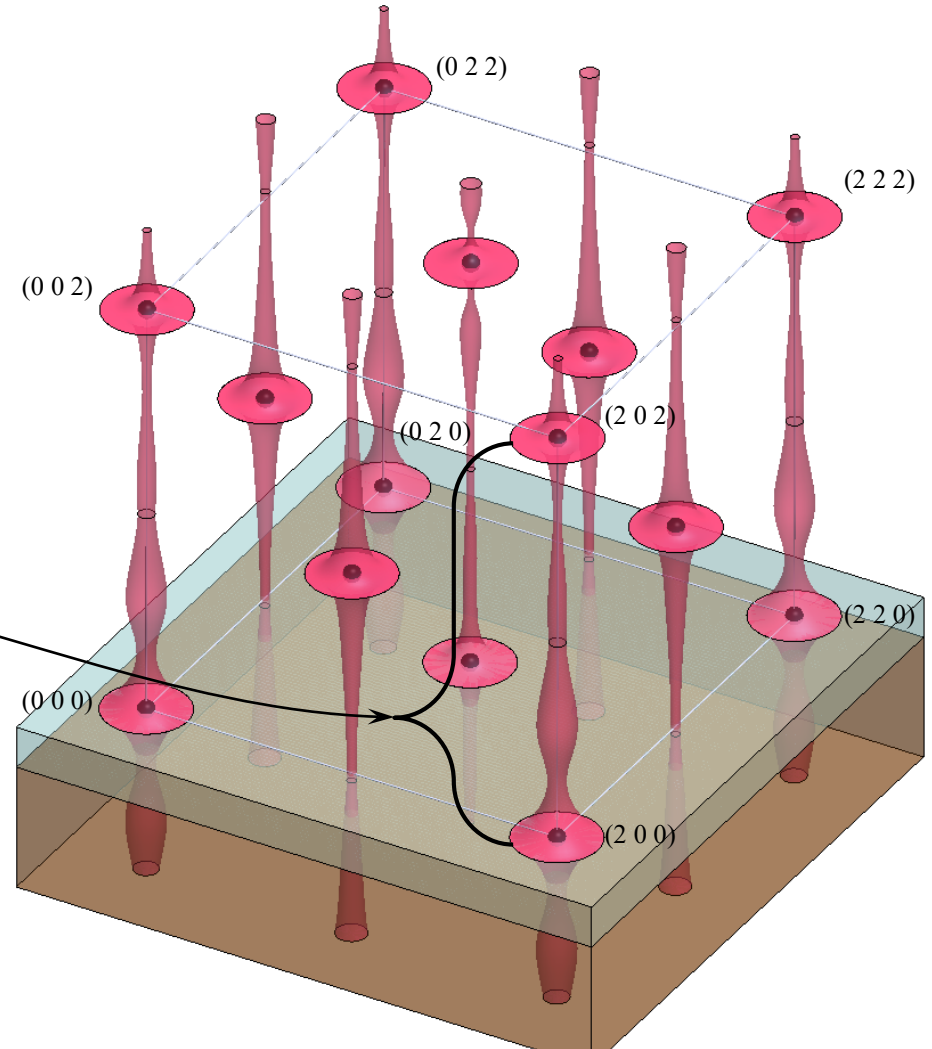
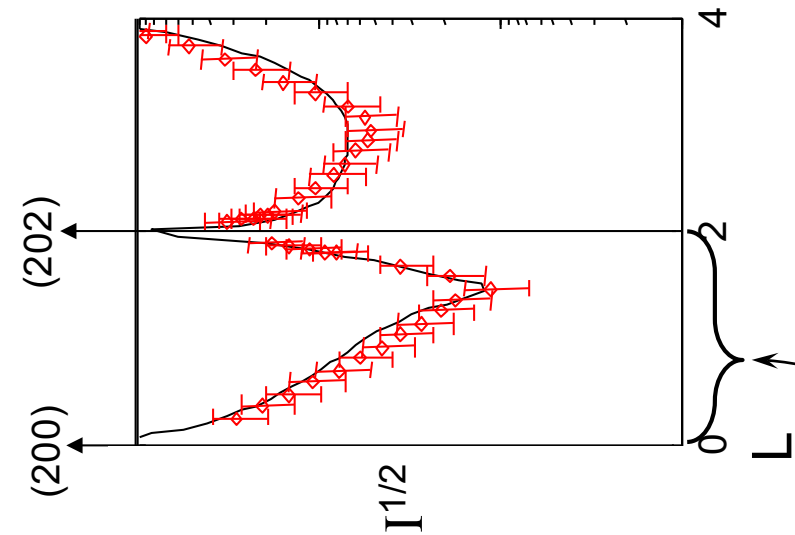


Reciprocal Space (FCC)
With a (001) Surface



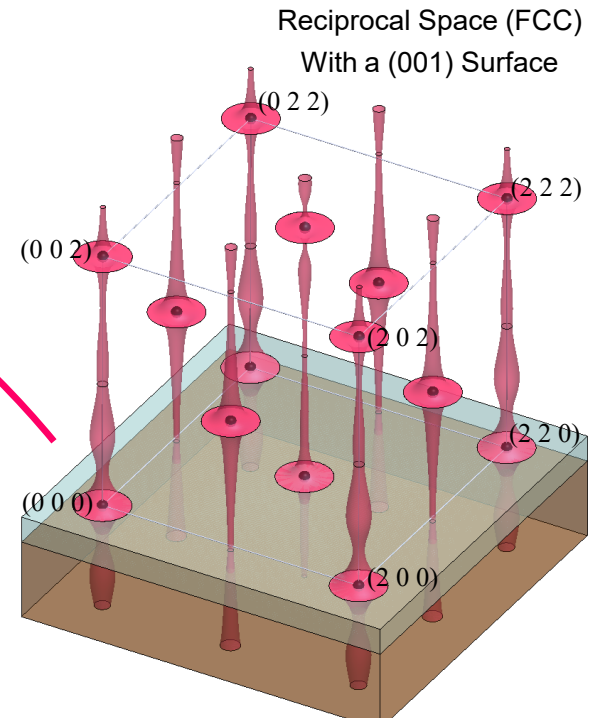
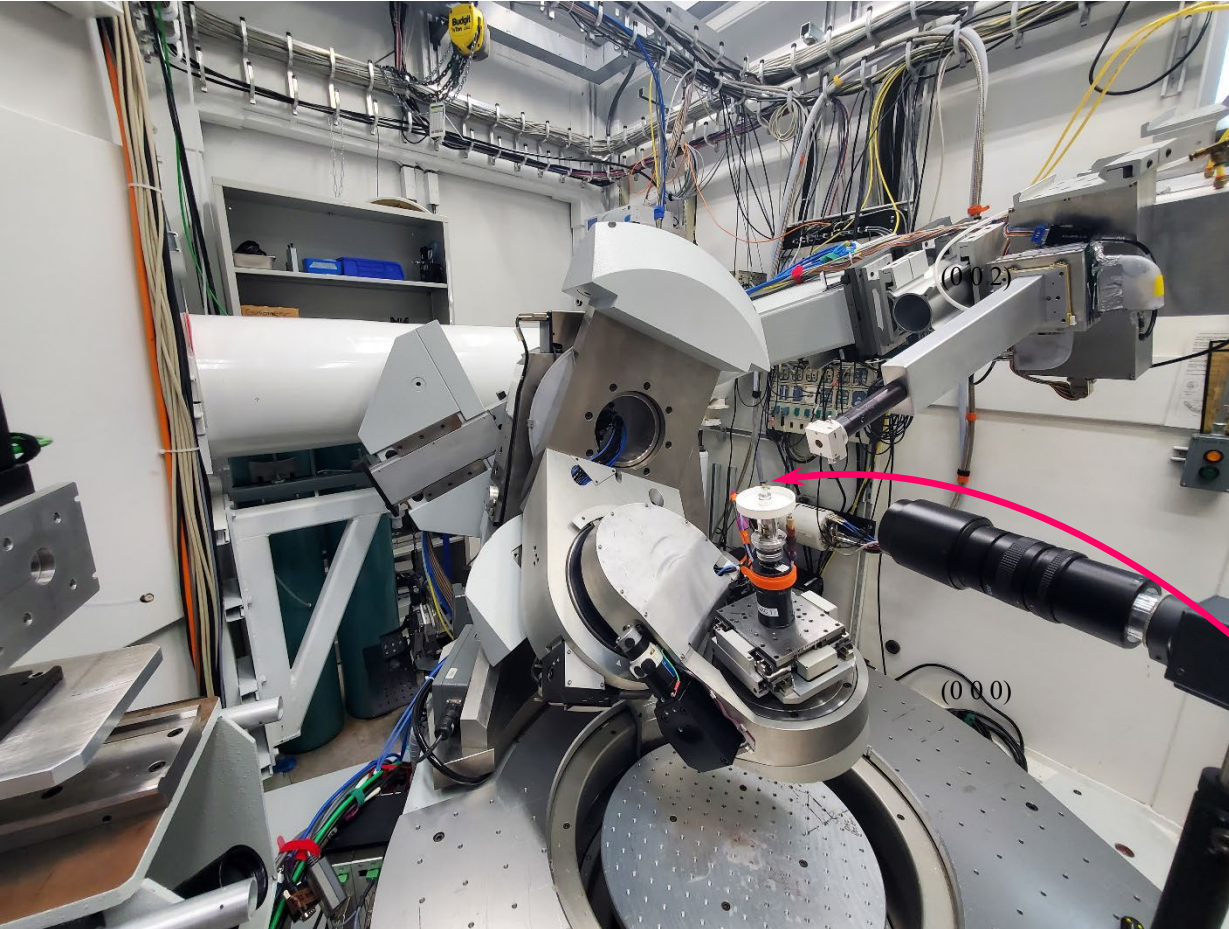
CTR Diffraction – Theory

Reciprocal Space (FCC)
With a (001) Surface

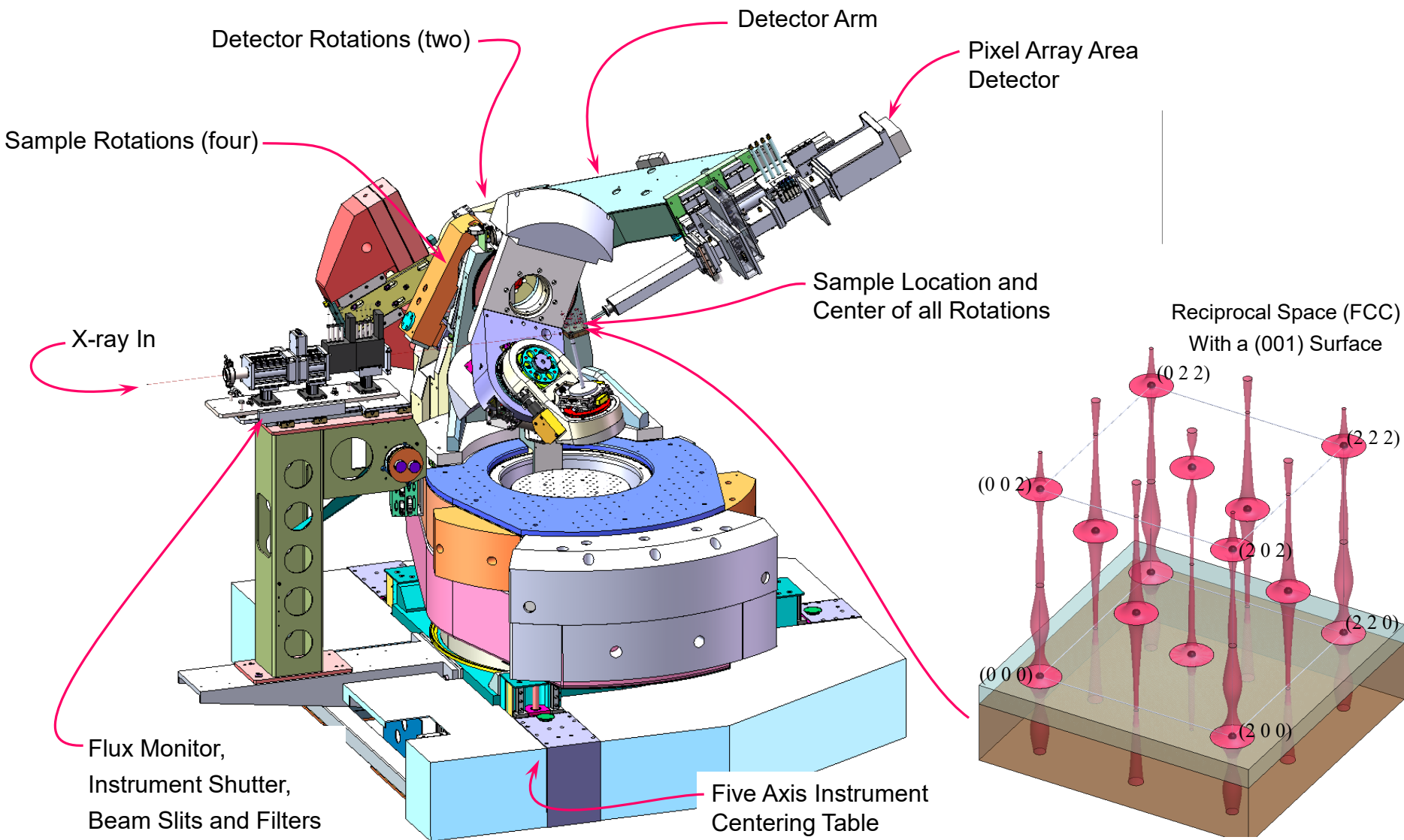


CTR Diffraction – On the Instrumentation

GSECARS 13BMC Diffractometer



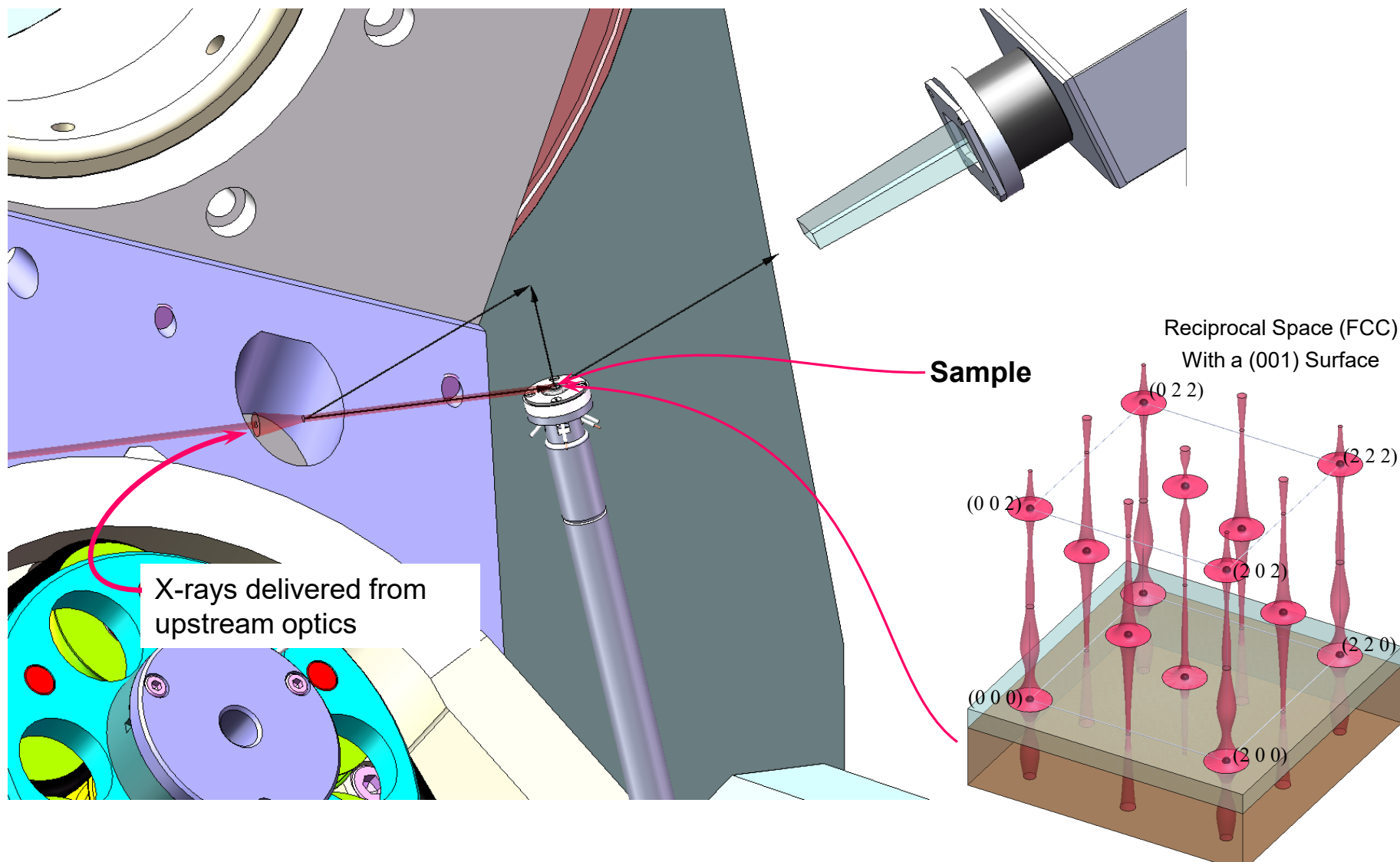
CTR Diffraction – On the Instrumentation



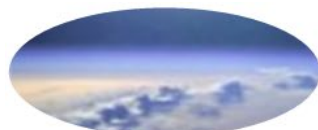
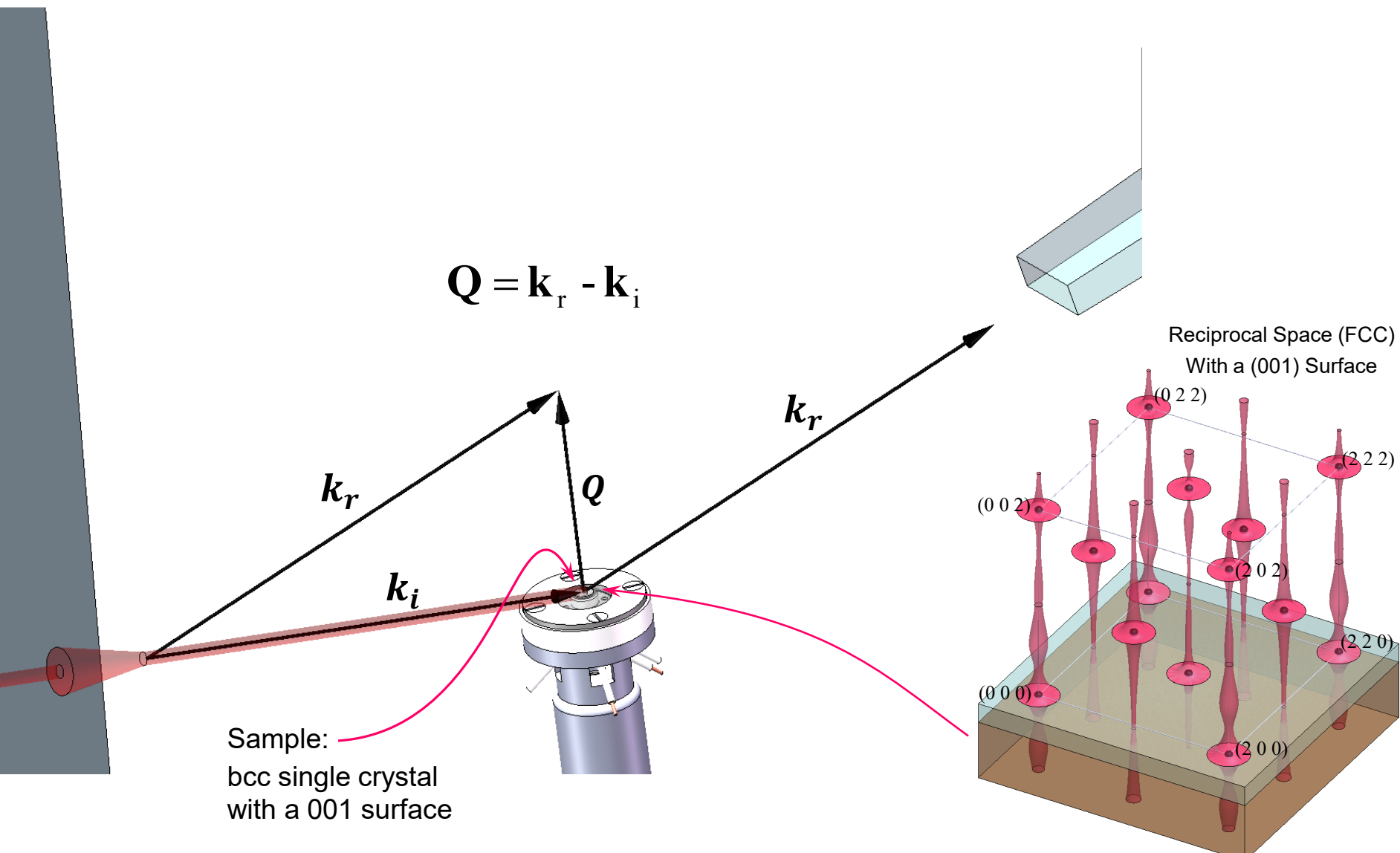
GeoSoilEnviroCARS 24th National School on Neutron and X-Ray Scattering

July 21st, 2022 Peter J. Eng

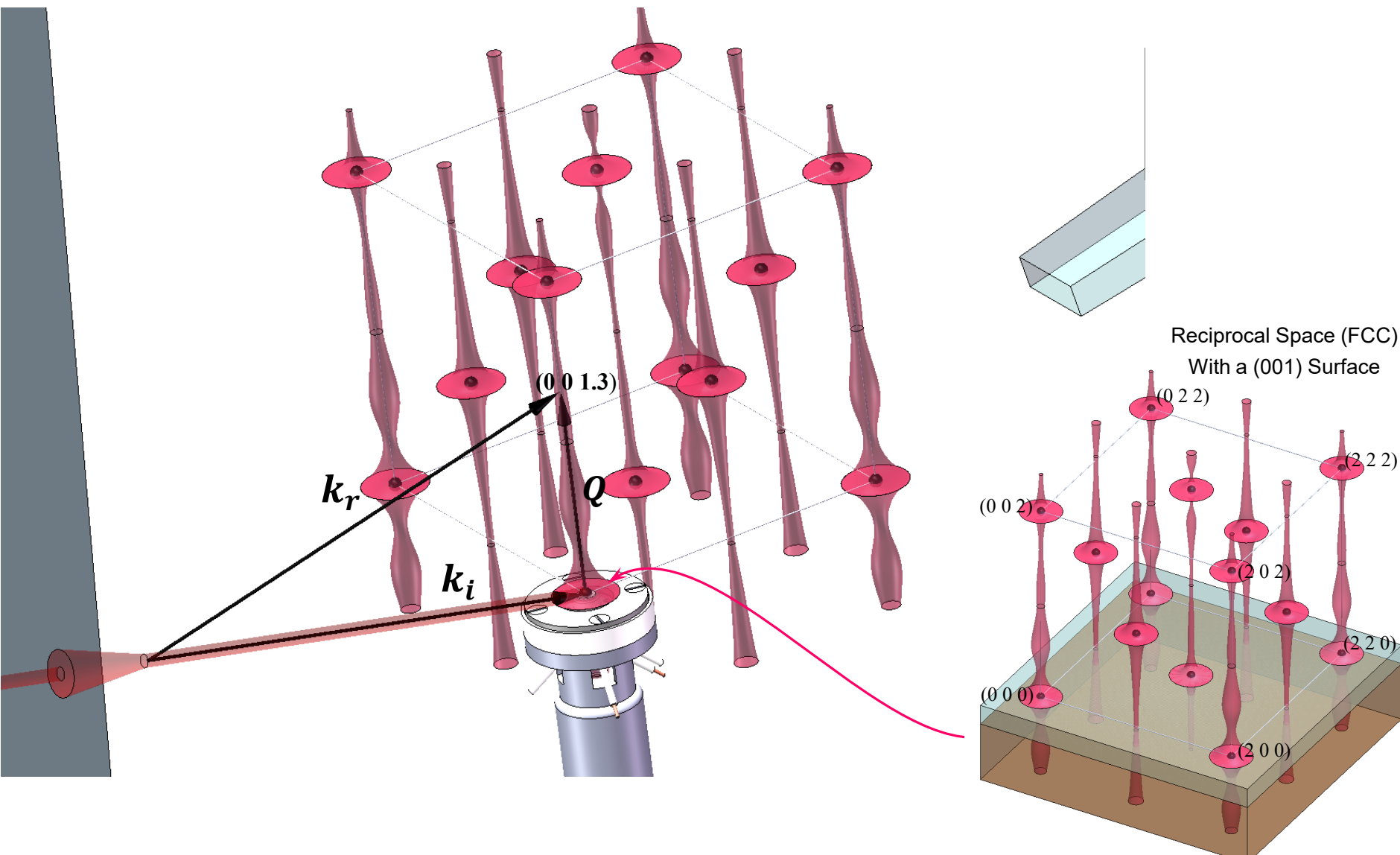
CTR Diffraction – On the Instrumentation



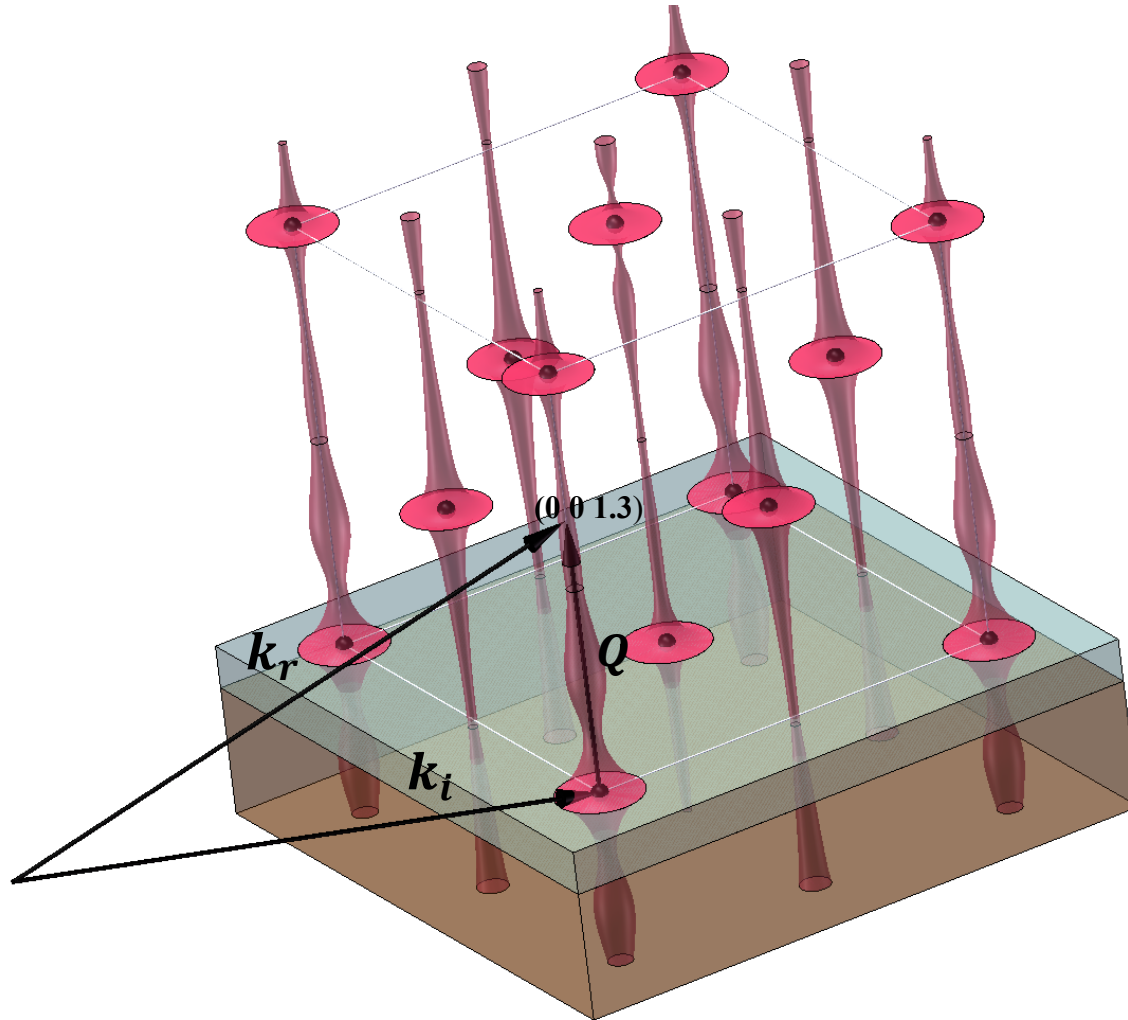
CTR Diffraction – On the Instrumentation



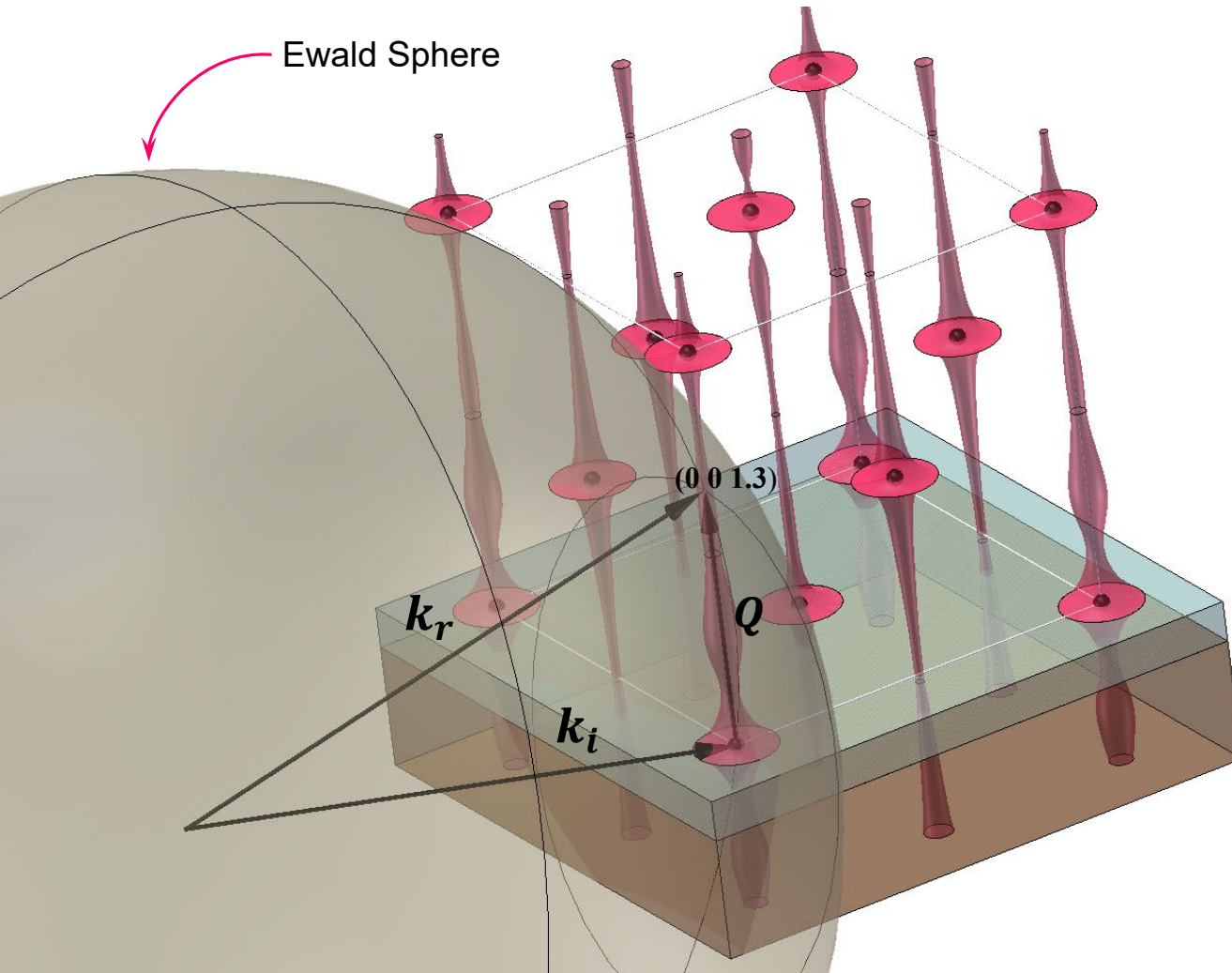
CTR Diffraction – On the Instrumentation



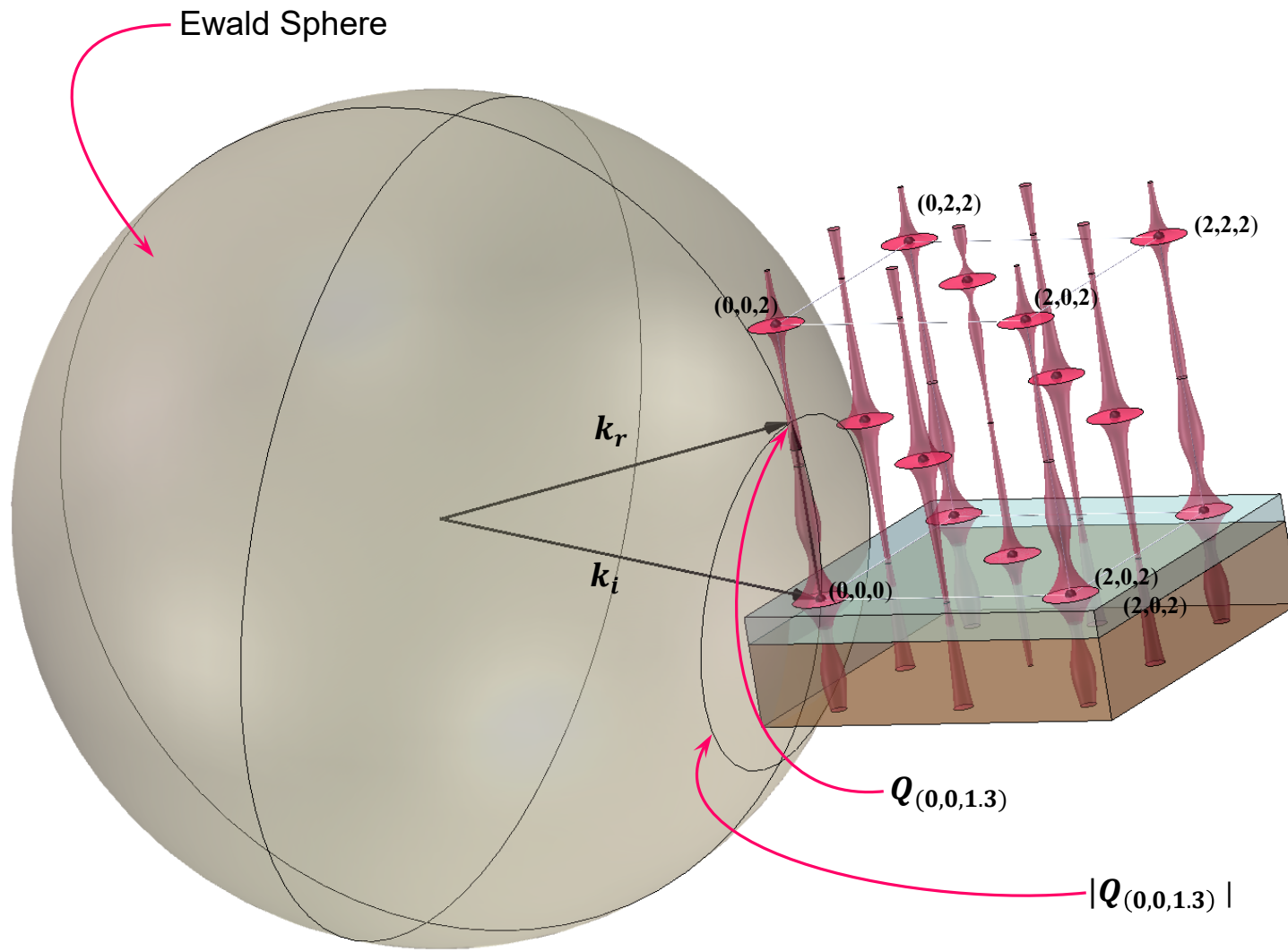
CTR Diffraction – Measurement



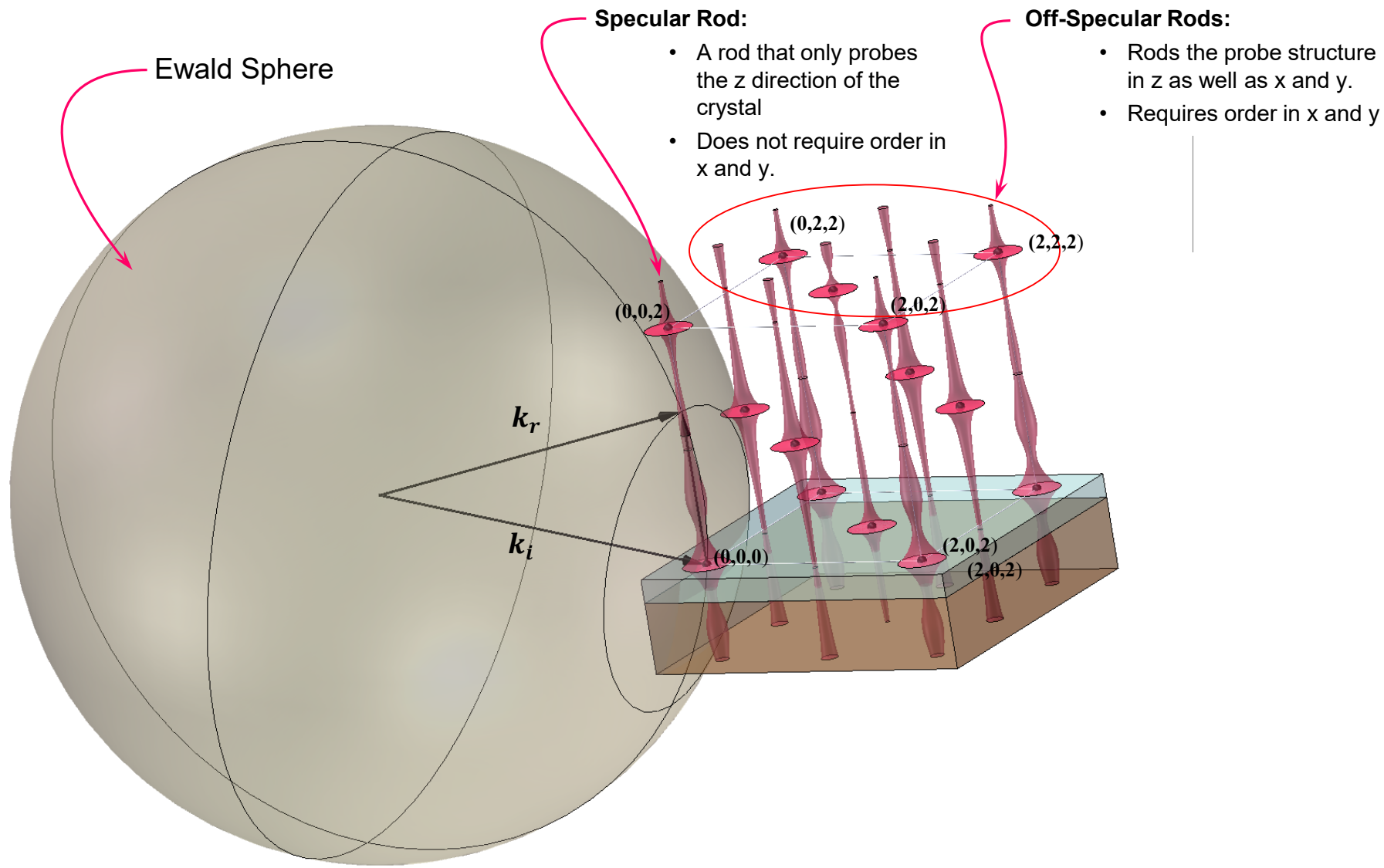
CTR Diffraction – Measurement



CTR Diffraction – Measurement

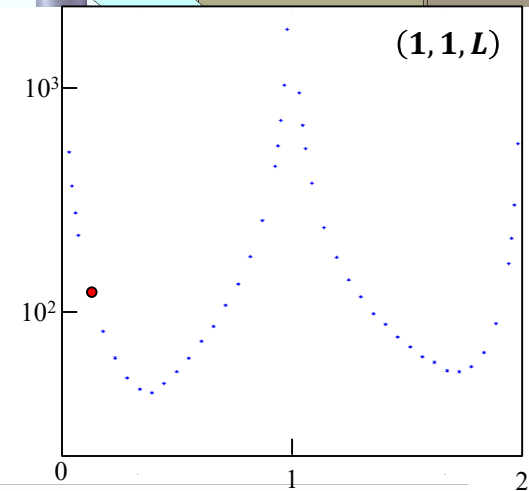
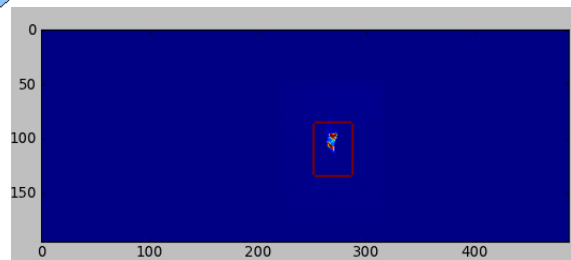
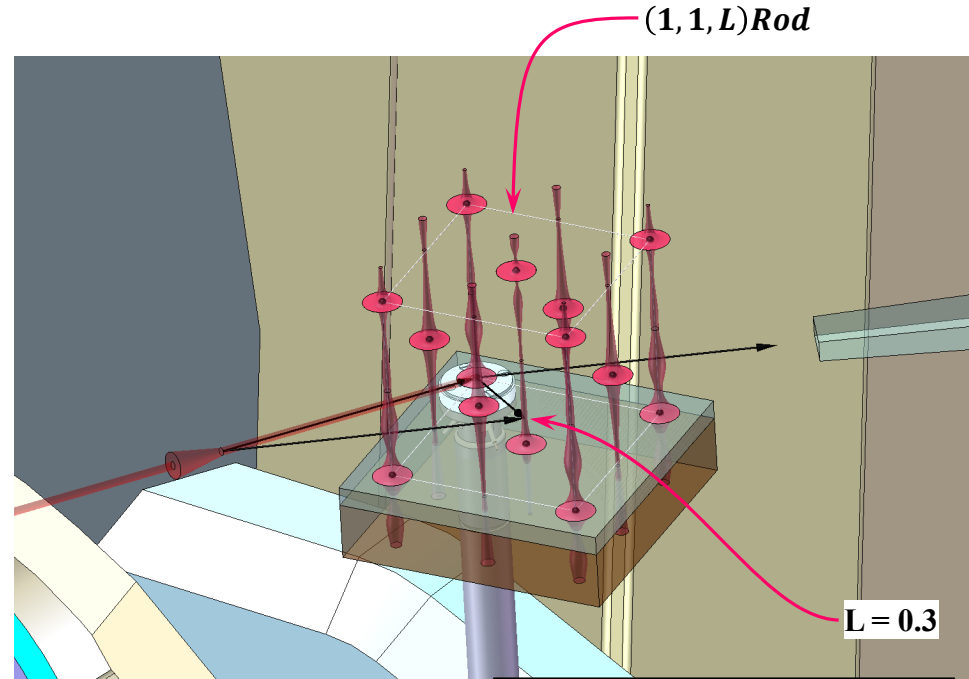
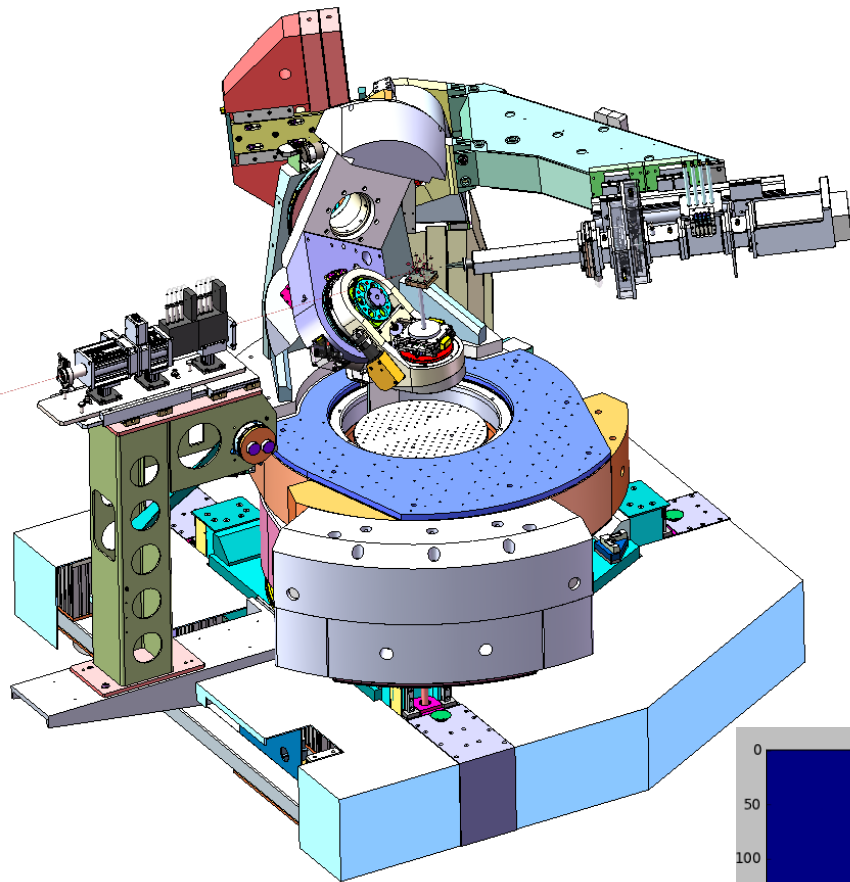


CTR Diffraction – Measurement



CTR Diffraction – Measurement– Off Specular Rod

$L = 0.3$

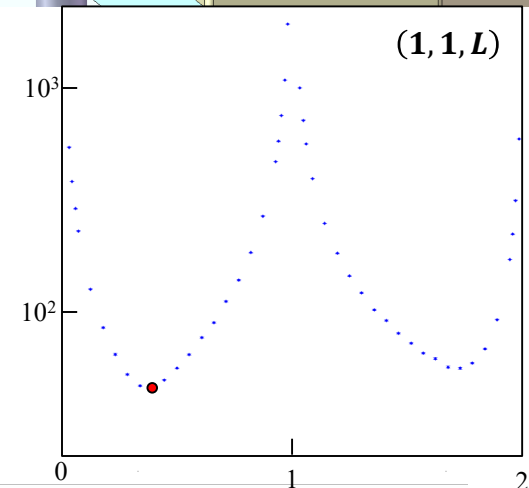
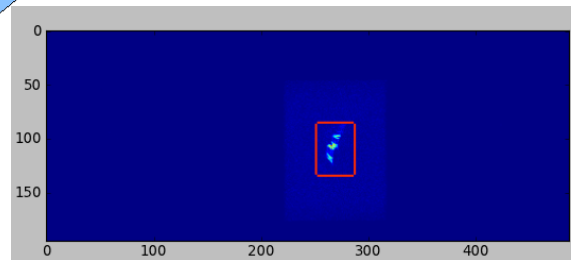
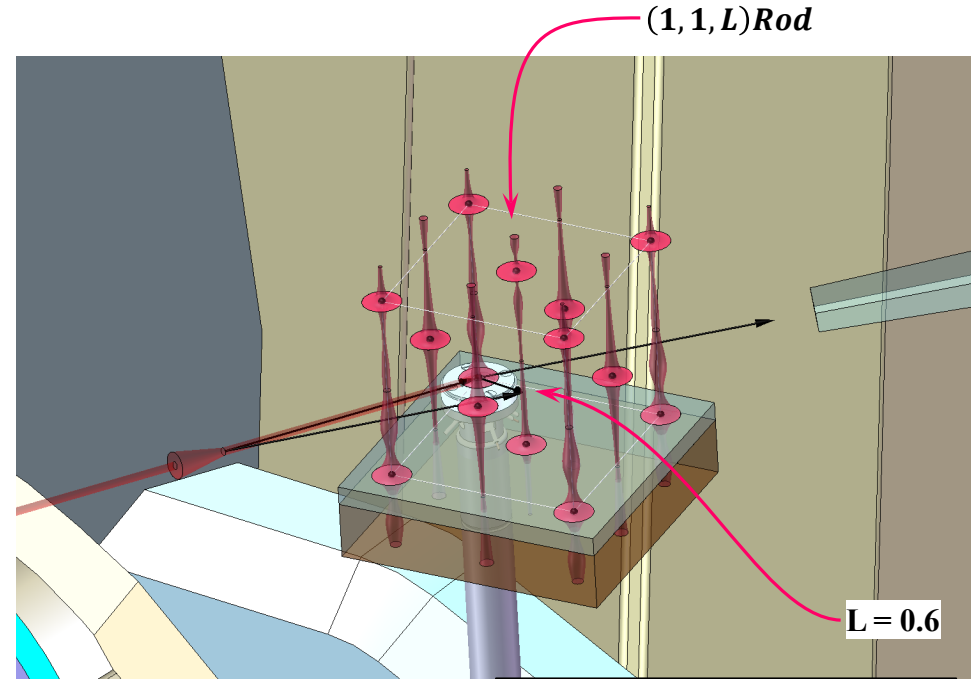
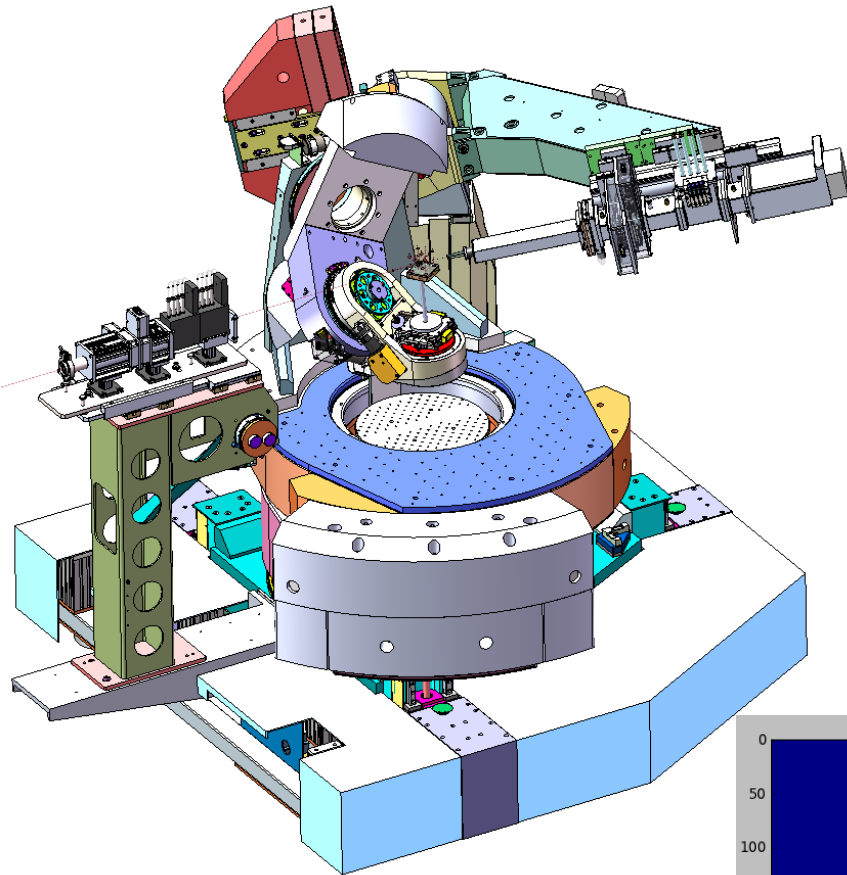


GeoSoilEnviroCARS 24th National School on Neutron and X-Ray Scattering

July 21st, 2022 Peter J. Eng

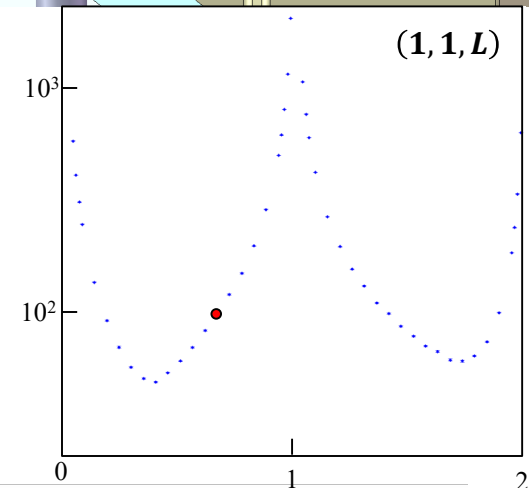
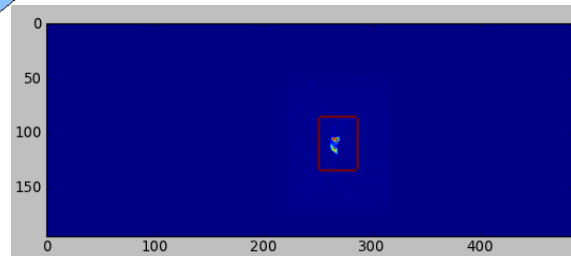
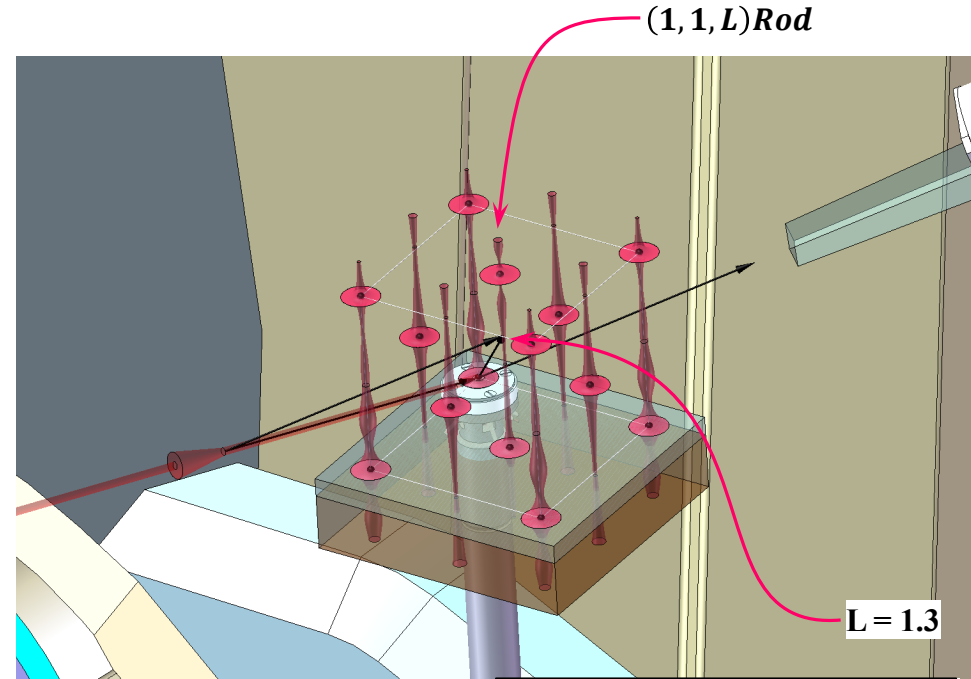
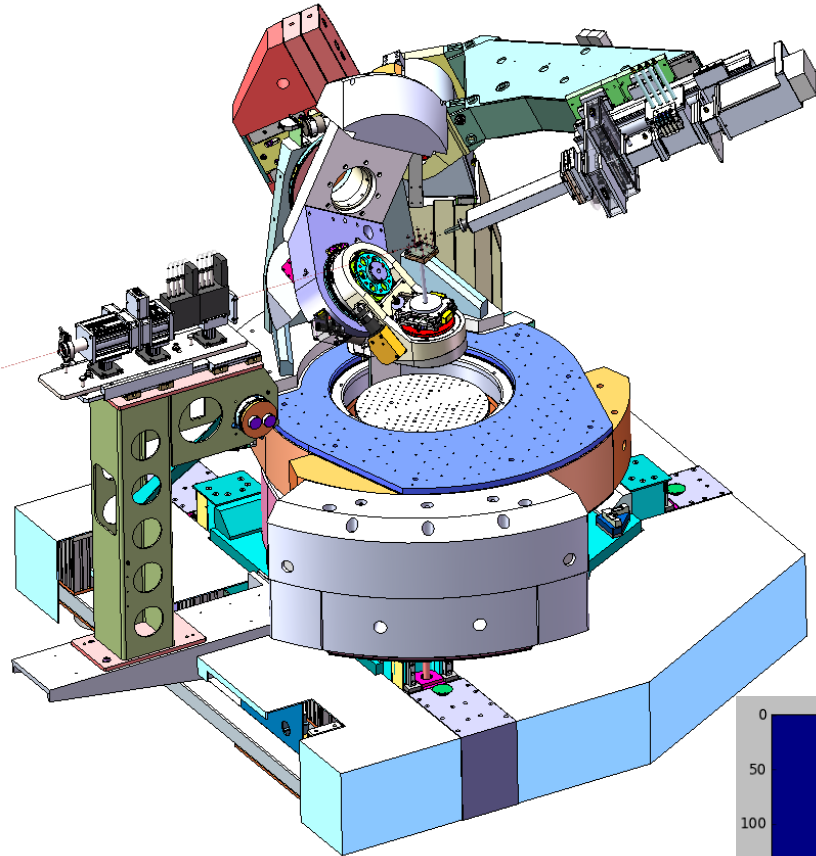
CTR Diffraction – Measurement– Off Specular Rod

$L = 0.6$



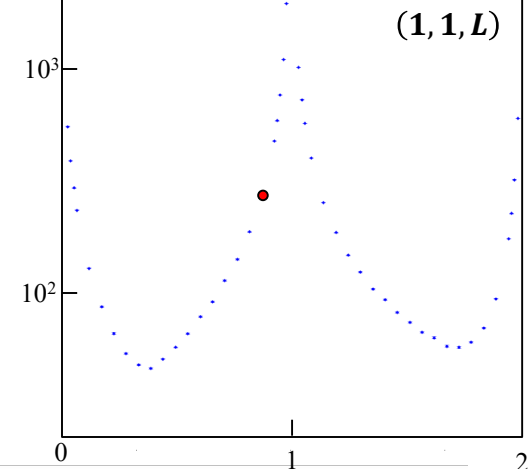
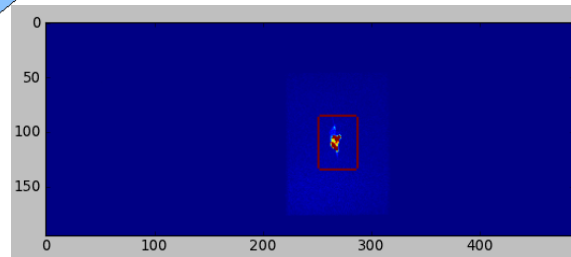
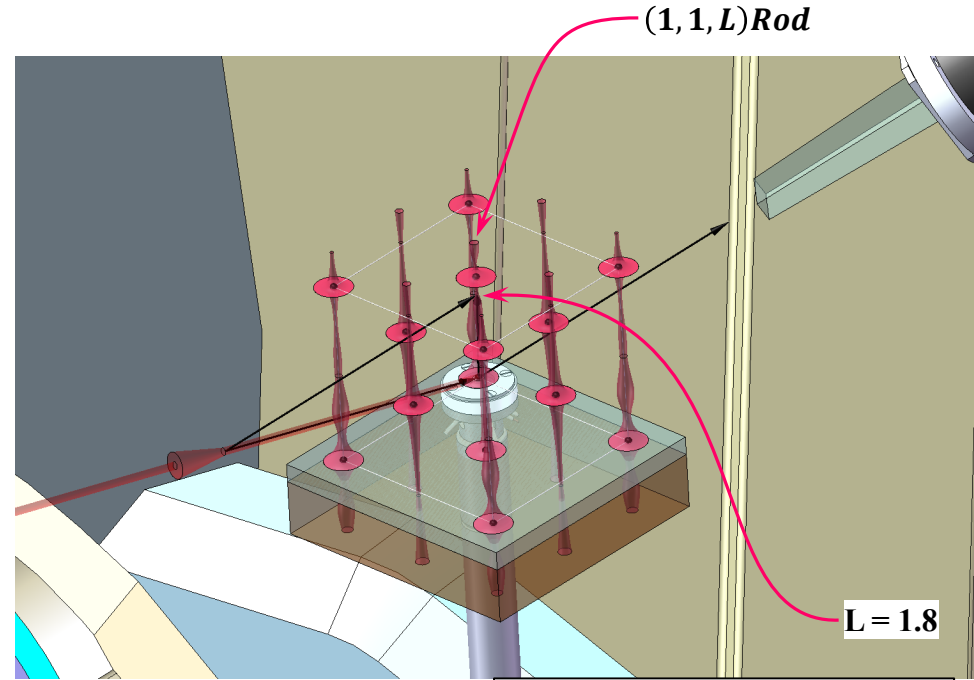
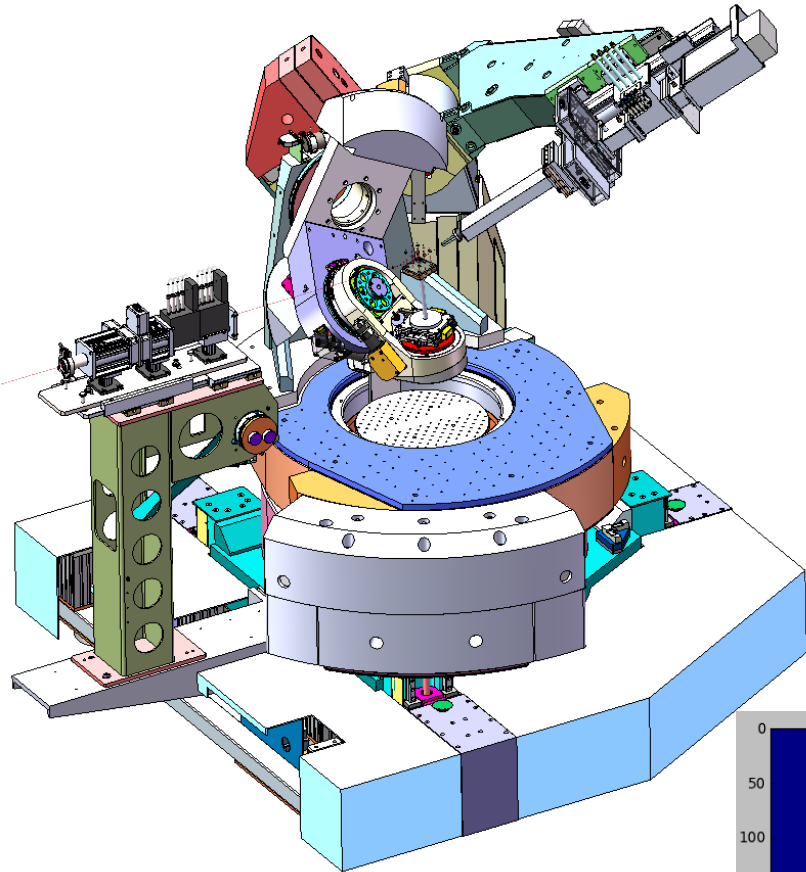
CTR Diffraction – Measurement– Off Specular Rod

$L = 1.3$

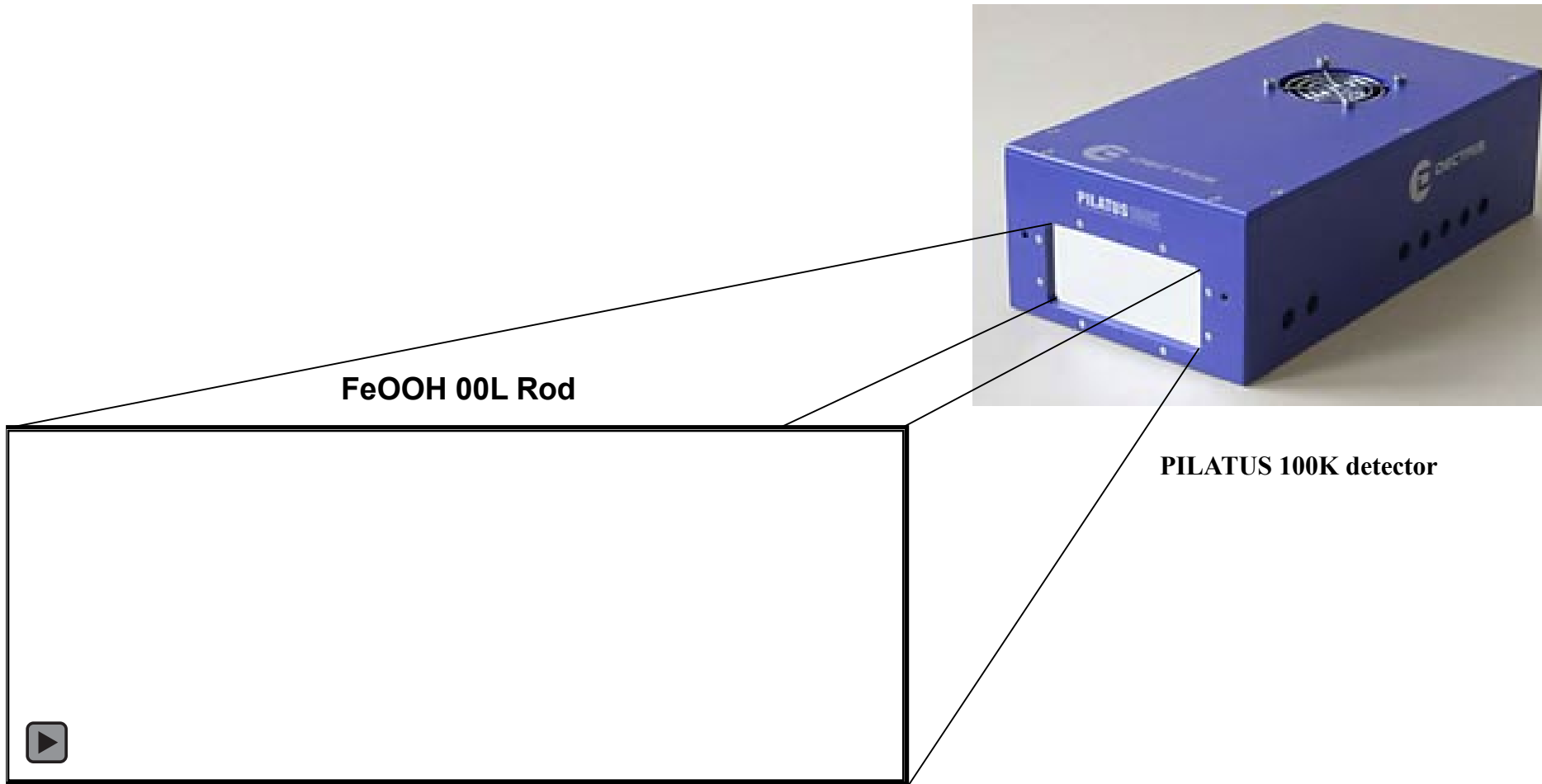


CTR Diffraction – Measurement– Off Specular Rod

$L = 1.8$



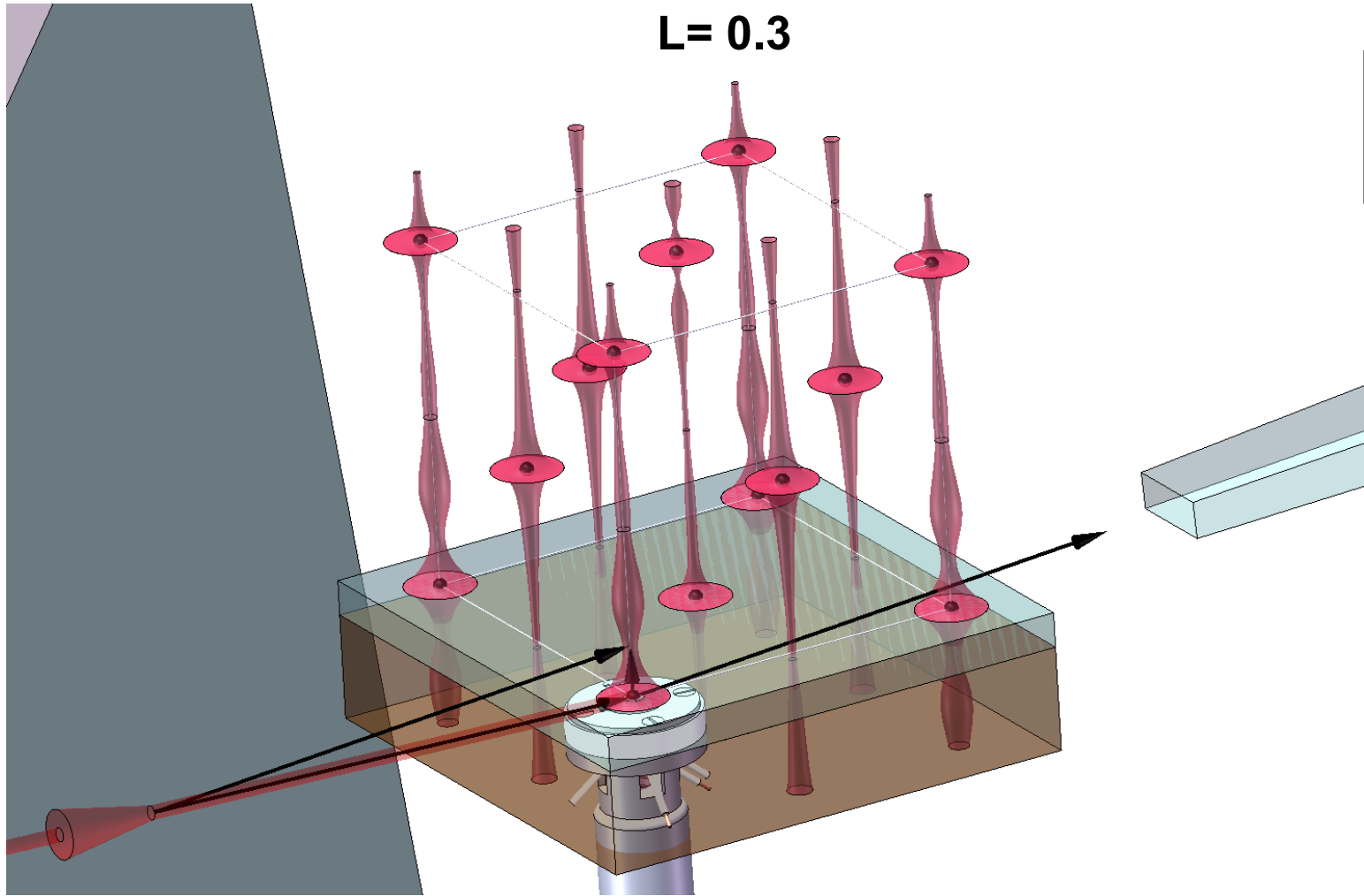
CTR Diffraction – Measurement – Pixel Array Detector



CTR Diffraction – Measurement – Specular Rod

$(0, 0, L)$ or (Specular)Rod

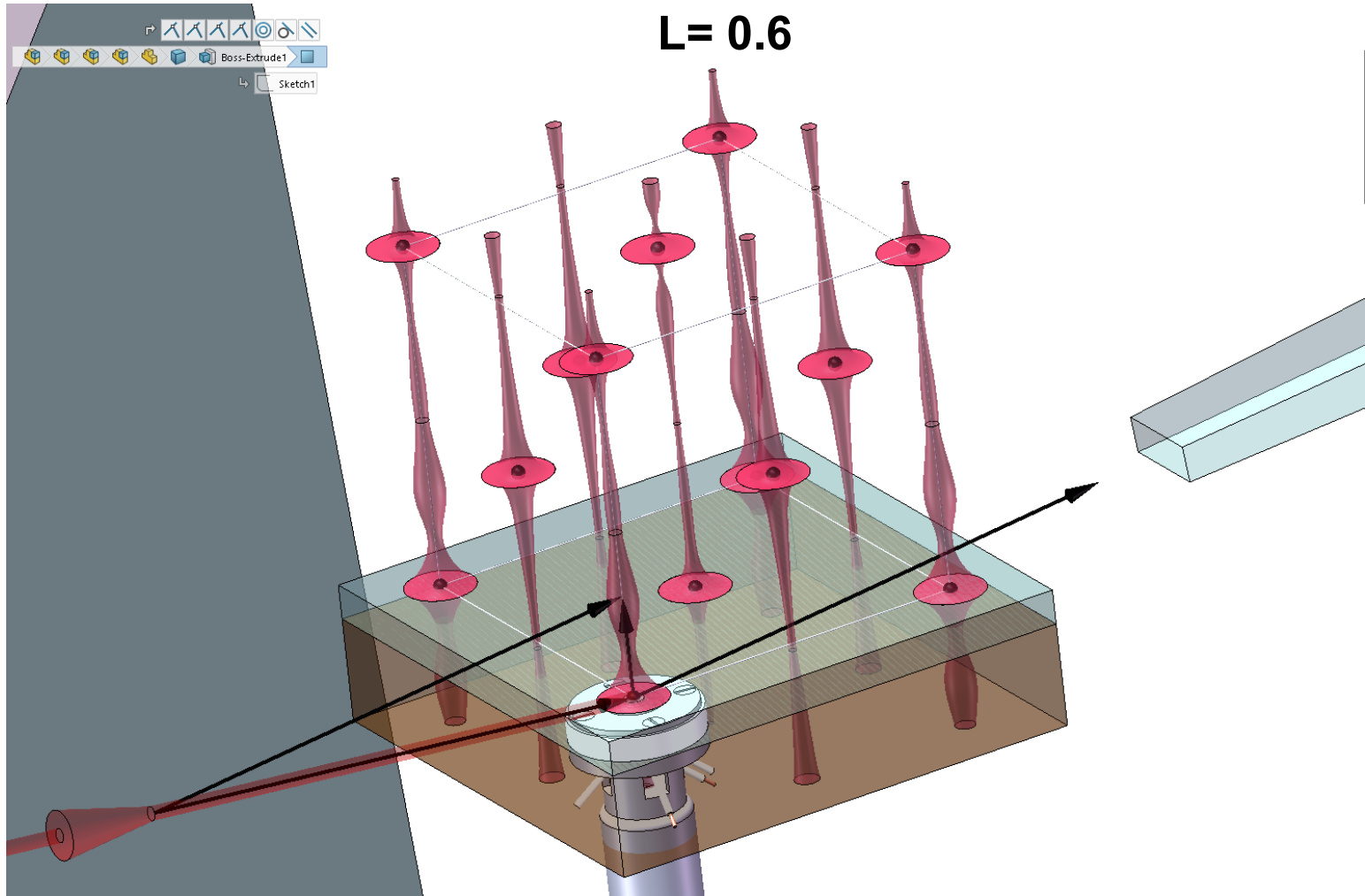
$L = 0.3$



CTR Diffraction – Measurement – Specular Rod

$(0, 0, L)$ or (Specular)Rod

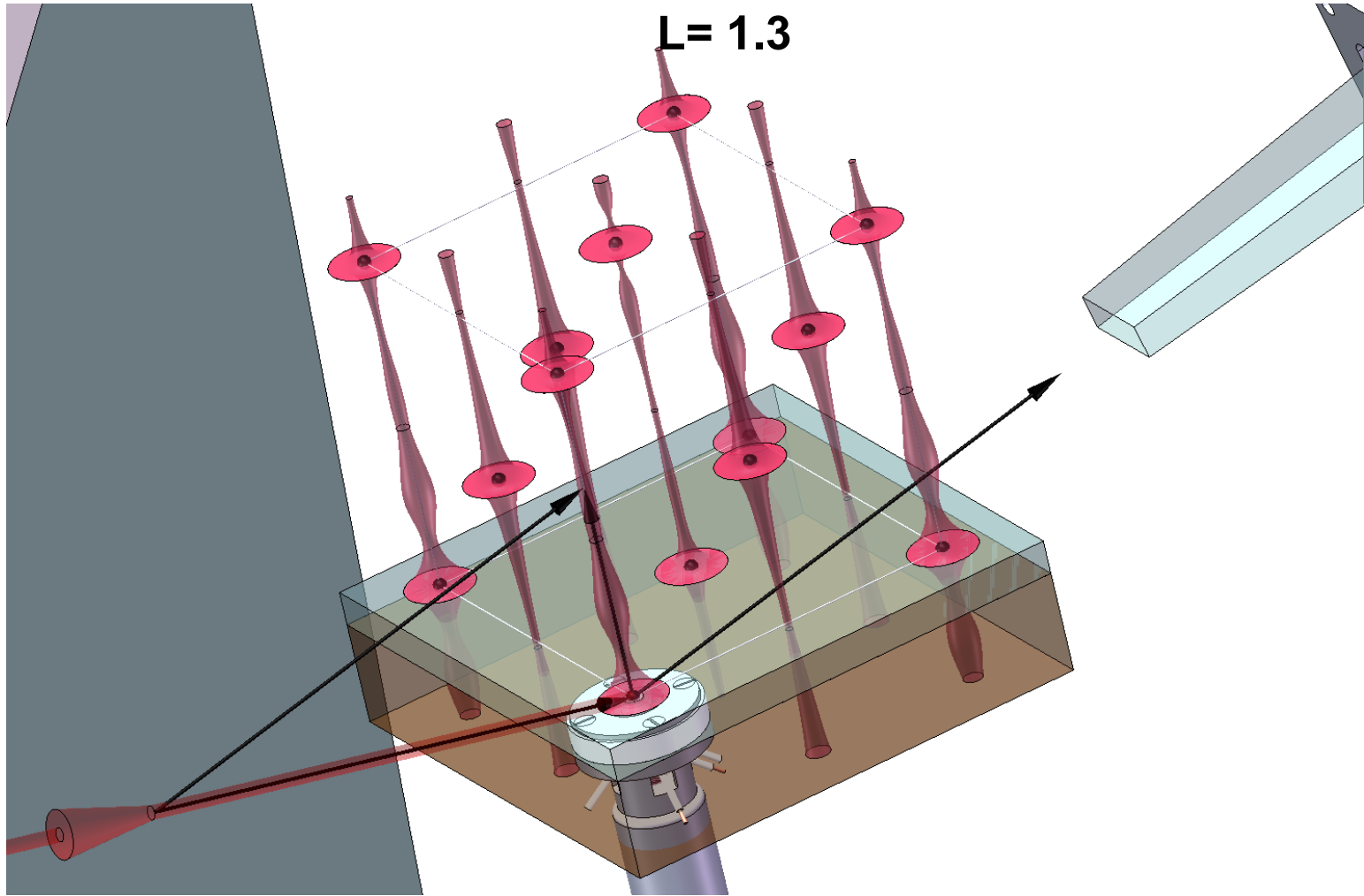
$L = 0.6$



CTR Diffraction – Measurement – Specular Rod

$(0, 0, L)$ or (Specular)Rod

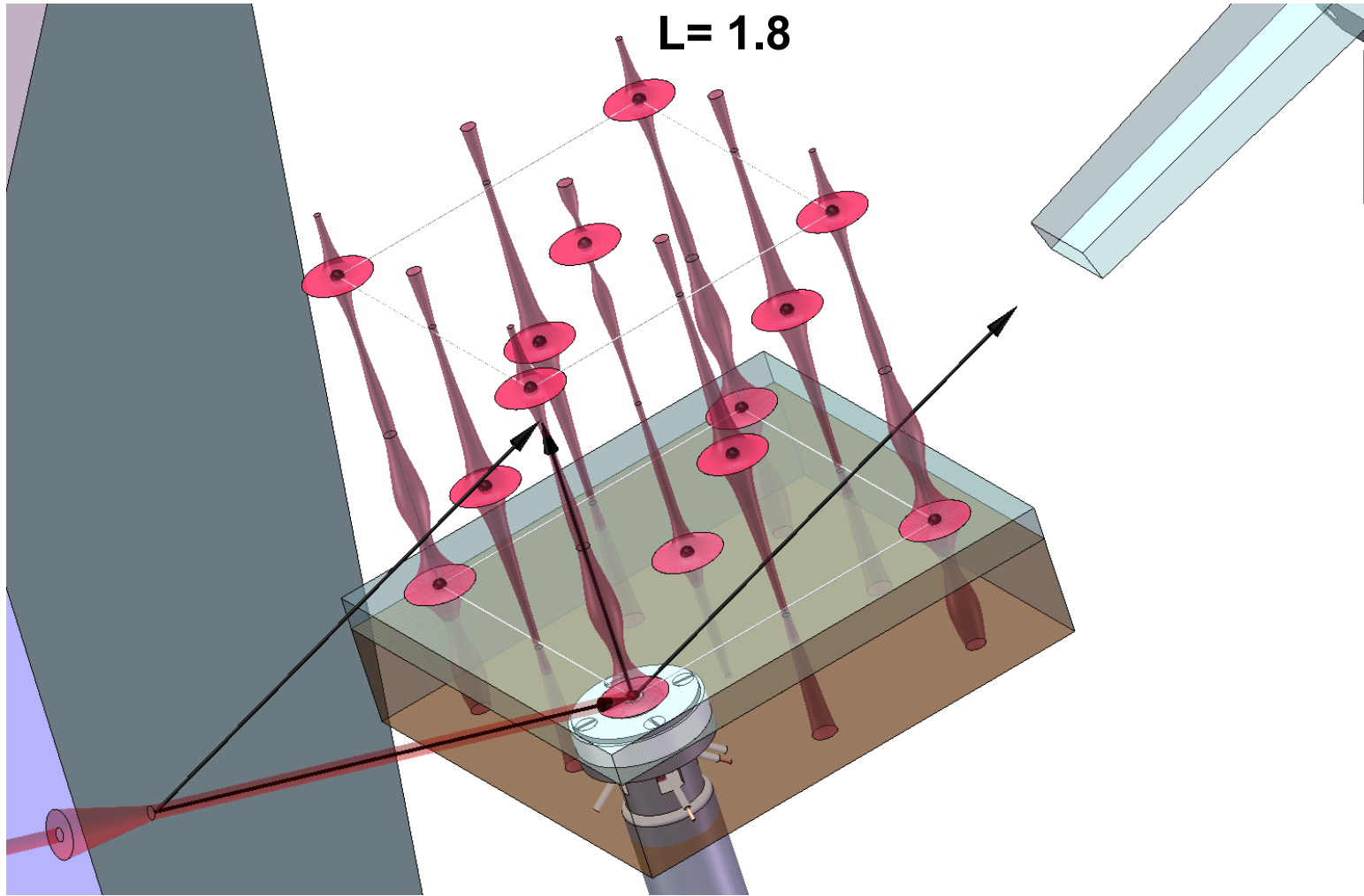
$L = 1.3$



CTR Diffraction – Measurement – Specular Rod

$(0, 0, L)$ or (Specular)Rod

$L = 1.8$



Data collection and reduction

Data integration → Data Shell:

Image view, ROI control, background subtraction and integration

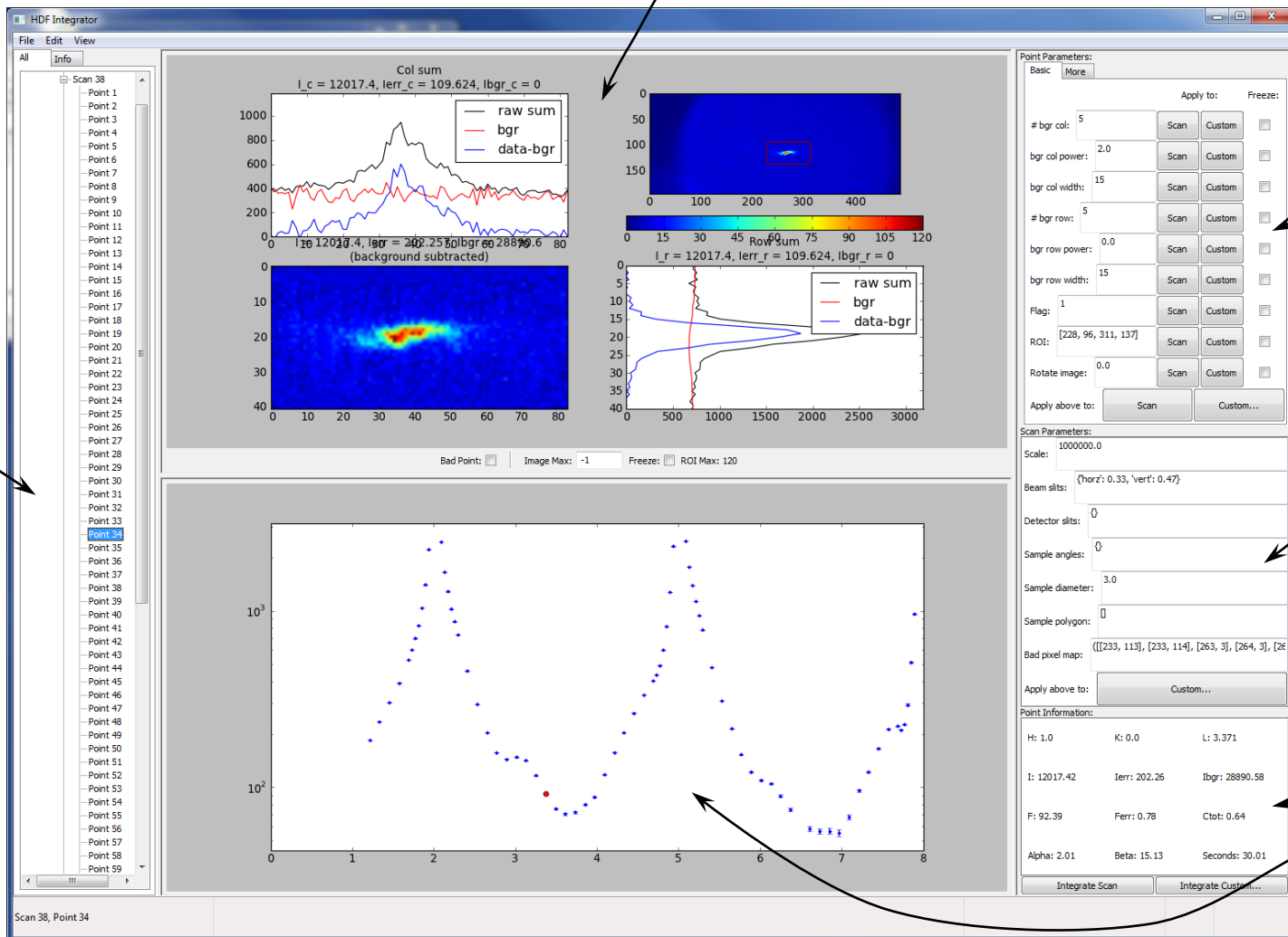
Scan and point tree

Integration parameters

Correction factors

Point information

Corrected structure factor

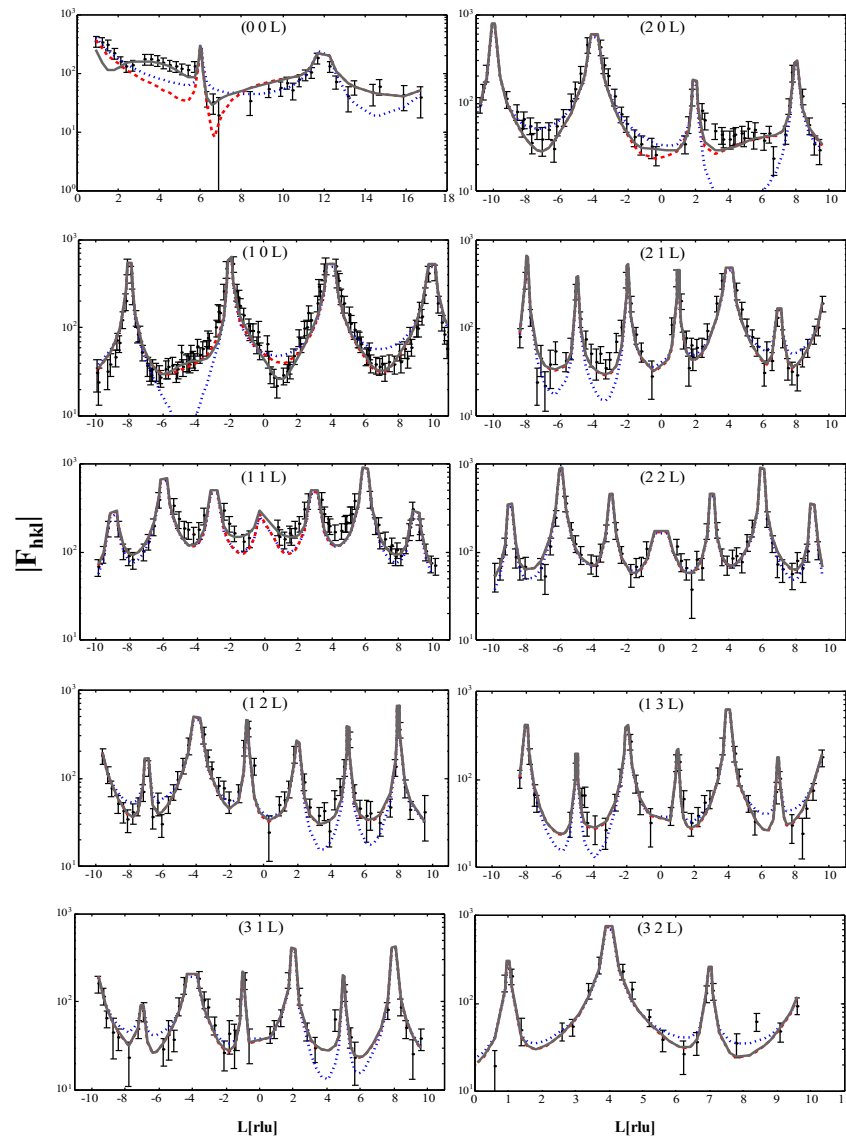
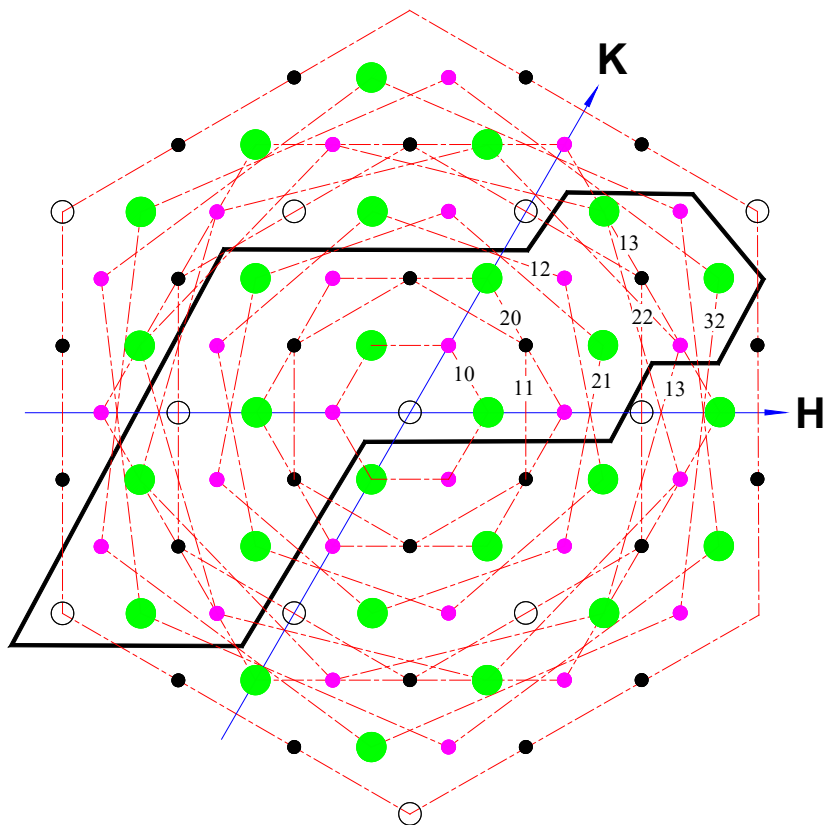


GeoSoilEnviroCARS 24th National School on Neutron and X-Ray Scattering

July 21st, 2022 Peter J. Eng

Data collection and reduction

Rod data set:



GeoSoilEnviroCARS 24th National School on Neutron and X-Ray Scattering

July 21st, 2022 Peter J. Eng

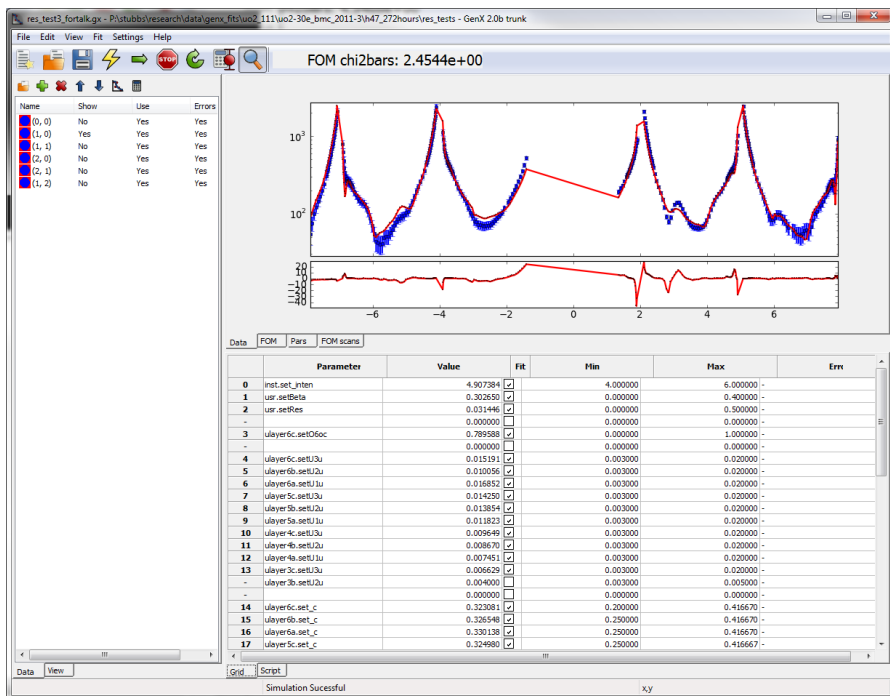
Data analysis

Fitting with GenX – genetic algorithm:

Journal of
Applied
Crystallography

GenX: an extensible X-ray reflectivity refinement program utilizing differential evolution

Matts Björck and Gabriella Andersson,
2011, *J. Appl. Cryst.* (2007)



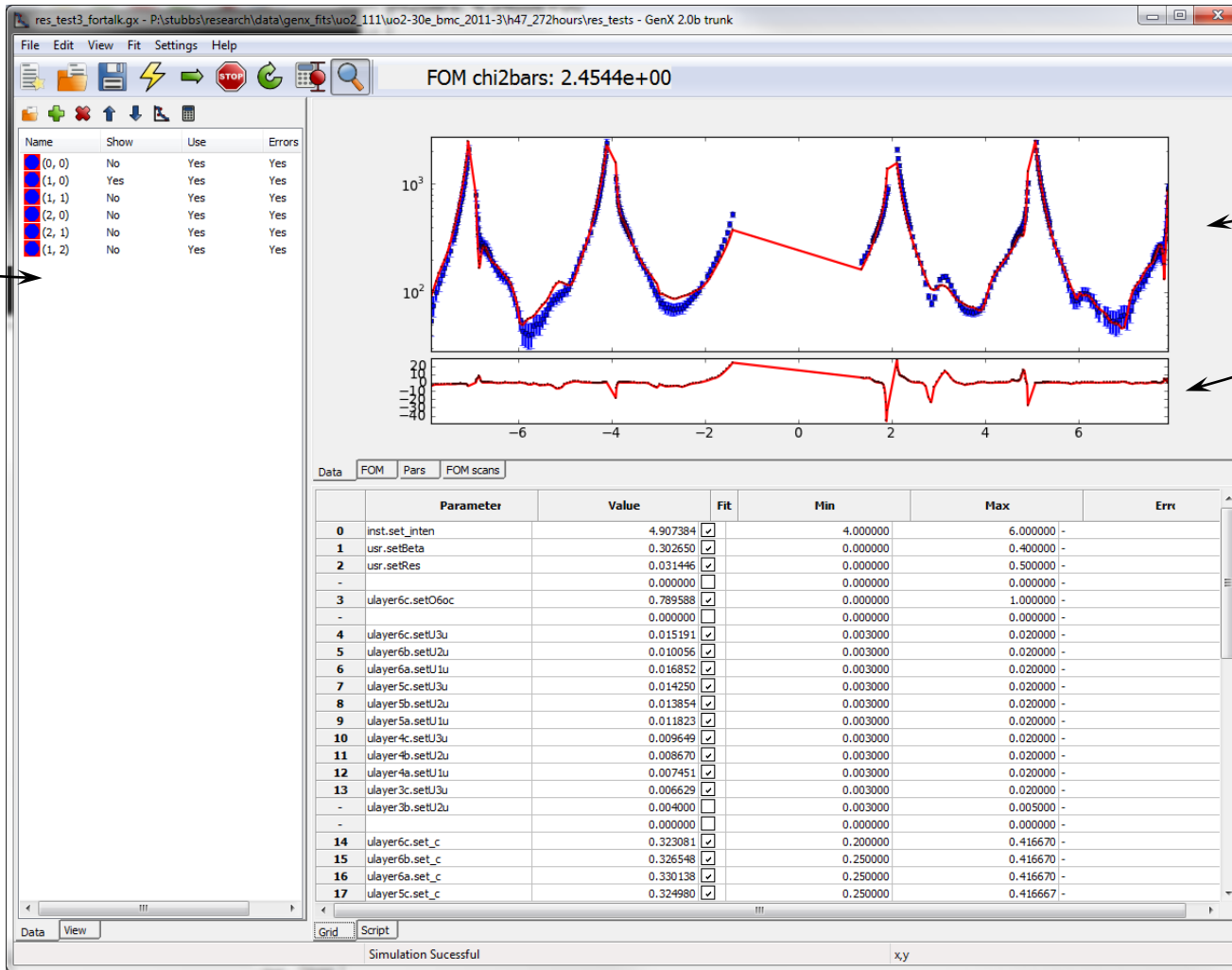
- X-ray reflectivity, CTR, multilayers
- Allows simultaneous stable refinement of many parameters
- Python - easily modified, extended
- Surface XRD code for layered structures
- User-friendly GUI

GeoSoilEnviroCARS 24th National School on Neutron and X-Ray Scattering

July 21st, 2022 Peter J. Eng

Data analysis

Fitting with GenX – genetic algorithm:



Data and fit results

Difference plot

Fit parameter:

- value
- valid range
- error



Data analysis

Fitting with GenX – genetic algorithm:

- Python scripting is used to setup the fit model
- Allows considerable customization and flexibility

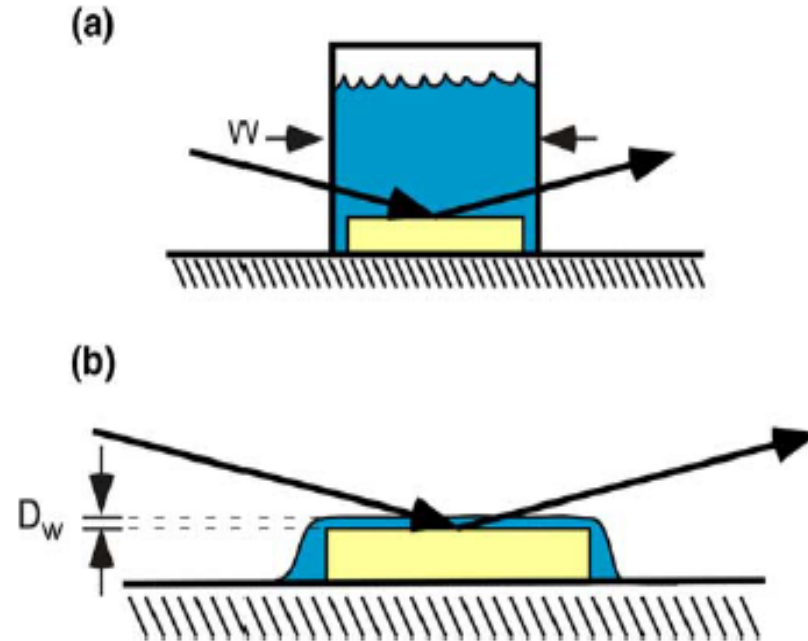


```
P:\stubs\research\data\genx_fts\wo2_111\wo2-30e_bmc_2011-3\h47_272hours\res_tests\script.py - Note...
File Edit Search View Encoding Language Settings Macro Run Plugins Window ?
script.py
1 # 1
2 import models.sxrd as model
3 from models.utils import UserVars
4 import numpy as np
5
6 # 2 Defining the unit cell parameters
7 unitcell = model.UnitCell(3.867, 3.867, 9.471, 90, 90, 120)
8 # 3 Define the instrument
9 inst = model.Instrument(wavel = .833, alpha = 2.0)
10
11 # 3.a Define beta for roughness model and resolution
12 usr=UserVars()
13 usr.new_var('beta', 0.0)
14 usr.new_var('res', 0.0)
15
16 # 4 Defining the bulk
17 bulk = model.Slab()
18 # 4.a Define the atoms
19 # atom name, element, x, y, z, Uiso, multiplicity
20 bulk.add_atom('U1', 'u4p', 0.0000, 0.0000, 0.0000, 0.00000, 0.004, 1.0)
21 bulk.add_atom('U2', 'u4p', 0.3333, 0.6667, 0.33333, 0.004, 1.0)
22 bulk.add_atom('U3', 'u4p', 0.6667, 0.3333, 0.66667, 0.004, 1.0)
23 bulk.add_atom('O1', 'o', 0.3333, 0.6667, 0.08333, 0.008, 1.0)
24 bulk.add_atom('O2', 'o', 0.0000, 0.0000, 0.25000, 0.008, 1.0)
25 bulk.add_atom('O3', 'o', 0.6667, 0.3333, 0.41667, 0.008, 1.0)
26 bulk.add_atom('O4', 'o', 0.3333, 0.6667, 0.58333, 0.008, 1.0)
27 bulk.add_atom('O5', 'o', 0.0000, 0.0000, 0.75000, 0.008, 1.0)
28 bulk.add_atom('O6', 'o', 0.6667, 0.3333, 0.91667, 0.008, 1.0)
29
30 # 6 Creating independent UO2 layers for top - note asymmetric unit cell
31 # 6.a bottom layer
32 ulayer1a = model.Slab(c = .333333333)
33 # 6.b Define the atoms
34 ulayer1a.add_atom('U1', 'u4p', 0.0000, 0.0000, 0.00, 0.004, 1.0, 1)
35 ulayer1a.add_atom('O1', 'o', 0.3333, 0.6667, 0.25, 0.008, 1.0, 1)
36 ulayer1a.add_atom('O7', 'o', 0.6667, 0.3333, 0.50, 0.008, 0.0, 1)
37 ulayer1a.add_atom('O2', 'o', 0.0000, 0.0000, 0.75, 0.004, 1.0, 1)
38
39 # 6.c middle layer
40 ulayer1b = model.Slab(c = .333333333)
41 # 6.d Define the atoms
42 ulayer1b.add_atom('U2', 'u4p', 0.3333, 0.6667, 0.00, 0.004, 1.0, 1)
43 ulayer1b.add_atom('O3', 'o', 0.6667, 0.3333, 0.25, 0.008, 1.0, 1)
44 ulayer1b.add_atom('O8', 'o', 0.0000, 0.0000, 0.50, 0.008, 0.0, 1)
45 ulayer1b.add_atom('O4', 'o', 0.3333, 0.6667, 0.75, 0.008, 1.0, 1)
46
47 # 6.e top layer
48 ulayer1c = model.Slab(c = .333333333)
49 # 6.f Define the atoms
50 ulayer1c.add_atom('U3', 'u4p', 0.6667, 0.3333, 0.00, 0.004, 1.0, 1)
51 ulayer1c.add_atom('O5', 'o', 0.0000, 0.0000, 0.25, 0.008, 1.0, 1)
52 ulayer1c.add_atom('O9', 'o', 0.3333, 0.6667, 0.50, 0.008, 0.0, 1)
53 ulayer1c.add_atom('O6', 'o', 0.6667, 0.3333, 0.75, 0.008, 1.0, 1)
54
55 ulayer2a = ulayer1a.copy()
56 ulayer2b = ulayer1b.copy()
57
length: 5166 lines: 130 Ln: 1 Col: 1 Sel: 0|0 Dos/Windows ANSI as UTF-8 INS
```



Sample Environments

In-situ liquid cells:



(a) Transmission and (b) thin film cells
(Fenter 2004)



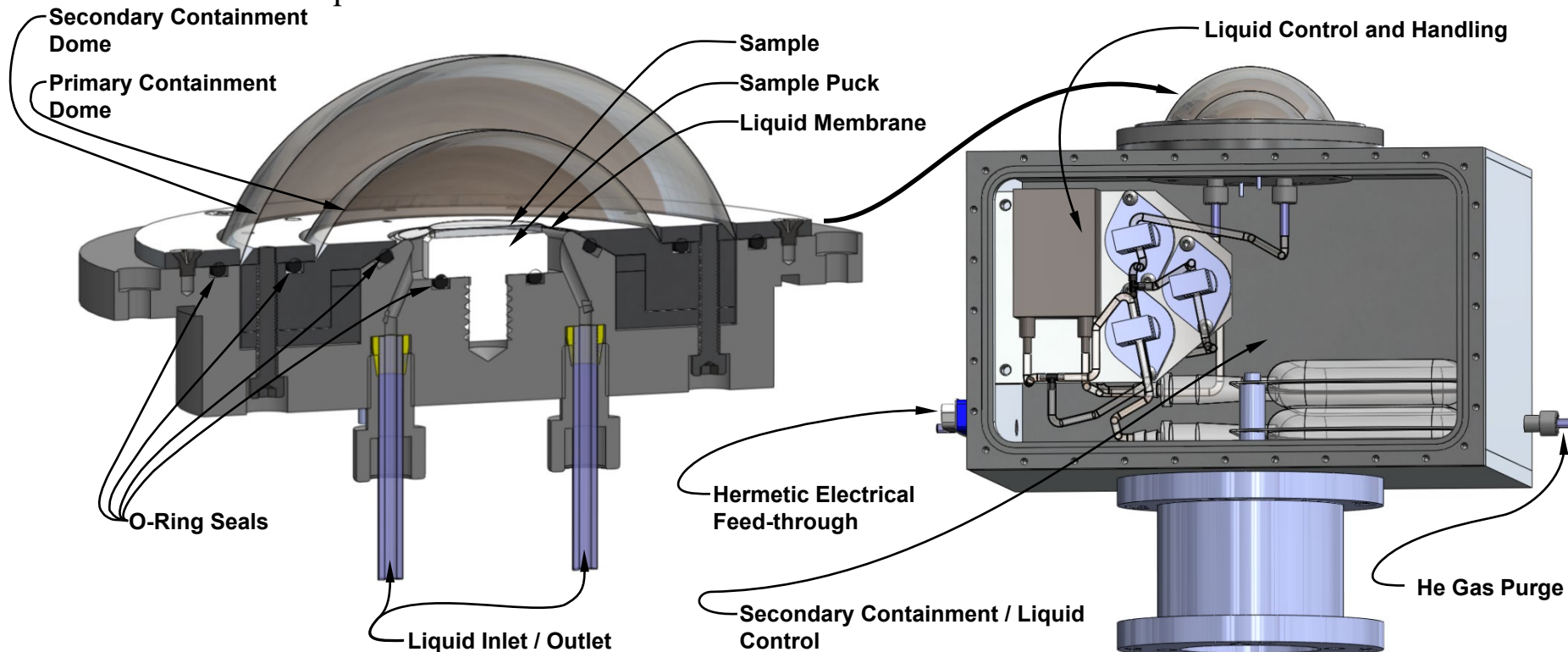
Sample Environments

GSECARS *in situ* liquid cell for radioactive material interface studies

Developed in collaboration with Moritz Schmidt, Paul Fenter and Lynda Soderholm (ANL)

The radiological hazard must be mitigated at the beamline during the measurements

- Multiple containment required
- X-ray scattering compatible
- Remote liquid control

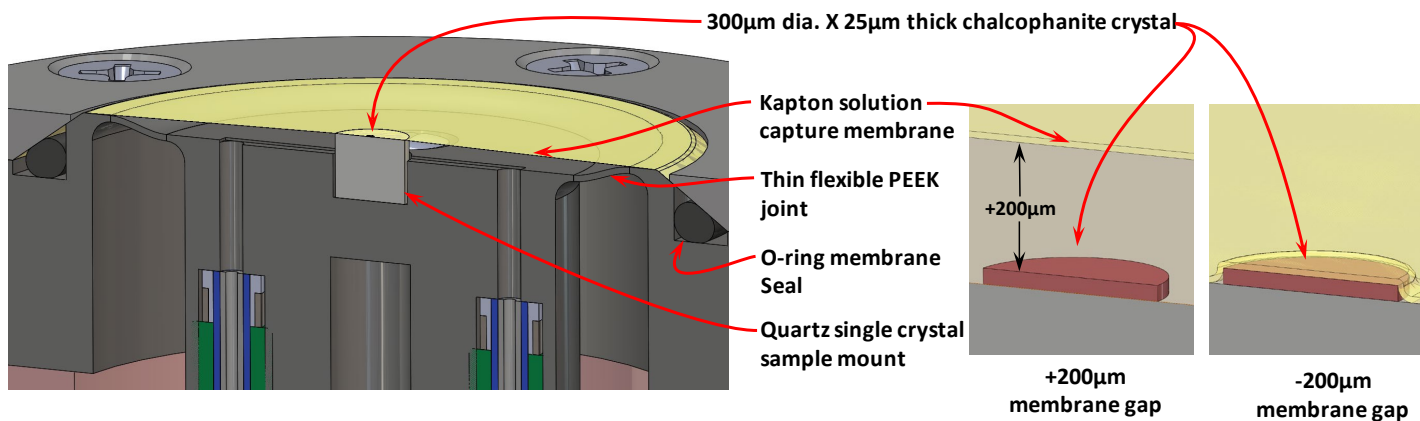
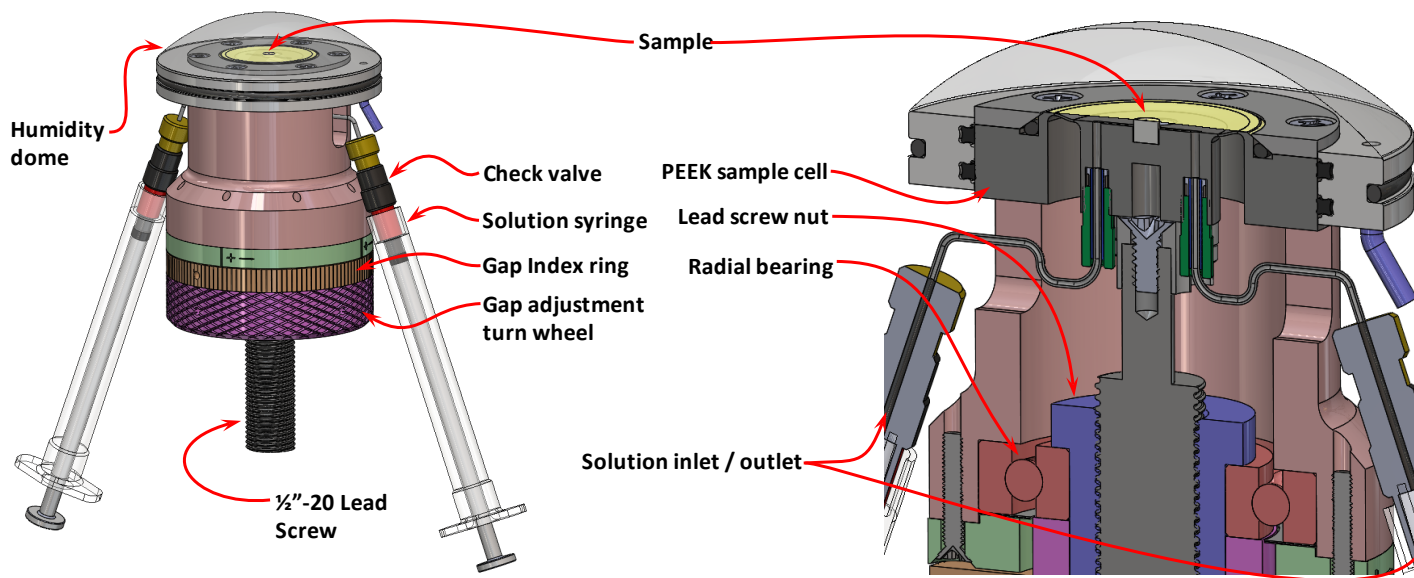


GeoSoilEnviroCARS 24th National School on Neutron and X-Ray Scattering

July 21st, 2022 Peter J. Eng

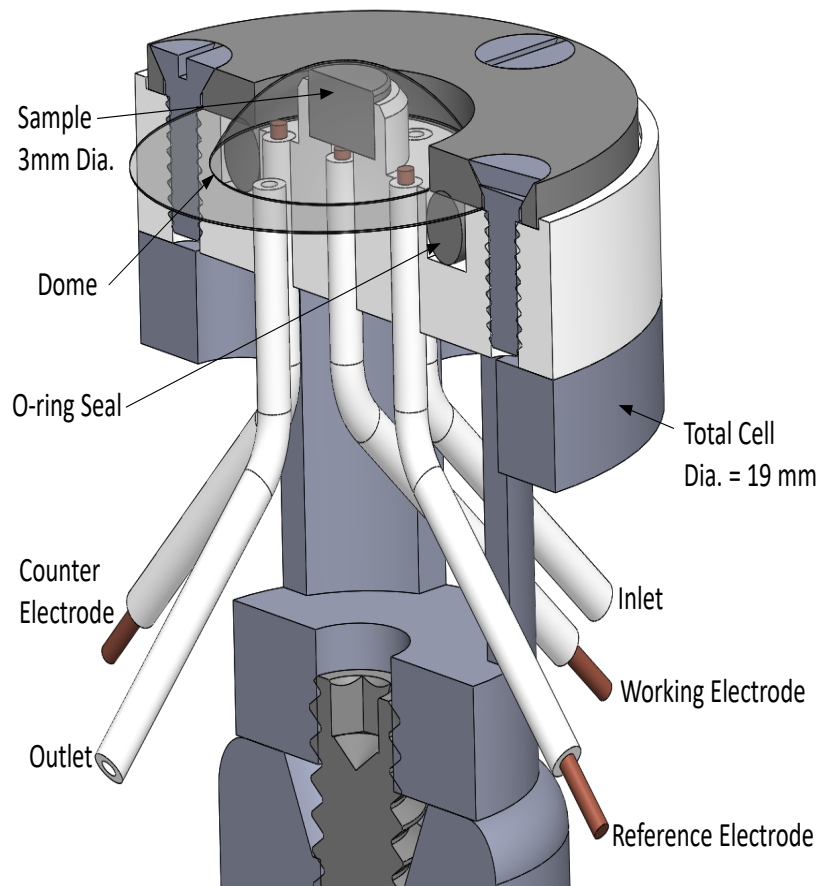
Sample Environments

Adjustable gap thin membrane cell



Sample Environments

Miniature electrochemistry cell



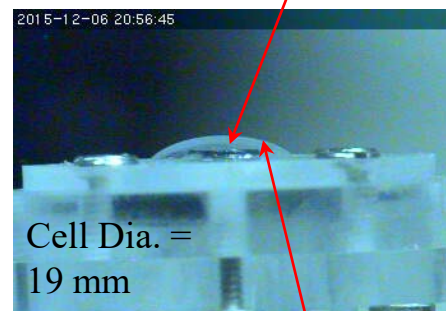
Solution ports Ag-AgCl reference electrode



Pt counter electrode

O-ring

3 mm Dia. hematite crystal



Spherical Tefzel dome traps 200-500 μm electrolyte solution

Collaboration with M. McBriarty, K. Rosso, PNNL

GeoSoilEnviroCARS 24th National School on Neutron and X-Ray Scattering

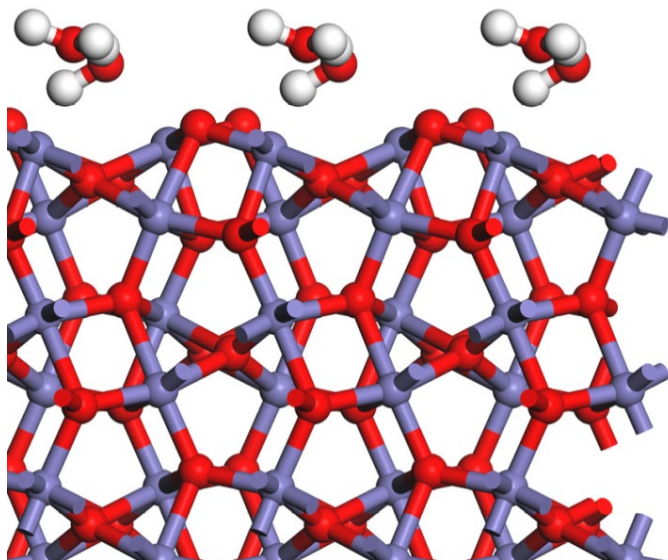
July 21st, 2022 Peter J. Eng

Electrochemistry at the (1-102) surface Hematite

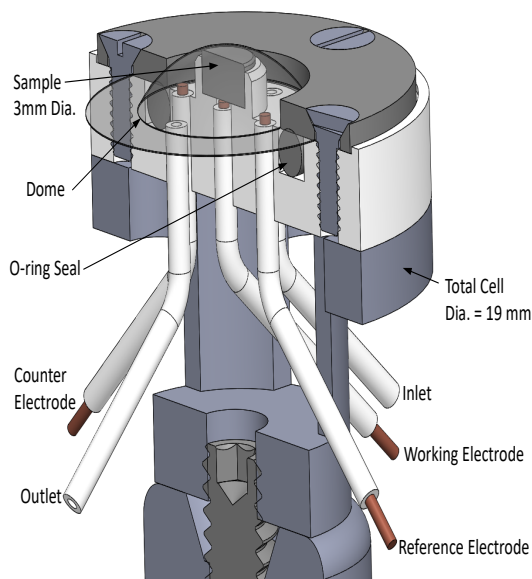
Potential-Specific Structure at the Hematite–Electrolyte Interface

M.E. McBriarty, J.E. Stubbs, P.J. Eng, K.M. Rosso (2018) *J. Phys. Chem. C* 121:12236

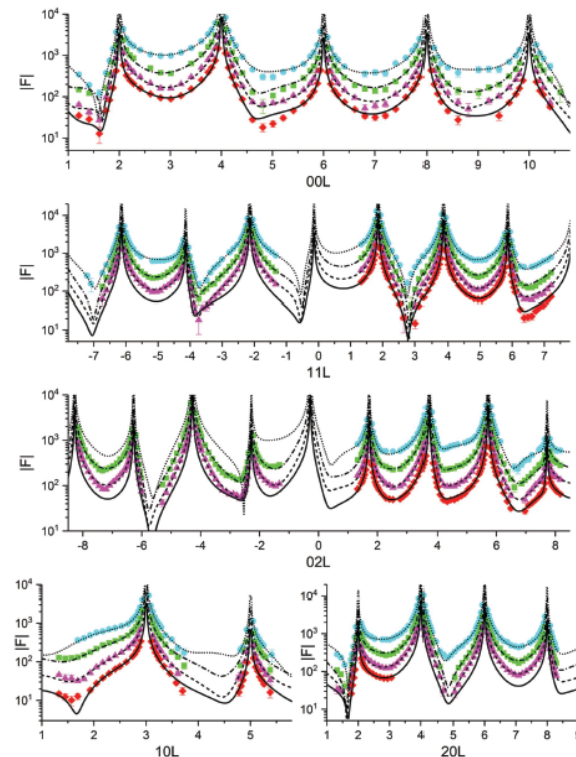
The atomic-scale structure of the interface between a transition metal oxide and aqueous electrolyte regulates the interfacial chemical reactions fundamental to (photo)electrochemical energy conversion and electrode degradation.



(1-102) surface of hematite ($\alpha\text{-Fe}_2\text{O}_3$)



Electrochemical Cell for Interface Scattering

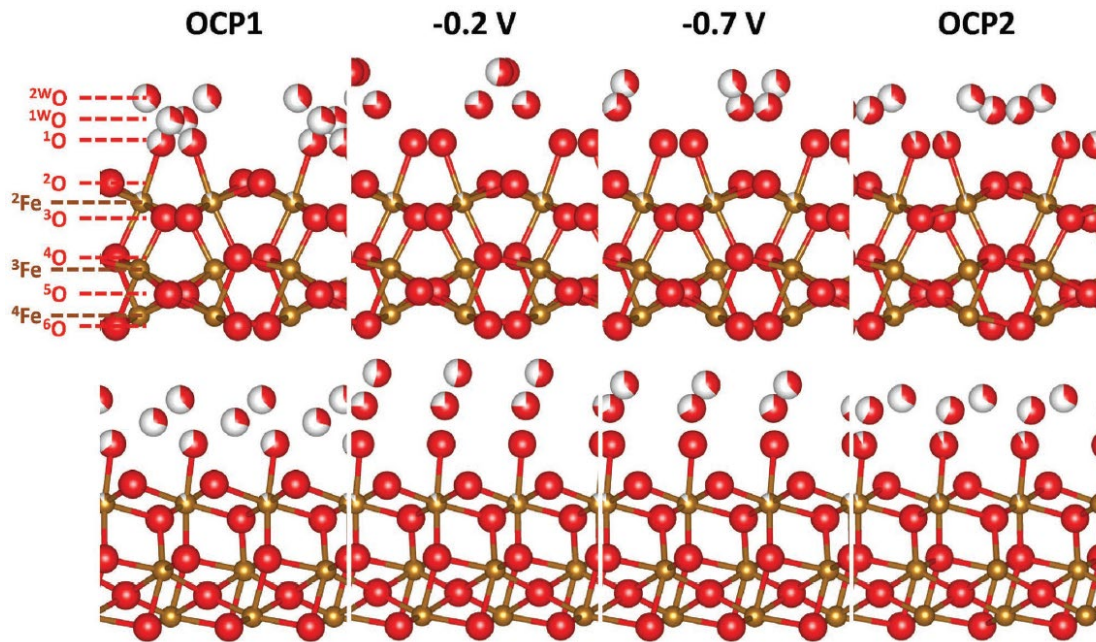


Crystal Truncation Rod Data Set



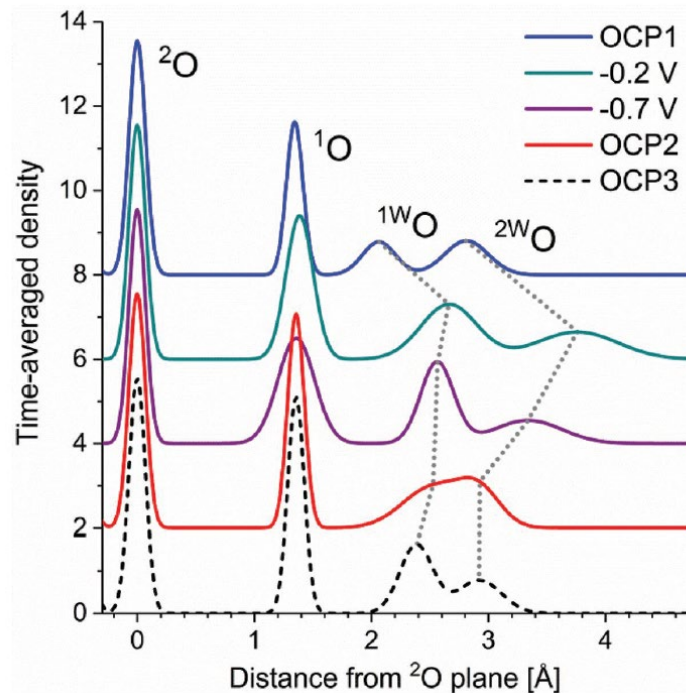
Electrochemistry at the (1-102) surface Hematite

Atomic models of the hematite–water interface derived from CTR fits.



Water molecules flip in response to applied potential at pH 7

Time-averaged atom density in the surface normal direction.



Resonant Anomalous X-ray Reflectivity (RAXR)

Adds elemental specificity to CTR measurements

The location, occupancy, and distribution width of a specific adsorbed element on a surface can be determined by measuring the structure factor as a function of energy through an absorption edge of the element at a fixed point on the CTR.

Non-resonant Structure factor - as a function of HKL at fixed energy far from absorption edge

$$F_c(H, K, L) = \sum_{k=1}^m f_{a,k} e^{i2\pi(x_k H + y_k K + z_k L)} e^{-M_j}$$

Sum over all non-resonant atoms in the unit cell

Non-resonant atomic scattering factor

Resonant Structure factor – as a function of energy through an absorption edge at fixed HKL

$$F_{c,res}(H, K, L, E) = \sum_{j=1}^m (f_j'(E) + i f_j''(E)) e^{i2\pi(x_j H + y_j K + z_j L)} e^{-M_j}$$

Sum over all resonant atoms in the unit cell

Anomalous dispersion terms

$$E_{surf}(HKL, E) = N_1 N_2 [F_c(HKL) + F_{c,res}(HKL, E)] e^{i\pi L}$$

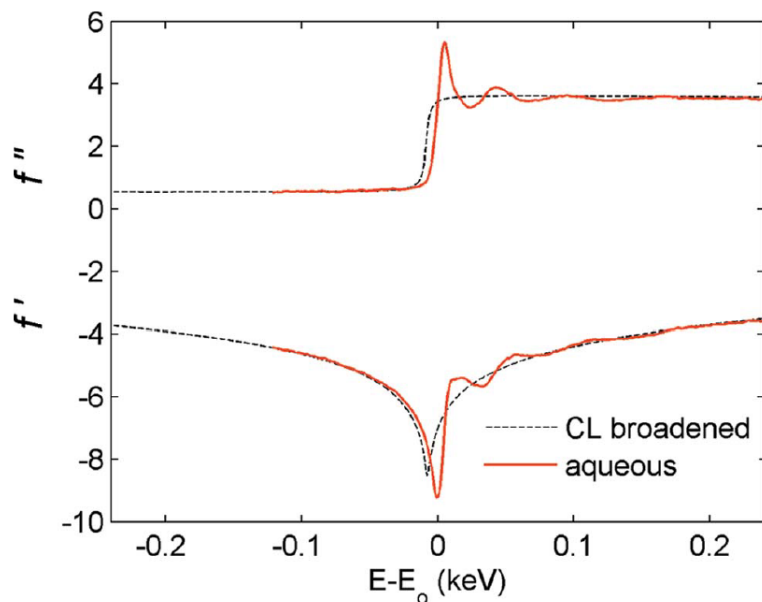


CTR Diffraction – RAXR

The resonant intensity results from the interference between the non-resonant and resonant components of the total structure factor

$$I(HKL,E) \propto N_1^2 N_2^2 \left| F_{c,bulk}(HKL)F_{ctr}(L) + [F_c(HKL) + F_{c,res}(HKL,E)]_{surf} \right|^2$$

The anomalous dispersion terms: $f_j'(E) + if_j''(E)$ are determined experimentally



Measured XANES profile of element of interest

Determined by difference Kramers-Kronig transform
Cross et al. Phys.Rev. B (1998)

(Park et al., *J Appl Crystallogr* 2007)

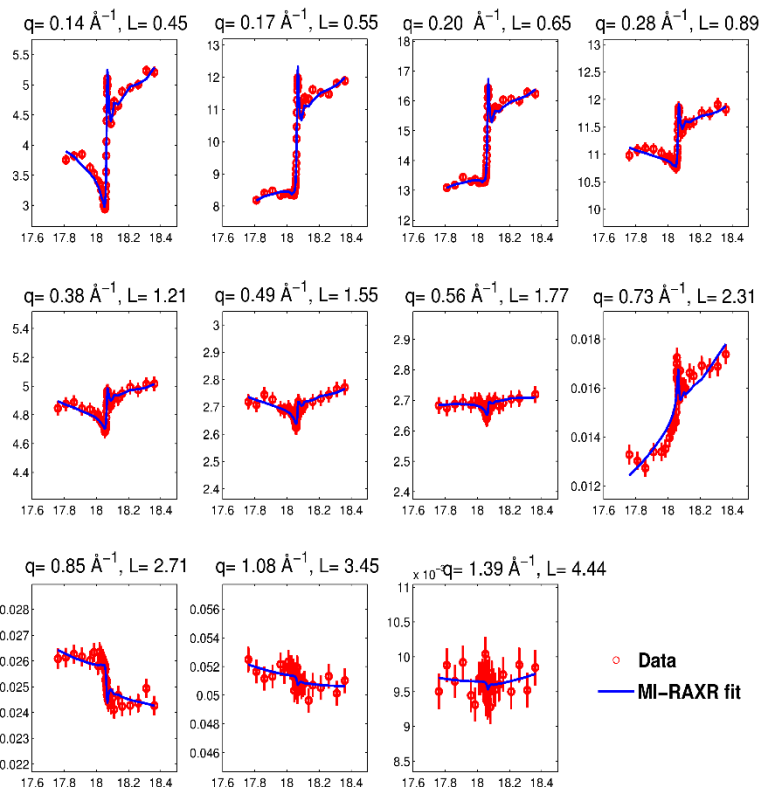
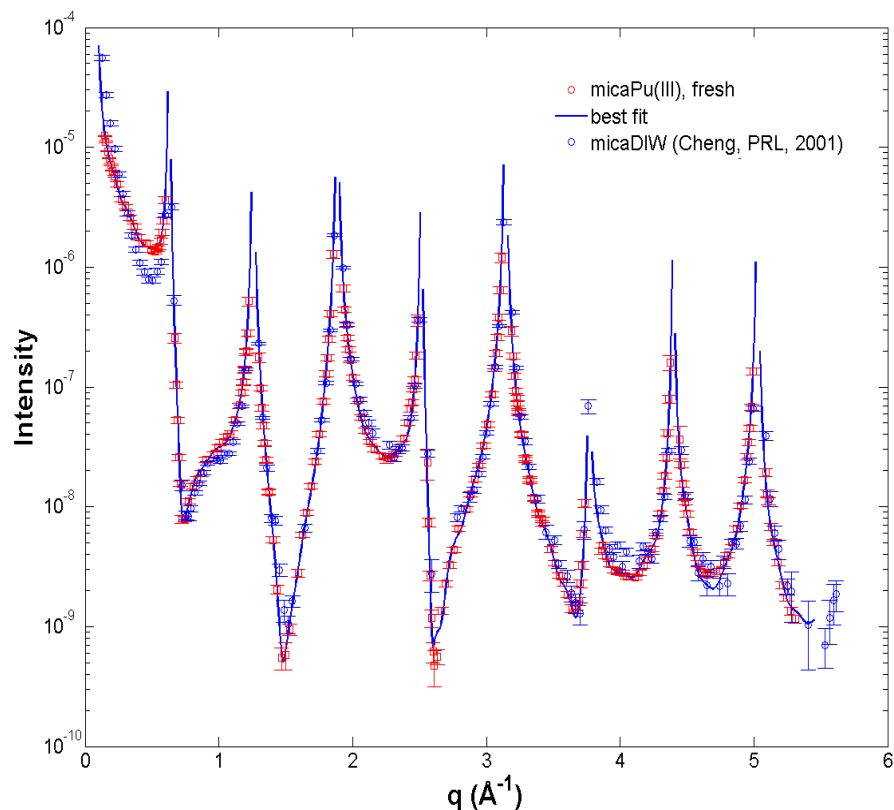
CTR Diffraction – RAXR

Surface-Mediated Formation of Pu(IV) Nanoparticles at the Muscovite-Electrolyte Interface

M. Schmidt, S.S. Lee, R.E. Wilson, K.E. Knope, F. Bellucci, P.J. Eng, J.E. Stubbs, L. Soderholm, P. Fenter (2013) *Environ. Sci. Technol.* 47: 14178-14184

Clean muscovite surface exposed to Pu(III) solution

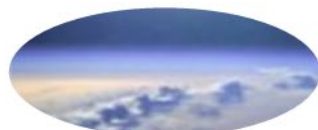
Specular CTR



RAXR spectra:

Energy scans across Pu L_{III} edge at fixed Q

Fit phase & amplitude for Pu height & coverage



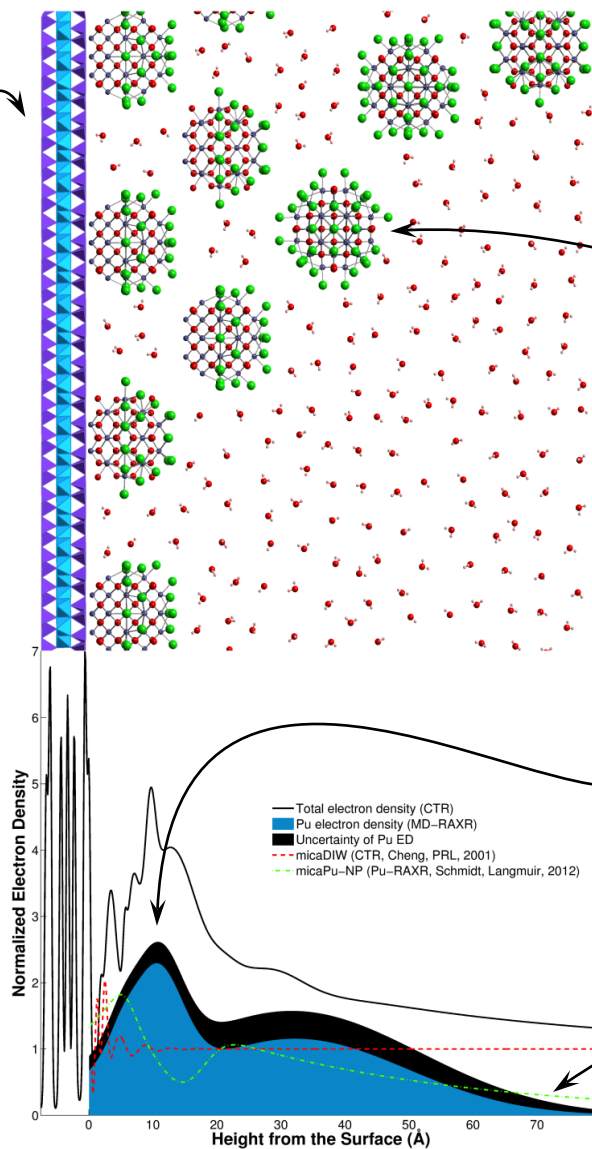
GeoSoilEnviroCARS 24th National School on Neutron and X-Ray Scattering

July 21st, 2022 Peter J. Eng

CTR Diffraction – RAXR

Muscovite surface

Pu(IV) Nanoparticles



Pu has broad vertical distribution, peaked at 10.5 Å and extends >70 Å



References

Reference texts:

Warren B.E. (1969) *X-ray Diffraction*. New York: Addison-Wesley.

Als-Nielsen J. and McMorrow D. (2001) *Elements of Modern X-ray Physics*. New York: John Wiley.

Sands D.E. (1982) *Vectors and Tensors in Crystallography*. New York: Addison-Wesley.

A few surface scattering methods papers:

Robinson I. K. (1986) *Phys. Rev. B* **33**(6), 3830-3836. (→ original reference)

Andrews S.R. and Cowley R.A. (1985) *J. Phys C*. **18**, 642-6439. (→ original reference)

Vlieg E., et. al. (1989) *Surf. Sci.* **210**(3), 301-321.

Vlieg E. (2000) *J. Appl. Crystallogr.* **33**(2), 401-405. (→ rod analysis code)

Trainor T. P., et. al.. (2002) *J App Cryst* **35**(6), 696-701. (→ rod analysis code)

Fenter P. and Park C. (2004) *J. App Cryst* **37**(6), 977-987.

Fenter P. A. (2002) *Reviews in Mineralogy & Geochemistry* **49**, 149-220. (→ Excellent tech. review)

Reviews

Fenter P. and Sturchio N. C. (2005) *Prog. Surface Science* **77**(5-8), 171-258.

Renaud G. (1998) *Surf. Sci. Rep.* **32**, 1-90.

Robinson I.K. and Tweet D.J. (1992) *Rep Prog Phys* **55**, 599-651.

Fuoss P.H. and Brennan S. (1990) *Ann Rev Mater Sci* **20** 365-390.

Feidenhans'l R. (1989) *Surf. Sci. Rep.* **10**, 105-188.

Coordinate transformations, reciprocal space, diffractometry

You H. (1999) *J. App Cryst.* **32** 614-623.

Vlieg E. (1997) *J. Appl. Crystallogr.* **30**(5), 532-543.

Toney M. (1993) *Acta Cryst* **A49**, 624-642



Feedback

Lecture – 9:45 – 10:45

Surface and Interface Scattering - Peter Eng

<https://forms.office.com/g/NLyUDMAupR>



GeoSoilEnviroCARS 24th National School on Neutron and X-Ray Scattering

July 21st, 2022 Peter J. Eng

Extra Slides



GeoSoilEnviroCARS 24th National School on Neutron and X-Ray Scattering

July 21st, 2022 Peter J. Eng

Total external reflection of x-rays – Arthur H. Compton 1922

Phil. *Total Reflexion of X-Rays.* 1123 123

radiation is considerably higher than the natural frequency of the electrons, this becomes very nearly,

$$\delta = \frac{nc^2}{2\pi n\nu^2}, \dots \dots \dots (4)$$

where n is the total number of electrons per unit volume of the medium.

If X-rays of wave-length 1.473 \AA . traverse calcite, this expression (4) indicates an index of refraction which is less than unity by about 8×10^{-6} . For $\lambda = 1.279$, $\delta = 6 \times 10^{-6}$, and for $\lambda = 1.096$, $\delta = 4.5 \times 10^{-6}$. The close correspondence between these theoretical values and the values calculated from Duane and Patterson's experiments can leave little doubt but that the consistent changes in apparent wave-length with order which they observe are due to refraction.

3. Observation of Total Reflexion of X-rays.

Since the refractive index is less than unity, a beam of X-rays striking a plane surface at a sufficiently large angle of incidence should be totally reflected. The critical glancing angle is given by

$$\cos \theta = \mu,$$

or

$$\sin \theta = \sqrt{2\delta}.$$

For 1.279 \AA ., the value of δ for crown glass of density 2.52 is given by equation (4) as 5.2×10^{-6} , in which case $2\theta = 22$ minutes of arc, which is a readily measurable deflexion*.

Fig. 1.

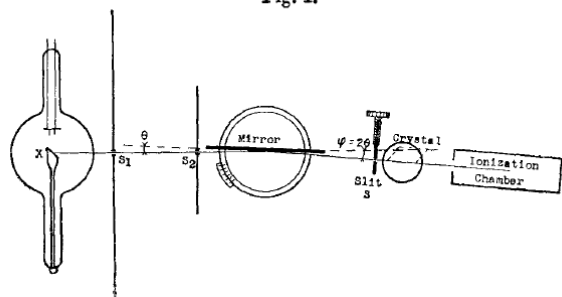
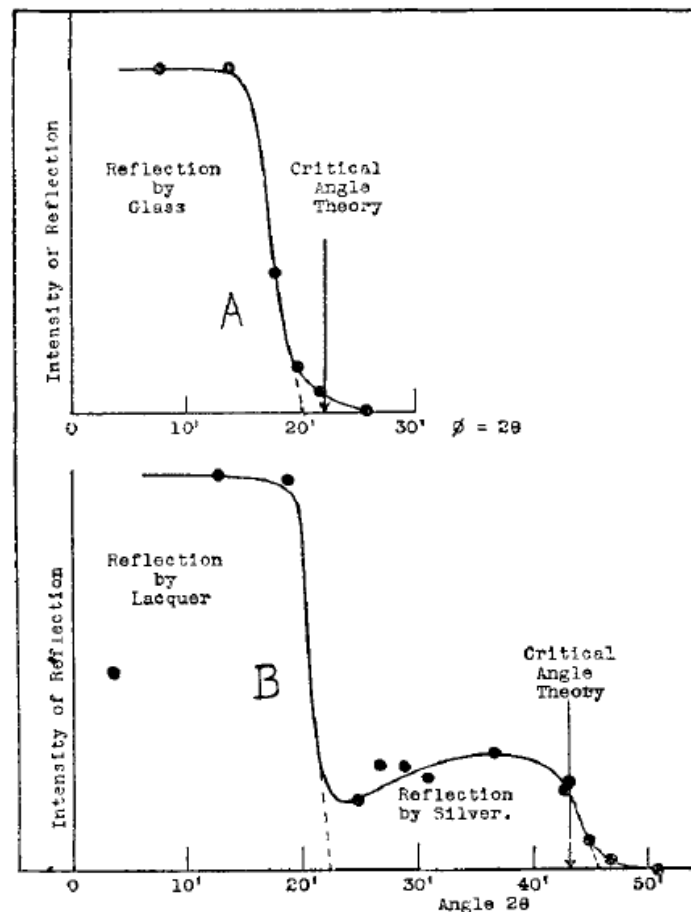


Fig. 4.



Total reflexion and critical angles for $\lambda = 1.279 \text{ \AA}$.



History

Critical angle for total external reflection of x-rays

Snell law:

$$n_1 \cos \theta_1 = n_2 \cos \theta_2$$

Let:

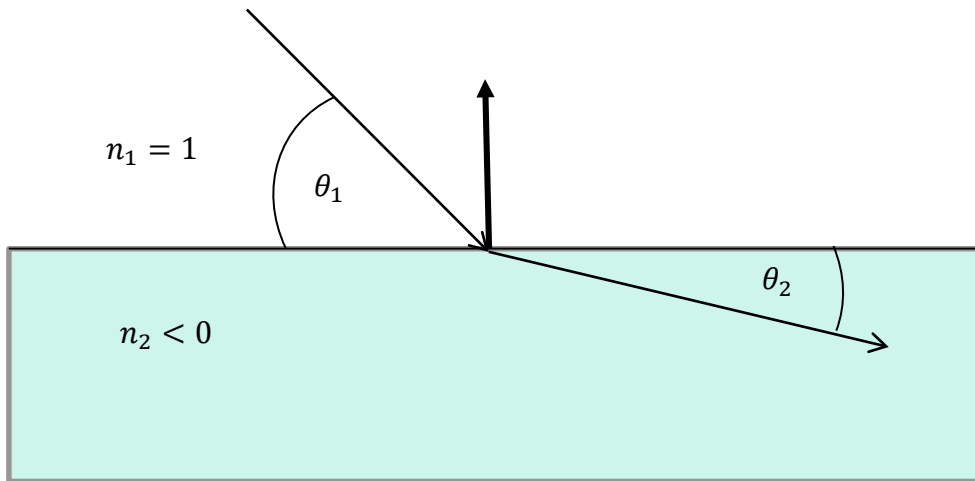
$$n_1 = 1, n = n_2 \text{ and } \theta_2 = 0$$

Then critical angle for total external reflection is:

$$\theta_c = \sqrt{2(1 - n)}$$

Let $n = 1 - \delta$ then:

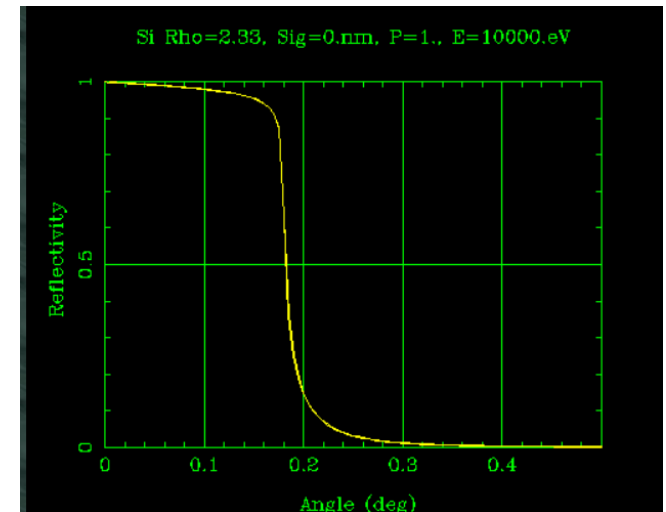
$$\theta_c [\text{mrad}] = \sqrt{2\delta} = 2.317 \lambda \sqrt{\rho \frac{Z}{A}}$$



For single crystal of Si at 10 keV:

$$\lambda = 1.24 \text{ \AA}, \rho = 2.33 \frac{\text{gm}}{\text{cm}^3}, Z = 14, A = 28.09 \text{ gm}$$

$$\theta_c = 3.1 \text{ mrad } (0.18^\circ)$$



From the CXRO Website:

http://henke.lbl.gov/optical_constants/mirror2.html



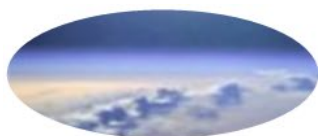
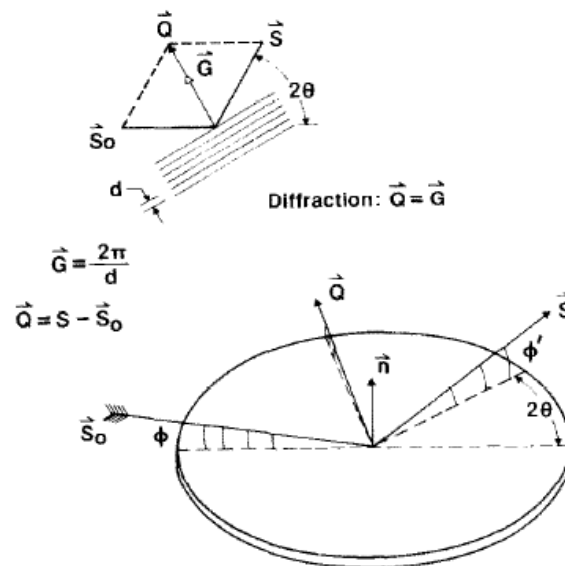
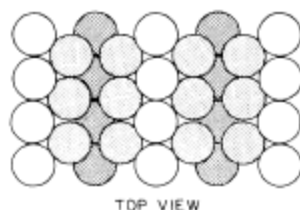
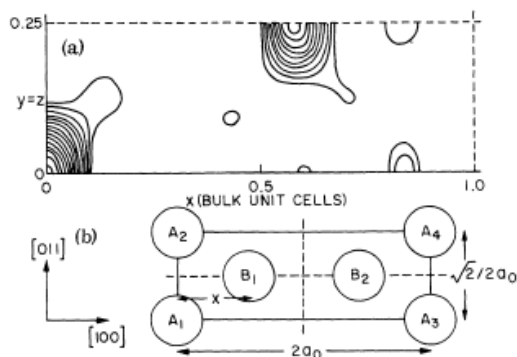
GeoSoilEnviroCARS 24th National School on Neutron and X-Ray Scattering

July 21st, 2022 Peter J. Eng

History

Surface x-ray diffraction measurements at grazing incidence

- Marra, Eisenberger and Cho 1979:
“X-ray total-external-reflection-Bragg diffraction: A structural study of the GaAs-Al interface”
J. Appl. Phys. 50, 4146 (1979)
- I. K. Robinson 1983:
“Direct Determination of Au(110) Reconstructed Surface by X-Ray Diffraction”
Phys. Rev. Lett. 50, 1145 (1983)
- S. Brennan 1985:
“Two-Dimensional X-Ray Scattering”
Surf. Sci. 153, 1 (1985)



History

3-D surface x-ray diffraction

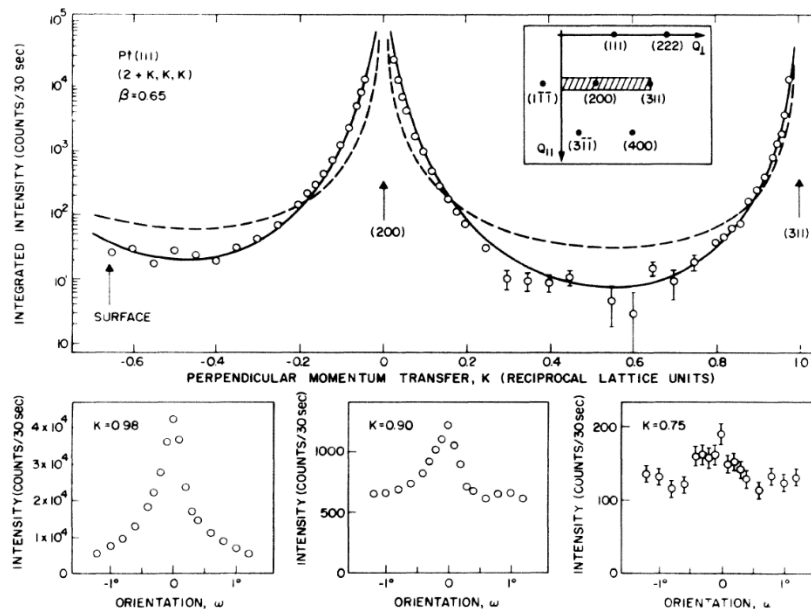
– I.K. Robinson 1986:

“Crystal truncation rods and surface roughness”

Phys. Rev. B 33, 3830 (1986)

$$|F(2\pi h/a_1, 2\pi k/a_2, q_3)|^2 = N_1^2 N_2^2 \frac{\sin^2(\frac{1}{2} N_3 q_3 a_3)}{\sin^2(\frac{1}{2} q_3 a_3)}$$

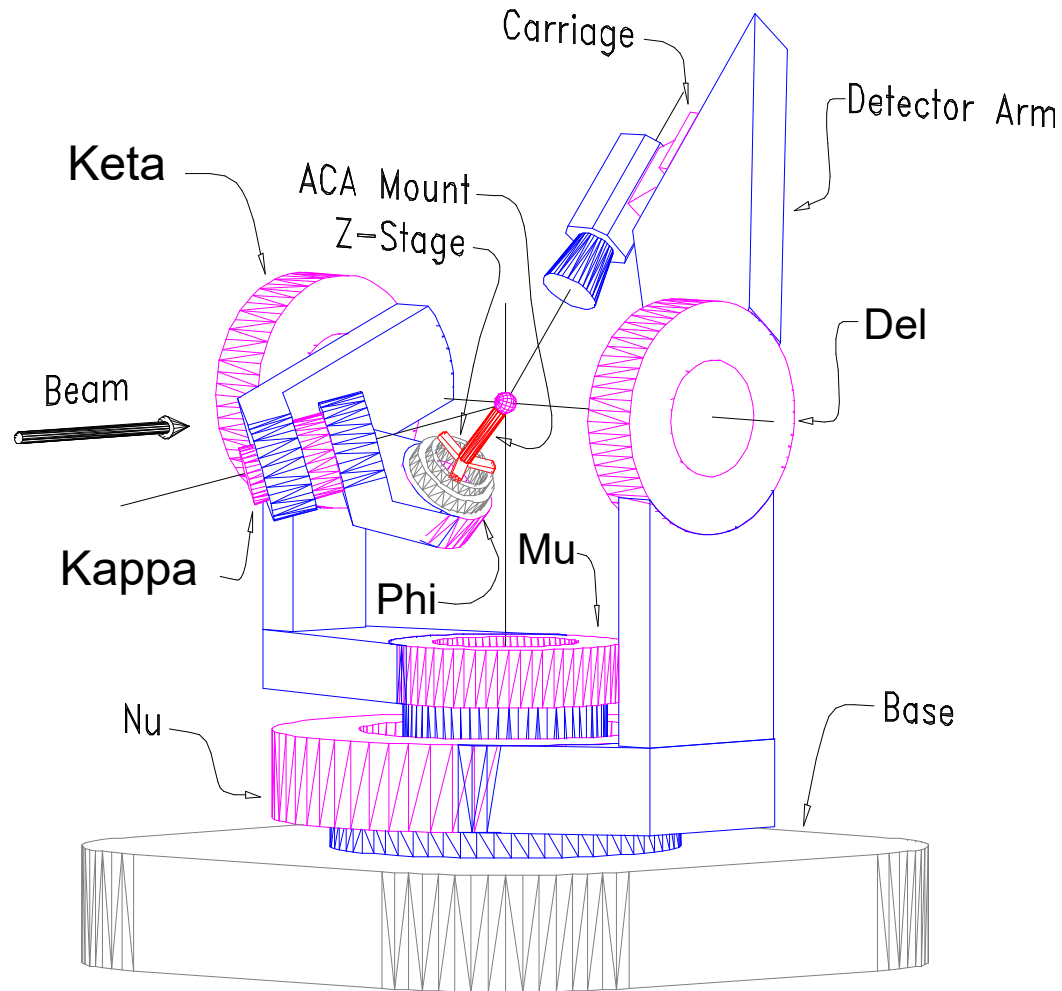
$$\rightarrow N_1^2 N_2^2 \frac{1}{2 \sin^2(\frac{1}{2} q_3 a_3)} \text{ as } N_3 \rightarrow \infty \text{ for } q_3 a_3 \neq 2\pi l$$



GEOSCIENCE 24th NATIONAL SCHOOL on neutron and X-Ray Scattering

July 21st, 2022 Peter J. Eng

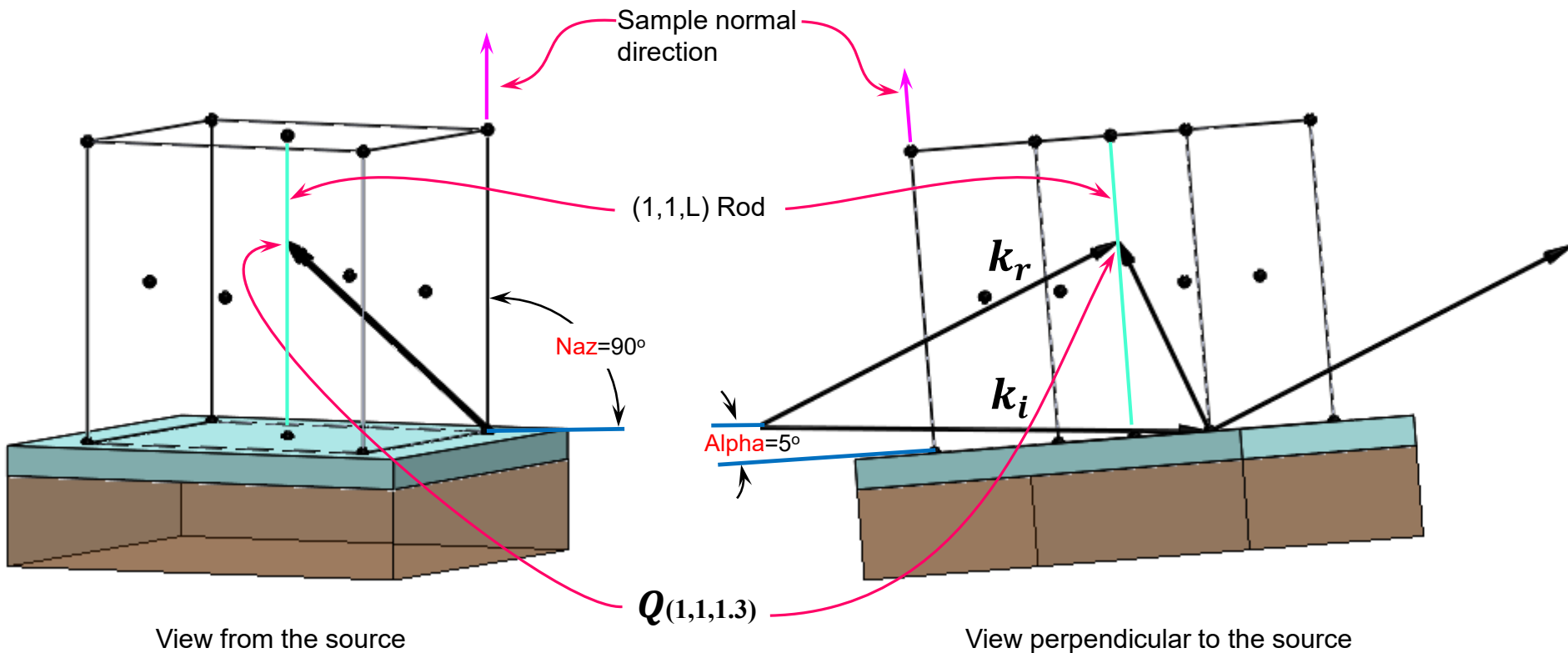
CTR Diffraction – On the Instrumentation



Diffractometer Geometry – Off-Specular Rods

For off-specular specify two diffraction geometry parameters:

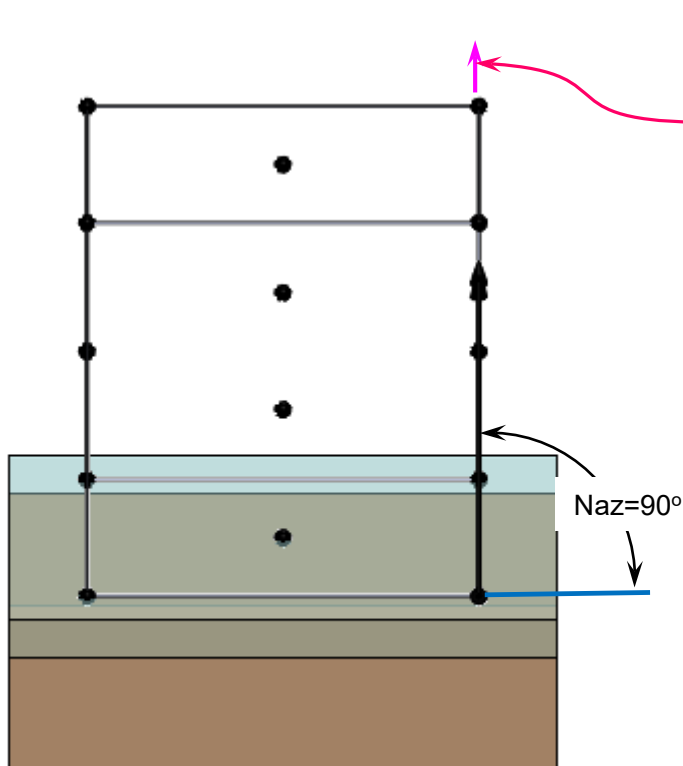
- 1) Incidence angle α that the k_i vector makes with the crystal surface
- 2) The angle N_{az} that the surface normal vector makes with the horizontal plane (a plane parallel to the floor in our lab)



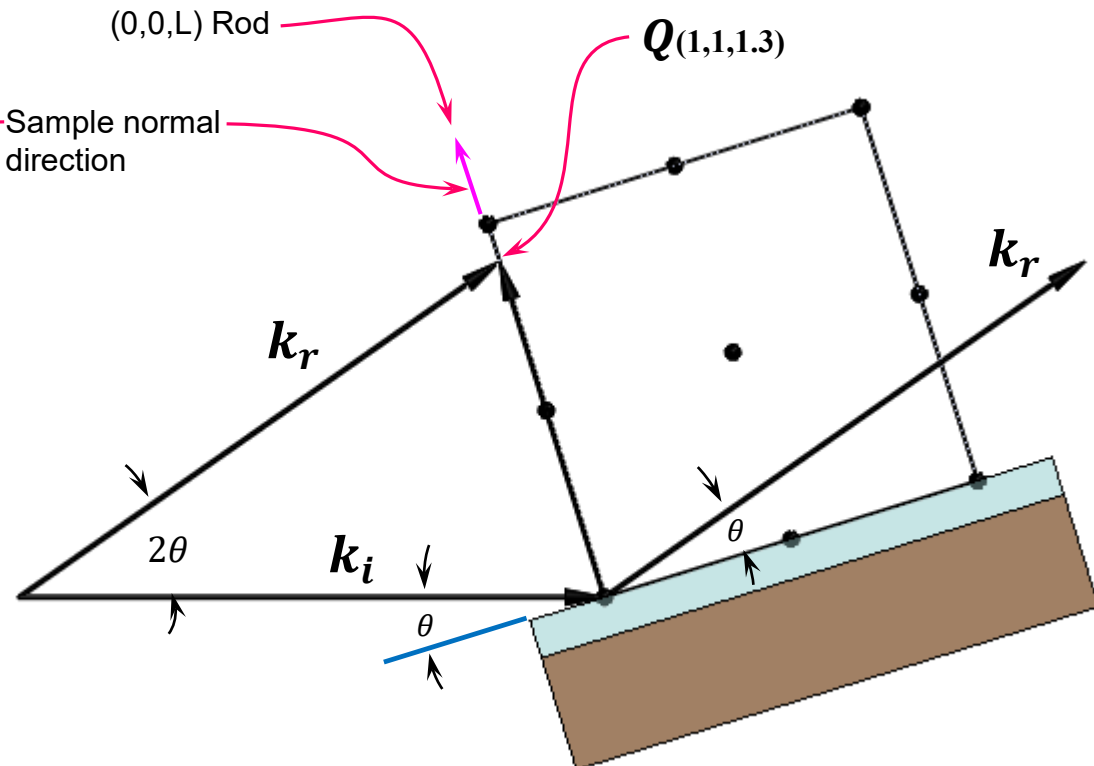
Diffractometer Geometry –Specular Rod

For specular specify one diffraction geometry parameters:

- 1) The angle N_{az} that the surface normal vector makes with the horizontal plane (a plane parallel to the floor in our lab).



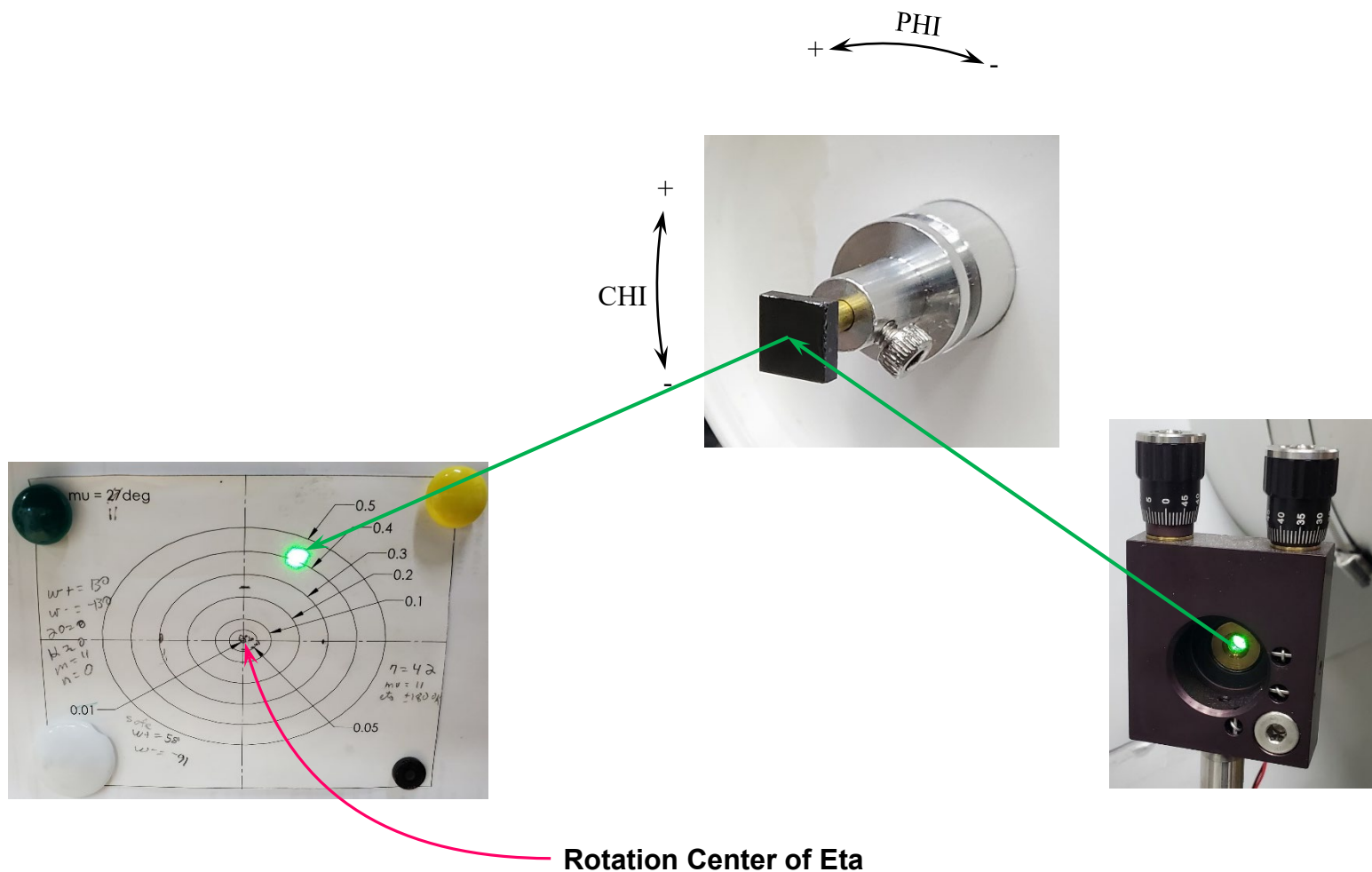
View from the source



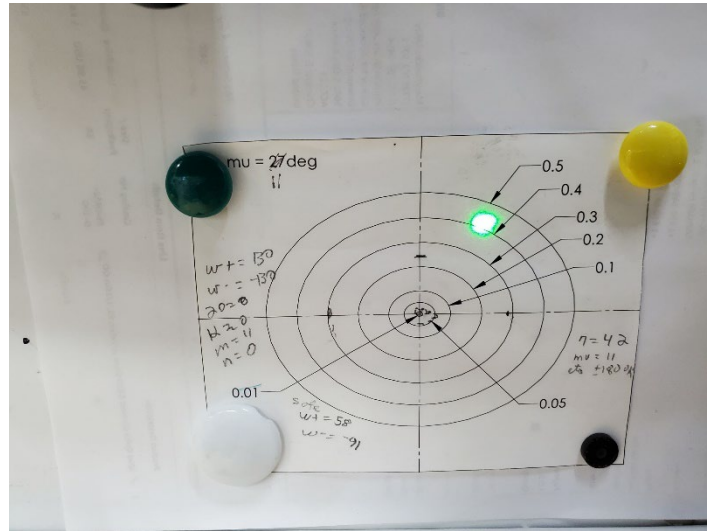
View perpendicular to the source



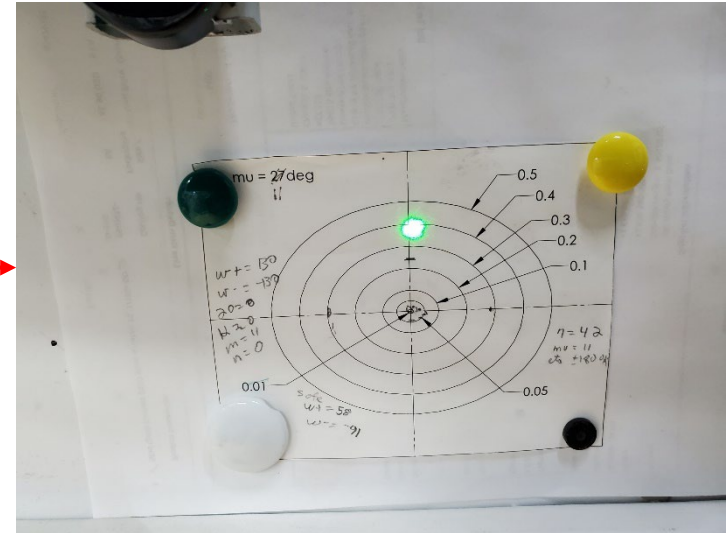
Diffractometer Geometry – Finding the Surface Normal



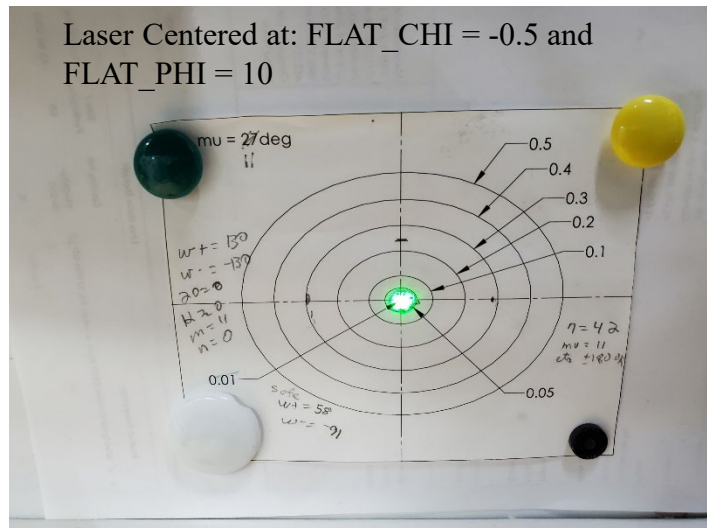
Diffractometer Geometry – Finding the Surface Normal



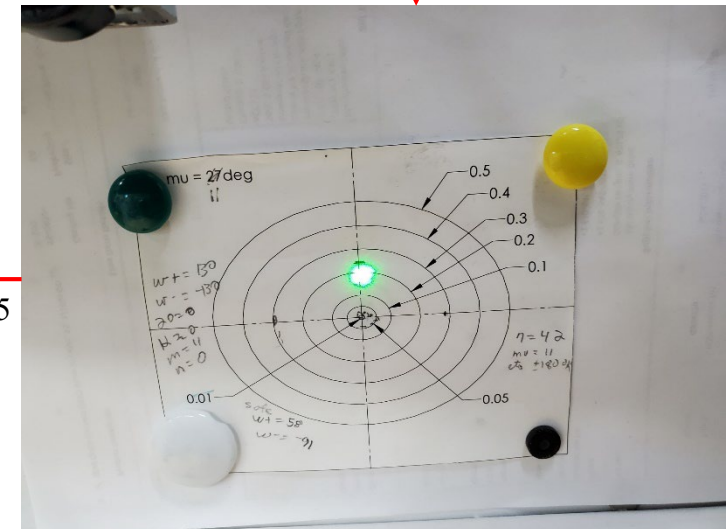
Phi +10



Chi -0.25

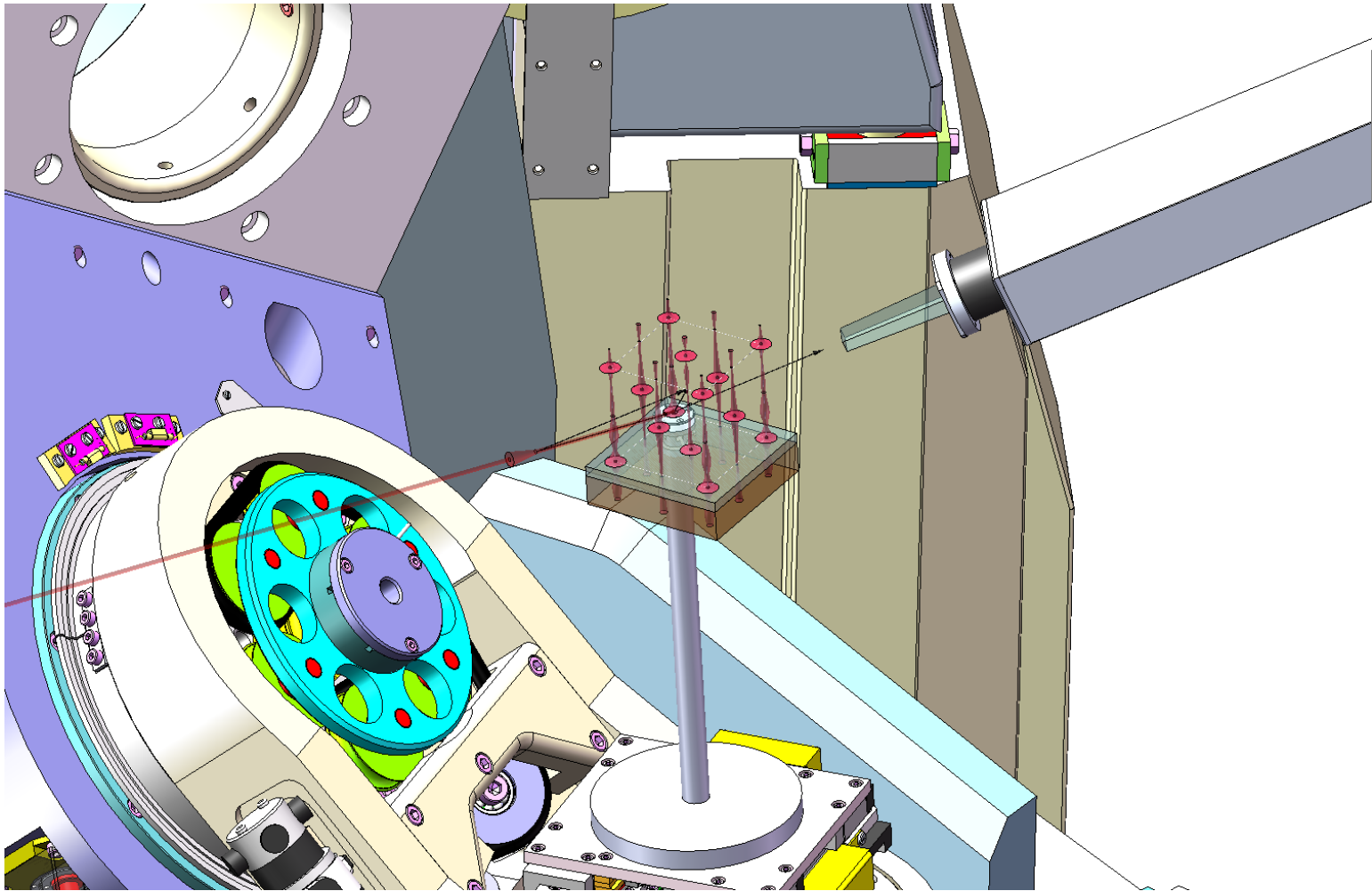


Chi -0.25



Diffractometer Geometry: (1,1,1.6), $N_{az} = 90^\circ$, $\alpha = 5^\circ$

Vertical Scattering Geometry



Diffractometer Geometry: (1,1,1.6), $N_{az} = 0^\circ$, $\alpha = 5^\circ$

Horizontal Scattering Geometry

